BEYOND THE STANDARD MODEL

Michael E. Peskin
SLAC, Stanford University, Stanford, California USA

Abstract

These lectures constitute a short course in 'Beyond the Standard Model' for students of experimental particle physics. I discuss the general ideas which guide the construction of models of physics beyond the Standard Model. The central principle, the one which most directly motivates the search for new physics, is the search for the mechanism of the spontaneous symmetry breaking observed in the theory of weak interactions. To illustrate models of weak-interaction symmetry breaking, I give a detailed discussion of the idea of supersymmetry and that of new strong interactions at the TeV energy scale. I discuss experiments that will probe the details of these models at future pp and e^+e^- colliders.

1. Introduction

Every year, the wise people who organize the European School of Particle Physics feel it necessary to subject young experimentalists to a course of lectures on 'Beyond the Standard Model'. They treat this subject as if it were a discipline of science that one could study and master. Of course, it is no such thing. If we knew what lies beyond the Standard Model, we could teach it with some confidence. But the interest in this subject is precisely that we do not know what is waiting for us there.

The confusion about 'Beyond the Standard Model' goes beyond students and summer school organizers to the senior scientists in our field. A theorist such as myself who claims to be able to explain things about physics beyond the Standard Model is very often met with skepticism that such explanations are even possible. 'Do we really have any idea', one is told, 'what we will find a higher energies?' 'Don't we just want the highest possible energy and luminosity?' 'The Standard Model works very well, so why must there be any new physics at all?'

And yet there are specific things that one can teach that should be relevant to physics beyond the Standard Model. Though we do not know what physics to expect at higher energies, the principles of physics that we have learned in the explication of the Standard Model should still apply there. In addition, we hope that some of the questions

not answered by the Standard Model should be answered there. This course will concentrate its attention on these two issues: What questions are likely to be addressed by new physics beyond the Standard Model, and what general methods of analysis can we use to create and analyze proposed answers to these questions?

A set of lectures on 'Beyond the Standard Model' should have one further goal as well. It is possible that the first sign of physics beyond the Standard Model could be discovered next year at LEP, or perhaps it is already waiting in the unanalyzed data from the Fermilab collider. On the other hand, it is possible that this discovery will have to wait for the great machines of the next generation. Many people feel dismay at the fact that the pace of discovery in high-energy physics is very slow, with experiments operating on the time scale of a decade familiar in planetary science rather than on the time scale of days or weeks. Because of the cost and complexity of modern elementary particle experiments, these long time scales are inevitable, and we have to adjust our expectations to them. But the long time scales also require that we set for ourselves very clear goals that we can try to realize a decade in the future. To do this, it is useful to have a concrete understanding of what experiments will look like at the next generation of colliders and what physics issues they address. Even if we cannot correctly predict what Nature will provide for us at higher energy, it is essential to take some models as illustrative examples and work out in complete detail how to analyze them experimentally. With luck, we can choose models will have features relevant to the ultimate correct theory of the next scale in physics. But even if we are not sufficiently lucky or insightful to predict what will appear, such a study will leave us prepared to solve whatever puzzles Nature has set.

This, then, is what I would like to accomplish in these lectures. I will set out some questions which I feel are the most important ones at the present stage of our understanding, and the ones which I feel are most likely to be addressed by the new phenomena of the next energy scale. I will explain some theoretical ideas that have come from our understanding of the Standard Model that I feel will play an important role at the next level. Building on these ideas, I will describe illustrative models of physics beyond the Standard Model. And, for each case, I will describe the program of experiments that will clarify the nature of the new physics that the model implies.

When we design a program of future high-energy experiments, we are also calling for the construction of new high-energy accelerators that would be needed to carry out this program. I hope that students of high-energy physics will take an interest in this practical or political aspect of our field of science. Those who think about this seriously know that we cannot ask society to support such expensive machines unless we can promise that these facilities will give back fundamental knowledge that is of the utmost importance and that cannot be obtained in any other way. I hope that they will be interested to see how central a role the CERN Large Hadron Collider (LHC) plays in each of the experimental programs that I will describe. Another proposed facility will also play a major role in my discussion, a high-energy e^+e^- linear collider with center-of-mass energy about 1 TeV. I will argue in these lectures that, with these facilities, the scientific justification changes qualitatively from that of the present colliders at CERN and Fermilab. Whereas at current energies, we search for new physics and try to place limits, at next step in energy we must find new physics that addresses one of the major gaps in the Standard Model.

This last issue leads to us to ask another, and perhaps unfamiliar, question about

the colliders of the next generation. Much ink has been wasted in comparing hadron and lepton colliders on the basis of energy reach and asking which is preferable. The real issue for these machines is a different one. We will see that illustrative models of new physics based on simple ideas will out to have rich and complex phenomenological consequences. Thus, it is a serious question whether we will be able to understand the model that Nature has put forward for us from experimental observations. I will argue through my examples that these two types of colliders, which focus on different and complementary aspects of the high-energy phenomena, can bring back a complete picture of the new phenomena of a clarity that neither, working alone, could achieve.

The outline of these lectures is as follows. In Section 2, I will introduce the question of the mechanism of electroweak symmetric breaking and also two related questions that influence the construction and analysis of models of new physics. In Sections 3 and 4, I will give one illustrative set of answers to these questions through a detailed discussion of models with supersymmetry at the weak-interaction scale. Section 3 will develop the formalism of supersymmetry and derive its connection to the questions I have set out. Section 4 will discuss more detailed properties of supersymmetric models which provide interesting experimental probes. In Section 5, I will discuss models with new strong interactions at the TeV mass scale, models which give very different answers to our broad questions about physics beyond the Standard Model. In Section 6, I will summarize the lessons of our study of these two very different types of models and draw some general conclusions.

2. Three Basic Questions

To begin our study of physics beyond the Standard Model, I will review some properties of the Standard Model and some insights that it provides. I will also discuss some questions that the Standard Model does not answer, but which might reasonably be answered at the next scale in fundamental physics.

2.1 Why not just the Standard Model?

To introduce the study of physics beyond the Standard Model, I must first explain what is wrong with the Standard Model. To see this, we only have to compare the publicity for the Standard Model, what we say about it to beginning students and to our colleagues in other fields, with the explicit expression for the Standard Model Lagrangian.

When we want to advertise the virtues of the Standard Model, we say that it is a model whose foundation is symmetry. We start from the principle of local gauge invariance, which tells us that the interactions of vector bosons are associated with a global symmetry group. The form of these interactions is uniquely specified by the group structure. Thus, from the knowledge of the basic symmetry group, we can write down the Lagrangian or the equations of motion. Specifying the group to be $U(1)$, we derive electromagnetism. To create a complete theory of Nature, we choose the group, in accord with observation, to be $SU(3) \times SU(2) \times U(1)$. This group is a product, and we are free to include a different coupling constant for each factor. But in the ideal theory, these would be the only parameters. Specify to which representations of the gauge group the matter particles belong, fix the three coupling constants, and we have a complete theory of Nature.

This set of ideas is tantalizing because it is so close to being true. The couplings of quarks and leptons to the strong, weak, and electromagnetic interactions are indeed fixed correctly in terms of three coupling constants. From the LEP and SLC experiments, we have learned that the pattern of weak-interaction couplings of the quarks and leptons follows the symmetry prediction to the accuracy of a few percent, and also that the strong-interaction coupling is universal among quark flavors at a similar level of accuracy.

On the other hand, the Lagrangian of the Minimal Standard Model tells a rather different story. Let me write it here for reference:

$$\begin{aligned}\mathcal{L} &= \overline{q} i \not{D} q + \overline{\ell} i \not{D} \ell - \frac{1}{4}(F^a_{\mu\nu})^2 \\ &\quad + |D_\mu \phi|^2 - V(\phi) \\ &\quad - \left(\lambda_u^{ij} \overline{u}^i_R \phi \cdot Q^j_L + \lambda_d^{ij} \overline{d}^i_R \phi^* \cdot Q^j_L + \lambda_\ell^{ij} \overline{e}^i_R \phi^* \cdot L^j_L + \text{h.c.} \right) \ . \end{aligned} \tag{1}$$

The first line of (1) is the pure gauge theory discussed in the previous paragraph. This line of the Lagrangian contains only three parameters, the three Standard Model gauge couplings g_s, g, g', and it does correctly describe the couplings of all species of quarks and leptons to the strong, weak, and electromagnetic gauge bosons.

The second line of (1) is associated with the Higgs boson field ϕ. The Minimal Standard Model introduces one scalar field, a doublet of weak interaction $SU(2)$, so that its vacuum expectation value can give a mass to the W and Z bosons. The potential energy of this field $V(\phi)$ contains at least two new parameters which play a role in determining the W boson mass. At this moment, there is no experimental evidence for the existence of the Higgs field ϕ and very little evidence that constrains the form of its potential.

The third line of (1) similarly gives an origin for the masses of quarks and leptons. In the Standard Model, the left- and right-handed quark fields belong to different representations of $SU(2) \times U(1)$; a similar conclusion holds for the leptons. On the other hand, a mass term for a fermion couples the left- and right-handed components. This is impossible as long as the gauge symmetry is exact. In the Standard Model, one can write a trilinear term linking a left- and right-handed pair of species to the Higgs field. When the Higgs field acquires a vacuum expectation value, this coupling turns into a mass term. Unfortunately, a generic fermion-fermion-boson coupling is restricted only rather weakly by gauge symmetries. The Standard Model gauge symmetry allows three complex 3×3 matrices of couplings, the paramaters λ^{ij} of (1). When ϕ acquires a vacuum expectation values, these matrices become the mass matrices of quarks and leptons. Thus, whereas the gauge couplings of quarks and leptons were strongly restricted by symmetry, the mass terms for these particles can be of general and, indeed, complex, structure.

If we consider (1) to be the fundamental Lagrangian of Nature, the situation is even worse. The Higgs coupling matrices λ^{ij} are renormalizable couplings in this Lagrangian. The property of renormalizability implies that, once these couplings are specified, the theory gives definite predictions. However, the specification of the renormalizable couplings is part of the statement of the problem. Except in very special field theories, these couplings cannot be determined from the internal consistency of the theory itself. The Standard Model Lagrangian then leaves us with the three matrices λ^{ij}, and the parameters of the Higgs potential $V(\phi)$, as conditions of the problem which cannot in principle be determined. In order to understand why the masses of the quarks, the leptons, and the W and

Z bosons have their observed values, we must find a deeper theory beyond the Standard Model from which the Lagrangian (1), or some replacement for it, can be derived.

Thus, it is a disappointing feature of the Minimal Standard Model that it has a large number of parameter which are undetermined, and which cannot be determined. This disappointment, though, has an interesting converse. Typically in physics, when we meet a system with a large number of parameters, what stands behind it is a system with a simple description which is realized with some complexity in its dynamics. The transport coefficients of fluids or the properties of electrons in a semiconductor are described in terms of a large number of parameters, but these parameters can be computed from an underlying atomic picture. Through this analogy, we would conclude that the gauge couplings of quarks and leptons are likely to reflect a fundamental structure, but that the Higgs boson is unlikely to be simple, minimal, or elementary. The multiplicity of undermined couplings of the Minimal Standard Model are precisely those of the Higgs boson. If we could break through and discover the simple underlying picture behind the Higgs boson, or behind the breaking of $SU(2) \times U(1)$ symmetry, we would then have the correct deeper viewpoint from which to understand the undetermined parameters of the Standard Model.

2.2 Three models of electroweak symmetry breaking

The argument given in the previous section leads us to the question: What is actually the mechanism of electroweak symmetry breaking? In this section, I would like to present three possible models for this phenomenon and to discuss their strengths and weaknesses.

The first of these is the model of electroweak symmetry breaking contained in the Minimal Standard Model. We introduce a Higgs field

$$\phi = \begin{pmatrix} \phi^+ \\ \phi^0 \end{pmatrix} \tag{2}$$

with $SU(2) \times U(1)$ quantum numbers $I = \frac{1}{2}$, $Y = \frac{1}{2}$. I will use $\tau^a = \sigma^a/2$ to denote the generators of $SU(2)$, and I normalize the hypercharge so that the electric charge is $Q = I^3 + Y$.

Take the Lagrangian for the field ϕ to be the second line of (1), with

$$V(\phi) = -\mu^2 \phi^\dagger \phi + \lambda (\phi^\dagger \phi)^2 \ . \tag{3}$$

This potential is minimized when $\phi^\dagger \phi = \mu^2/2\lambda$. Thus, one particular vacuum state is given by

$$\langle \phi \rangle = \begin{pmatrix} 0 \\ \frac{1}{\sqrt{2}} v \end{pmatrix} \ , \tag{4}$$

where $v^2 = \mu^2/\lambda$.

The most general ϕ field configuration can be written in the same notation as

$$\phi = e^{i\alpha(x)\cdot\tau} \begin{pmatrix} 0 \\ \frac{1}{\sqrt{2}}(v + h(x)) \end{pmatrix} \ . \tag{5}$$

In this expression, $\alpha^a(x)$ parametrizes an $SU(2)$ gauge transformation. The field $h(x)$ is a gauge-invariant fluctation away from the vacuum state; this is the physical Higgs field.

The mass of this field is given by

$$m_h^2 = 2\mu^2 = 2\lambda v^2 \ . \tag{6}$$

Notice that, in this model, $h(x)$ is the only gauge-invariant degree of freedom in $\phi(x)$, and so the symmetry-breaking sector gives rise to only one new particle, the Higgs scalar.

If we insert (4) into the kinetic term for ϕ, we obtain a mass term for W and Z; this is the usual Higgs mechanism for producing these masses. If g and g' are the $SU(2)\times U(1)$ coupling constants, one finds the familiar result

$$m_W = g\frac{v}{2} \ , \qquad m_Z = \sqrt{g^2 + g'^2}\frac{v}{2} \ . \tag{7}$$

The measured values of the masses and couplings then lead to

$$v = 246 \text{ GeV} \ . \tag{8}$$

This is a very simple model of $SU(2) \times U(1)$ symmetry breaking. Perhaps it is even too simple. If we ask the question, why is $SU(2)\times U(1)$ broken, this model gives the answer 'because $(-\mu^2) < 0$.' This is a perfectly correct answer, but it teaches us nothing. Normally, the grand qualitative phenomena of physics happen as the result of definite physical mechanisms. But there is no physically understandable mechanism operating here.

One often hears it said that if the minimal Higgs model is too simple, one can make the model more complex by adding a second Higgs doublet. For our next case, then, let us consider a model with two Higgs doublets ϕ_1, ϕ_2, both with $I = \frac{1}{2}$, $Y = \frac{1}{2}$. The Lagrangian of the Higgs fields is

$$\mathcal{L} = |D_\mu \phi_1|^2 + |D_\mu \phi_1|^2 - V(\phi_1, \phi_2) \ , \tag{9}$$

with

$$V = -\left(\begin{array}{cc} \phi_1^\dagger & \phi_2^\dagger \end{array}\right) M^2 \begin{pmatrix} \phi_1 \\ \phi_2 \end{pmatrix} + \cdots \ , \tag{10}$$

where M^2 is a 2×2 matrix. It is not difficult to engineer a form for V such that, at the minimum, the vacuum expectation values of ϕ_1 and ϕ_2 are aligned:

$$\langle \phi_1 \rangle = \begin{pmatrix} 0 \\ \frac{1}{\sqrt{2}} v_1 \end{pmatrix} \ , \qquad \langle \phi_2 \rangle = \begin{pmatrix} 0 \\ \frac{1}{\sqrt{2}} v_2 \end{pmatrix} \ . \tag{11}$$

The ratio of the two vacuum expectation values is conventionally parametrized by an angle β,

$$\tan\beta = \frac{v_2}{v_1} \ . \tag{12}$$

To reproduce the correct values of the W and Z mass,

$$v_1^2 + v_2^2 = v^2 = (246 \text{ GeV})^2 \ . \tag{13}$$

The field content of this model is considerably richer than that of the minimal model. An infinitesimal gauge transformation of the vacuum configuration (11) leads to a field configuration

$$\delta\phi_1 = \frac{1}{2}\begin{pmatrix} v_1(\alpha_1 + i\alpha_2) \\ v_1(i\alpha_3) \end{pmatrix} \ , \qquad \delta\phi_2 = \frac{1}{2}\begin{pmatrix} v_2(\alpha_1 + i\alpha_2) \\ v_2(i\alpha_3) \end{pmatrix} \ . \tag{14}$$

The fluctuations of the field configuration which are orthogonal to this lead to new physical particles. These include the motions

$$\delta\phi_1 = \frac{1}{2}\begin{pmatrix} \sin\beta\cdot(h_1+ih_2) \\ \sin\beta\cdot(ih_3)\end{pmatrix}\ , \qquad \delta\phi_2 = \frac{1}{2}\begin{pmatrix} -\cos\beta\cdot(h_1+ih_2) \\ -\cos\beta\cdot(ih_3)\end{pmatrix}\ , \tag{15}$$

as well as the fluctuations $v_i \to v_i + H_i$ of the two vacuum expectation values. Thus we find five new particles. The fields h_1 and h_2 combine to form charged Higgs bosons $H^\pm$. The field h_3 is a CP-odd neutral boson, usually called A^0. The two fields H_i typically mix to form mass eigenstates called h^0 and H^0.

I have discussed this structure in some detail because we will later see it appear in specific model contexts. But it does nothing as far as answering the physical question that I posed a moment ago. Again, if one asks what is the mechanism of weak interaction symmetry breaking, the answer this model gives is that the matrix $(-M^2)$ has a negative eigenvalue.

The third model I would like to discuss is a model of a very different kind proposed in 1979 by Weinberg and Susskind [1, 2]. Imagine that the fundamental interactions include a new gauge interaction which is almost an exact copy of QCD with two quark flavors. The new interactions differ from QCD in only two respects: First, the quarks are massless; second, the nonperturbative scales Λ and m_ρ are much larger in the new subsection. The two flavors of quarks should be coupled to $SU(2)\times U(1)$ just as (u,d) are, and I will call them (U,D).

In QCD, the strong interactions between quarks and antiquarks leads to the generation of large effective masses for the u and d. This mass generation is associated with spontaneous symmetry breaking. The strong interactions between very light quarks and antiquarks make it energetically favorable for the vacuum of space to fill up with quark-antiquark pairs. This gives vacuum expectation values to operators built from quark and antiquark fields.

The analogue of this phenomenon should occur in our theory of new interactions—for just the same reason—and so we should find

$$\left\langle \overline{U}U\right\rangle = \left\langle \overline{D}D\right\rangle = -\Delta \neq 0\ . \tag{16}$$

In terms of chiral components,

$$\overline{U}U = U_L^\dagger U_R + U_R^\dagger U_L\ , \tag{17}$$

and similarly for $\overline{D}D$. But, in the weak-interaction theory, the left-handed quark fields transform under $SU(2)$ while the right-handed fields do not. Thus, the vacuum expectation value in (16) signals $SU(2)$ symmetry breaking. In fact, under $SU(2)\times U(1)$, the operator $\overline{Q}_L U_R$ has the same quantum numbers $I=\frac{1}{2}$, $Y=\frac{1}{2}$ as the elementary Higgs boson that we introduced in our earlier model. The vacuum expectation value of this operator then has the same effect: It breaks $SU(2)\times U(1)$ to the $U(1)$ symmetry of electromagnetism and gives mass to the three weak-interaction bosons.

I will explain in Section 5.1 that the pion decay constant F_π of the new strong interaction theory plays the role of v in (7) in determining the mass scale of m_W and m_Z. If we were to set F_π to the value given in (8), we would need to scale up QCD by the factor

$$\frac{246\ \text{GeV}}{93\ \text{MeV}} = 2600. \tag{18}$$

Then the hadrons of these new strong interactions would be at TeV energies.

For me, the Weinberg-Susskind model is much more appealing as a model of electroweak symmetry breaking than the Minimal Standard Model. The reason for this is that, in the Weinberg-Susskind model, electroweak symmetry breaking happens naturally, for a reason, rather than being included as the result of an arbitrary choice of parameters. I would like to emphasize especially that the Weinberg-Susskind model is preferable even though it is more complex. In fact, this complexity is an essential part of its foundation. In this model, *something happens*, and that physical action gives rise to a set of consequences, of which electroweak symmetry breaking is one.

This notion that the consequences of physical theories flow from their complexity is familiar from the theories in particle physics that we understand well. In QCD, quark confinement, the spectrum of hadrons, and the parton description of high-energy reactions all flow out of the idea of a strongly-coupled non-Abelian gauge interaction. In the weak interactions, the $V\!-\!A$ structure of weak couplings and all of its consequences for decays and asymmetries follow from the underlying gauge structure.

Now we are faced with a new phenomenon, the symmetry breaking of $SU(2)\times U(1)$, whose explanation lies outside the realm of the known gauge theories. Of course it is possible that this phenomenon could be explained by the simplest, most minimal addition to the laws of physics. But that is not how we have seen Nature work. In searching for an explanation of electroweak symmetry breaking, we should not be searching for a simplistic theory but rather for a simple idea from which deep and rich consequences might flow.

2.3 Questions for orientation

The argument of the previous section gives focus to the study of physics beyond the Standard Model. We have a phenomenon necessary to the working of weak-interaction theory, the symmetry-breaking of $SU(2)\times U(1)$, which we must understand. This symmetry-breaking is characterized by a mass scale, v in (8), which is close to the energy scales now being probed at accelerators. At the same time, it is a new qualitative phenomenon which cannot originate from the known gauge interactions. Therefore, it calls for new physics, and in an energy region where we can hope to discover it. For me, this is the number one question of particle physics today:

*** What is the mechanism of electroweak symmetry breaking?**

Along with this question come two subsidiary ones. Both of these are connected to the fact that electroweak symmetry breaking is necessary for the generation of masses for the weak-interaction bosons, the quarks, and the leptons. Perhaps there are also other particles which cannot obtain mass until $SU(2)\times U(1)$ is broken. Then these particles also must have masses at the scale of a few hundred GeV or below. The heaviest of these particles must be especially strongly coupled to the fields that are the basic cause of the symmetry-breaking. At the very least, the top quark belongs to this class of very heavy particles, and other members of this class might well be found. Thus, we are also led to ask,

*** What is the spectrum of elementary particles at the 1 TeV energy scale?**

*** Is the mass of the top quark generated by weak couplings or by new strong interactions?**

In the remainder of this section, I will comment on these three questions. In the following sections, when we consider explicit models of electroweak symmetry breaking, I

will develop the models theoretically to propose answer these questions. At any stage in the argument, though, you should have firmly in mind that these answers will ultimately come from experiment, and, in particular, from direct observations of TeV-energy phenomena. The goal of my theoretical arguments, then, will be to suggest particular phenomena which could be observed experimentally to shed light on these questions. We will see in Sections 4 and 5 that models which attempt to explain electroweak symmetry breaking typically suggest a variety of new experimental probes, which may allow us to uncover a whole new layer of the fundamental interactions.

2.4 General features of electroweak symmetry breaking

Since the question of electroweak symmetry breaking will be our main concern, it is important to state at the beginning what we do know about this phenomenon. Unfortunately, our knowledge is very limited. Basically it consists of only three items.

First, we know the general scale of electroweak symmetry breaking, which is set by the scale of m_W and m_Z,

$$v = 246 \text{ GeV} . \tag{19}$$

If there are new particles associated with the mechanism of electroweak symmetry breaking, their masses should be at the scale v. Of course, this is only an order-of-magnitude estimate. The precise relation between v and the masses of new particles depends on the specific model of electroweak symmetry breaking. In the course of these lectures, I will discuss examples in which the most important new particles lie below v and other examples in which they lie higher by a large factor.

Second, we know that the electroweak boson masses follow the pattern (7), that is,

$$\frac{m_W}{m_Z} = \cos\theta_w , \qquad m_\gamma = 0 . \tag{20}$$

In terms of the original $SU(2)$ and $U(1)$ gauge bosons A^a_μ, B_μ, this pattern tells us that the mass matrix had the form

$$m^2 = \frac{v^2}{2} \begin{pmatrix} g^2 & & & \\ & g^2 & & \\ & & g^2 & -gg' \\ & & -gg' & g'^2 \end{pmatrix} \tag{21}$$

acting on the vector $(A^1_\mu, A^2_\mu, A^3_\mu, B_\mu)$. Notice that the 3×3 block of this matrix acting on the $SU(2)$ bosons is diagonal. This would naturally be a consequence of an unbroken $SU(2)$ symmetry under which $(A^1_\mu, A^2_\mu, A^3_\mu)$ form a triplet [3, 4]. This strongly suggests that an unbroken $SU(2)$ symmetry, called *custodial* $SU(2)$, should be included in any successful model of electroweak symmetry breaking.

The Minimal Standard Model actually contains such a symmetry accidentally. the complex doublet ϕ can be viewed as a set of four real-valued fields,

$$\phi = \frac{1}{\sqrt{2}} \begin{pmatrix} \phi^1 + i\phi^2 \\ \phi^3 + i\phi^4 \end{pmatrix} . \tag{22}$$

The Higgs potential (3) is invariant to $SO(4)$ rotations of these fields. The vacuum expectation value (4) gives an expectation value to one of the four components and so breaks

$SO(4)$ spontaneously to $SO(3) = SU(2)$. In the Weinberg-Susskind model, there is also a custodial $SU(2)$ symmetry, the isospin symmetry of the new strong interactions. In this case, the custodial symmetry is not an accident, but rather a component of the new idea.

Third, we know that the new interactions responsible for electroweak symmetry breaking contribute very little to precision electroweak observables. I will discuss this constraint in somewhat more detail in Section 5.2. For the moment, let me point out that, if we take the value of the electromagnetic coupling α and the weak interaction parameters G_F and m_Z as input parameters, the value of the weak mixing angle $\sin^2\theta_w$ that governs the forward-backward and polarization asymmetries of the Z^0 can be shifted by radiative corrections involving particles associated with the symmetry breaking. In the Minimal Standard Model, this shift is rather small,

$$\delta(\sin^2\theta_w) = \frac{\alpha}{\cos^2\theta_w - \sin^2\theta_w} \frac{1 + 9\sin^2\theta_w}{24\pi} \log\frac{m_h}{m_Z} \ . \tag{23}$$

The coefficient of the logarithm has the value 6×10^{-4}. The accuracy of the LEP and SLC experiments is such that the size of the logarithm cannot be much larger than 1, and larger radiative corrections from additional sources are forbidden. In models of electroweak symmetry breaking based on new strong interactions, this can be an important constraint.

2.5 The evolution of couplings

Now I would like to comment similarly on the two subsidiary questions that I put forward in Section 2.3. I will begin with the first of these questions: What is the spectrum of elementary particles at the 1 TeV energy scale? In the discussion above, I have already argued for the importance of this question. Because mass generation in quantum field theory is associated with symmetry breaking, and because one of the major symmetries of Nature is broken at the scale v, we might expect a sizeable multiplet of particles to have masses of the order of magnitude of v, that is, in the range of hundreds of GeV. Well above the scale of v, these particles are effectively massless species characterized by their definite quantum numbers under $SU(2) \times U(1)$.

It is important to note that, at energies much higher than v, the basic species are chiral. For example, the right- and left-handed components of the u quark have the following quantum numbers in this high-energy world:

$$u_R \ : \ I = 0, \ Y = \frac{2}{3} \qquad \begin{pmatrix} u \\ d \end{pmatrix}_L \ : \ I = \frac{1}{2}, \ Y = -\frac{1}{6} \ . \tag{24}$$

There are no relations between these two species; each half of the low-energy u quark has a completely different fundamental assignment. And, each multiplet is prohibited from acquiring mass by $SU(2) \times U(1)$ symmetry.

It is tempting to characterize the full set of elementary particles at 1 TeV—the particles, that is, that we have a chance of observing at accelerators in the foreseeable future—as precisely those which are forbidden to acquire mass until $SU(2) \times U(1)$ is broken. This would explain why these particles are left over from the truly high-energy dynamics of Nature, the dynamics which generates and perhaps unifies the gauge and flavor interactions, to survive down to the much lower energy scales accessible to our experiments.

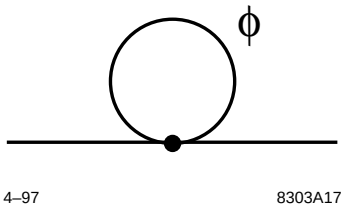

Figure 1: The simplest diagram which generates a Higgs boson mass term in the Minimal Standard Model.

Before giving in to this temptation, however, I would like to point out that the Minimal Standard Model contains a glaring counterexample to this point of view, the Higgs boson itself. The mass term for the Higgs field

$$\Delta\mathcal{L} = -\mu^2 \phi^\dagger \phi \tag{25}$$

respects all of the symmetries of the Standard Model whatever the value of μ. This model, then, gives no reason why μ^2 is of order v rather than being, for example, twenty orders of magnitude larger.

Further, if we arbitrarily set $\mu^2 = 0$, the μ^2 term would be generated by radiative corrections. The first correction to the mass is shown in Figure 1. This simple diagram is formally infinite, but we might cut off its integral at a scale Λ where the Minimal Standard Model breaks down. With this prescription, the diagram contributes to the Higgs boson mass $m^2 = -\mu^2$ in the amount

$$\begin{aligned} -im^2 &= -i\lambda \int \frac{d^4k}{(2\pi)^4} \frac{i}{k^2} \\ &= -i\frac{\lambda}{16\pi^2}\Lambda^2 \ . \end{aligned} \tag{26}$$

Thus, the contribution of radiative corrections to the Higgs boson mass is *nonzero*, *divergent*, and *positive*. The last of these properties is actually the worst. Since electroweak symmetry breaking requires that m^2 be negative, the contribution we have just calculated must be cancelled by the Higgs boson bare mass term, and this cancellation must be made more and more fine to achieve a negative m^2 of the order of $-v^2$ in models where Λ is very large. This problem is often called the 'gauge hierarchy problem'. I think of it as just a special aspect of the fact that the Minimal Standard Model does not explain why $-\mu^2$ is negative or why electroweak symmetry is broken. Once we have left this fundamental question to a mere choice of a parameter, it is not surprising that the radiative corrections to this parameter might drive it in an unwanted direction.

To continue, however, I would like to set this issue aside and think more carefully about the properties of the massless, chiral particle multiplets that we find at the TeV energy scale and above. If these particles are described by a renormalizable field theory but we can ignore any mass parameters, the interactions of these particles are governed by the dimensionless couplings of their renormalizable interactions. The scattering amplitudes generated by these couplings will reflect the maximal parity violation of the field content, with forward-backward and polarization asymmetries in scattering processes typically of order 1.

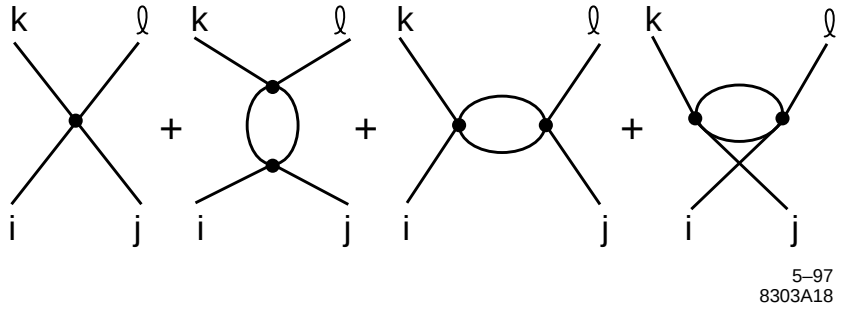

Figure 2: Diagrams which renormalize the Higgs coupling constant in the Minimal Standard Model.

For massless fermions, there is an ambiguity in writing the quantum numbers in such a chiral situation becuase a left-handed fermion has a right-handed antifermion, and vice versa. For reasons that will be clearer in the next section, I will choose the convention of writing all species of fermions in terms of their left-handed components, viewing all right-handed particles as antiparticles. Thus, I will now recast the right-handed u quark in (24) as the antiparticle of a left-handed species $\overline{u}$ which belongs to the $\overline{3}$ representation of color $SU(3)$. The fermions of the Standard Model thus belong to the left-handed multiplets

$$\begin{aligned} L &: I = \frac{1}{2},\ Y = -\frac{1}{2} & \qquad Q &: I = \frac{1}{2},\ Y = \frac{1}{6} \\ \overline{e} &: I = 0,\ Y = 1 & \qquad \overline{u} &: I = 0,\ Y = -\frac{2}{3} \\ & & \qquad \overline{d} &: I = 0,\ Y = \frac{1}{3}\ . \end{aligned} \tag{27}$$

Here L is the left-handed lepton doublet and Q is the left-handed quark doublet. Q is a color 3, and $\overline{u}$, $\overline{d}$ are color $\overline{3}$'s. The right-handed electron is the antiparticle of $\overline{e}$, and there is no right-handed neutrino. This set of quantum numbers of repeated for each quark and lepton generation.

If the dimensionless couplings of the theory at TeV energies are small, these coupling will run according to their renormalization group equations, but only at a logarithmic rate. Thus, above the TeV scale, the description of elementary particles would change very slowly. In this circumstance, it is reasonable to extrapolate many orders of magnitude above the TeV energy scale and to derive definite physical conclusions from that extrapolation. I will now describe two consequences of this idea.

The first of these concerns the coupling constant of the minimal Higgs theory. For this analysis, it is best to write the Higgs multiplet as four real-valued fields as in (22). Then the Higgs Lagrangian (ignoring the mass term) takes the form

$$\mathcal{L} = \frac{1}{2}(\partial_\mu \phi^i)^2 - \frac{1}{2}\lambda_b \left((\phi^i)^2\right)^2\ , \tag{28}$$

where $i = 1, \ldots, 4$. I have given the coupling a subscript b to remind us that this is the bare coupling. The value of the first, tree-level, diagram shown in Figure 2 is

$$-2i\lambda_b \left(\delta^{ij}\delta^{k\ell} + \delta^{ik}\delta^{j\ell} + \delta^{i\ell}\delta^{jk}\right)\ . \tag{29}$$

To compute the three one-loop diagrams in Figure 2, we need to contract two of these structures together, using $\delta^{ii} = 4$ where necessary. The easiest way to do this is to isolate the terms in each diagram which are proportional to $\delta^{ij}\delta^{k\ell}$. Since the set of three diagrams is symmetric under crossing, the other two index contractions must appear also with equal coefficients. The contributions to this term from the three loop diagrams shown in Figure 2 have the form

$$\frac{(-2i\lambda_b)^2}{2} \int \frac{d^4k}{(2\pi)^4} \frac{i}{k^2} \frac{i}{k^2} \left([8+2+2]\delta^{ij}\delta^{k\ell} + \cdots \right) \ , \tag{30}$$

where I have ignored the external momentum, and the numbers in the bracket give the contribution from each diagram. In a scattering process, this expression is a good approximation when k lies in the range from the momentum transfer Q up to the scale Λ at which the Minimal Standard Model breaks down. Then the sum of the diagrams in Figure 2 is

$$-2i\lambda_b \left(1 - \frac{12\lambda_b^2}{(4\pi)^2} \log \frac{\Lambda^2}{Q^2} \right) \cdot \left[\delta^{ij}\delta^{k\ell} + \cdots \right] \ . \tag{31}$$

The coefficient in this expression can be thought of as the effective value of the Higgs coupling constant for scattering processes at the momentum transfer Q. Often, we trade the bare coupling λ_b for the value of the effective coupling at a low-energy scale (for example, v), which we call the renormalized coupling λ_r. In terms of λ_r, (31) takes the form

$$-2i\lambda_r \left(1 + \frac{12\lambda_r^2}{(4\pi)^2} \log \frac{Q^2}{v^2} \right) \cdot \left[\delta^{ij}\delta^{k\ell} + \cdots \right] \ . \tag{32}$$

Whichever description we choose, the effective coupling $\lambda(Q)$ has a logarithmically slow variation with Q. The most convenient way to describe this variation is by writing a differential equation, called the *renormalization group equation* [5]

$$\frac{d}{d\log Q} \lambda(Q) = \frac{3}{2\pi^2} \lambda^2(Q) \ . \tag{33}$$

If the coupling is not so weak, we should add further terms to the right-hand side which arise from higher orders of perturbation theory.

The solution of (33) is

$$\lambda(Q) = \frac{\lambda_r}{1 - (3\lambda/2\pi^2)\log Q/v} \tag{34}$$

It is interesting that the effective coupling is predicted to become strong at high energy, specifically, at the scale

$$Q_* = v \exp \left[\frac{2\pi^2}{3\lambda} \right] \ . \tag{35}$$

Either the minimal Higgs Lagrangian is a consequence of strong-interaction behavior at the scale Q_*, or, at some energy scale below Q_* the simple Higgs theory must become a part of some more complex set of interactions.

Making use of (6), we can relate this bound on the validity of the simple Higgs theory to the value of the Higgs mass, be rewriting (35) as

$$Q_* = v \exp \left[\frac{4\pi^2 v^2}{3m_h^2} \right] \ . \tag{36}$$

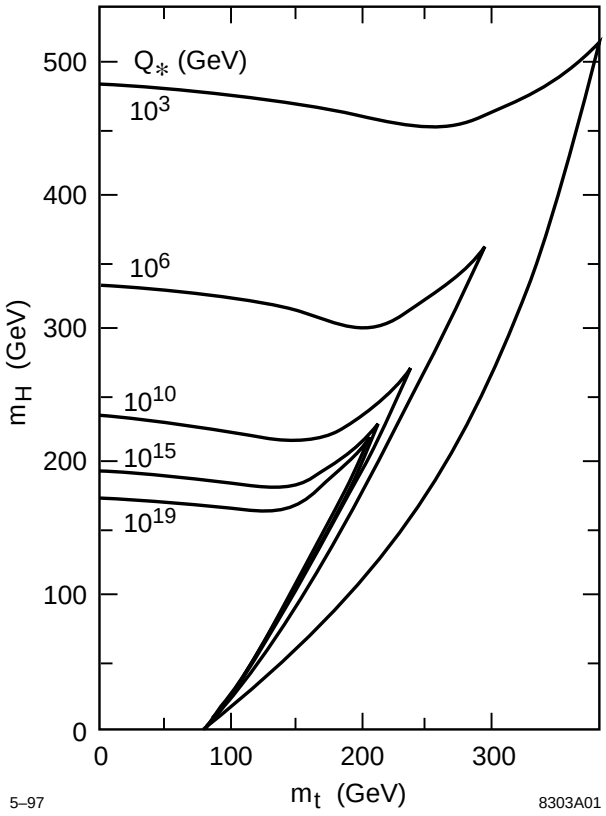

Figure 3: Region of validity of the minimal Higgs model in the (m_h, m_t) plane, including two-loop quantum corrections to the Higgs potential, from [6].

This is a remarkable formula, because the mass of the Higgs boson sits in the denominator of an exponential. Thus, for small m_h or a small value of λ at v, the energy scale Q_* up to which the minimal Higgs theory can be valid is very high. On the other hand, as m_h increases above v, the value of Q_* decreases catastrophically. Here is a table of the values predicted by (36):

m_h	Q_*
150 GeV	6×10^{17} GeV
200 GeV	1×10^{11} GeV
300 GeV	2×10^{6} GeV
500 GeV	6×10^{3} GeV
700 GeV	1×10^{3} GeV

(37)

Notice that, as the mass of the Higgs boson goes above 700 GeV, the scale Q_* comes down to m_h. Larger values of the Higgs boson mass in the minimal model are self-contradictory.

A more accurate evaluation of the limit Q_* in the Standard Model, including the full field content of the model and terms in perturbation theory beyond the leading logarithms, is shown in Figure 3 [6]. Note that, in this more sophisticated calculation, the limit Q_* depends on the value of the top quark mass when m_t becomes large. The calculation I have just described explains the top boundary of the regions indicated in the figure; I will describe the physics that leads to the right-hand boundary in Section 2.6.

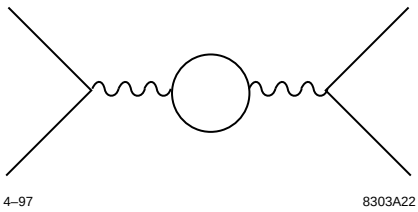

Figure 4: A one-loop diagram contributing to the renormalization-group evolution of a gauge coupling constant.

The same idea, that the basic coupling constants can evolve slowly on a logarithmic scale in Q due to loop corrections from quantum field theory, can be applied to the $SU(3) \times SU(2) \times U(1)$ gauge couplings. The renormalization group equation for the gauge coupling g_i which includes the effects of one-loop diagrams such as that shown in Figure 4 has the form

$$\frac{d}{d \log Q} g_i(Q) = -\frac{b_i}{(4\pi)^2} g_i^3 \ . \tag{38}$$

That is, the rate of change of g_i^2 with $\log Q$ is proportional to g_i^4, as the diagram indicates.

The b_i are constants which depend on the gauge group and on the matter multiplets to which the gauge bosons couple. For $SU(N)$ gauge theories with matter in the fundamental representation,

$$b_N = \left(\frac{11}{3} N - \frac{1}{3} n_f - \frac{1}{6} n_s \right) \ , \tag{39}$$

where n_f is the number of chiral (left-handed) fermions and n_s is the number of complex scalars which couple to the gauge bosons. For a $U(1)$ gauge theory in which the matter particles have charges t, the corresponding formula is

$$b_1 = -\frac{2}{3} \sum_f t_f^2 - \frac{1}{3} \sum_s t_s^2 \ . \tag{40}$$

I will not derive these formulae here; you can find their derivation in any textbook of quantum field theory (for example, [5]). In the $SU(N)$ case, when n_f and n_s are sufficiently small, b_N is positive, leading to a decrease of the effective coupling as Q increases. This is the remarkable phenomenon of *asymptotic freedom*.

It is especially interesting that the effect of asymptotic freedom is stronger for $SU(3)$ than for $SU(2)$ while the $SU(3)$ gauge coupling is larger at the energy of Z boson mass. This suggests that, if we extrapolate to very high energy, the strong- and weak-interaction coupling constants should become equal, and perhaps the three different interactions that make up the Standard Model may become unified [7]. In the remainder of this section, I will investigate this question quantitatively.

In order to discuss the unification of gauge couplings, there is one small technical point that we must address first. For a non-Abelian group, we conventionally normalize the generators t^a so that, in the fundamental representation,

$$\mathrm{tr}[t^a t^b] = \frac{1}{2} \delta^{ab} \ . \tag{41}$$

Also, for any simple non-Abelian group, $\mathrm{tr}[t^a] = 0$. For example, the matrices $\tau^a = \sigma^a/2$ which we used to represent the $SU(2)$ generators below (2) obey these conditions. However, for a $U(1)$ group there is no similar natural way to normalize the charges. In principle, we could hypothesize that the $SU(2)$ and $SU(3)$ charges are unified with a charge proportional to the hypercharge,

$$t_Y = c \cdot Y \tag{42}$$

for any value of the scale factor c.

In building a theory of unified strong, weak, and electromagnetic interactions, we might not want to assume that all fermion species necessarily belong to the fundamental representation of some $SU(N)$ group; thus, we would not wish to impose the condition (41) on t_Y. But it is not so unreasonable to insist that there is a single large non-Abelian group for which t_Y and the $SU(2)$ and $SU(3)$ charges are all generators, and that the quarks and leptons of the Standard Model form a representation of this group. This leads to the normalization condition for t_Y,

$$\mathrm{tr}(t_Y)^2 = \mathrm{tr}(t)^2 \ , \tag{43}$$

where t is a generator of $SU(2)$ or $SU(3)$. Any such generator gives the same constraint. For convenience, I will choose to implement this condition using $t = t^3$, the third component of weak-interaction isospin. The trace could be taken over three or over one Standard Model generations. Before evaluating c, it is interesting to sum over the fermions with quantum numbers in the table (27), to check that t_Y has zero trace. Indeed, including each species in (27) with its $SU(2)$ and color multiplicity, we find

$$\begin{aligned} \mathrm{tr}[t_Y] &= c\mathrm{tr}[Y] \\ &= c\left[-\frac{1}{2}\cdot 2 + 1\cdot 1 + \frac{1}{6}\cdot 6 - \frac{2}{3}\cdot 3 + \frac{1}{3}\cdot 3\right] \\ &= 0 \end{aligned} \tag{44}$$

Then we can compute

$$\mathrm{tr}(t^3)^2 = \left(\frac{1}{2}\right)^2 \cdot 2 \cdot 4 = 2 \ , \tag{45}$$

and

$$\mathrm{tr}(t_Y)^2 = c^2\left[\left(\frac{1}{2}\right)^2\cdot 2 + 1\cdot 1 + \left(\frac{1}{6}\right)^2\cdot 6 + \left(\frac{2}{3}\right)^2\cdot 3 + \left(\frac{1}{3}\right)^2\cdot 3\right] = c^2\cdot\frac{10}{3} \ . \tag{46}$$

Equating these expressions, we find $c = \sqrt{3/5}$; that is,

$$t_Y = \sqrt{\frac{3}{5}}Y \ , \tag{47}$$

or, writing the $U(1)$ gauge coupling $g'Y = g_1 t_Y$,

$$g_1 = \sqrt{\frac{5}{3}}g' \ . \tag{48}$$

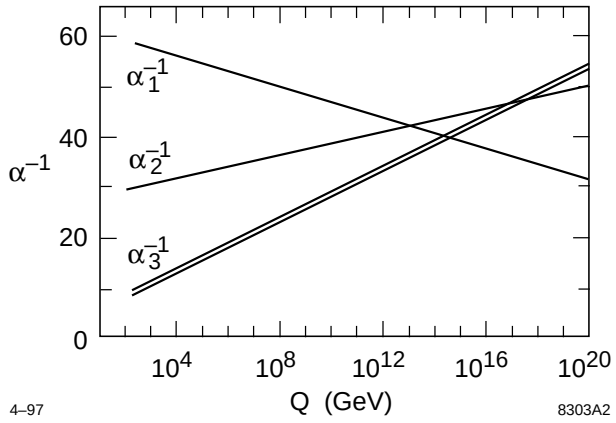

Figure 5: Evolution of the $SU(3) \times SU(2) \times U(1)$ gauge couplings to high energy scales, using the one-loop renormalization group equations of the Standard Model. The double line for α_3 indicates the current experimental error in this quantity; the errors in α_1 and α_2 are too small to be visible.

These formulae give the normalization of the $U(1)$ coupling which unifies with $SU(2)$ and $SU(3)$ in the $SU(5)$ and $SO(10)$ grand unfied theories, and in many more complicated schemes of unification.

In the Standard Model, the $U(1)$ coupling constant g_1 and the $SU(2)$ and $SU(3)$ couplings g_2 and g_3 evolve with Q according to the renormalization group equation (38) with

$$\begin{aligned} b_3 &= 11 - \frac{4}{3} n_g \\ b_2 &= \frac{22}{3} - \frac{4}{3} n_g - \frac{1}{6} n_h \\ b_1 &= -\frac{4}{3} n_g - \frac{1}{10} n_h \ . \end{aligned} \tag{49}$$

In this formula, n_g is the number of quark and lepton generations and n_h is the number of Higgs doublet fields. Note that a complete generation of quarks and leptons has the same effect on all three gauge couplings, so that (at the level of one-loop corrections), the validity of unification is independent of the number of generations. The solution to (38) can be written, in terms of the measured coupling constants at $Q = m_Z$, as

$$g_i^2(Q) = \frac{g_i^2(m_Z)}{1 + (b_i/8\pi^2) \log Q/m_Z} \ . \tag{50}$$

Alternatively, if we let $\alpha_i = g_i^2/4\pi$,

$$\alpha_i^{-1}(Q) = \alpha_i^{-1}(m_Z) + \frac{b_i}{2\pi} \log \frac{Q}{m_Z} \ . \tag{51}$$

The evolution of coupling constants predicted by (49) and (51), with $n_h = 1$, is shown in Figure 5. It is disappointing that, although the values of the coupling constants do converge, they do not come to a common value at any scale.

We can be a bit more definite about this test of the unification of couplings as follows: I will work in the $\overline{MS}$ scheme for defining coupling constants. The precisely known values of α, m_Z, and G_F imply $\alpha^{-1}(m_Z) = 127.90 \pm .09$, $\sin^2\theta_w(m_Z) = 0.2314 \pm .003$ [11]; combining this with the value of the strong interaction coupling $\alpha_s(m_Z) = 0.118 \pm .003$ [8], we find for the $\overline{MS}$ couplings at $Q = m_Z$:

$$\begin{aligned} \alpha_1^{-1} &= 58.98 \pm .08 \\ \alpha_2^{-1} &= 29.60 \pm .04 \\ \alpha_3^{-1} &= 8.47 \pm .22 \end{aligned} \tag{52}$$

On the other hand, if we assume that the three couplings come to a common value at a scale m_U, we can put $Q = m_U$ into the three equations (51), eliminate the unknowns $\alpha^{-1}(m_U)$ and $\log(m_U/m_Z)$, and find one relation among the measured coupling constants at m_Z. This relation is

$$\alpha_3^{-1} = (1+B)\alpha_2^{-1} - B\alpha_1^{-1} \ , \tag{53}$$

where

$$B = \frac{b_3 - b_2}{b_2 - b_1} \ . \tag{54}$$

From the data, we find

$$B = 0.719 \pm .008 \pm .03 \ , \tag{55}$$

where the second error reflects the omission of higher order corrections, that is, finite radiative corrections at the thresholds and two-loop corrections in the renormalization group equations.

On the other hand, the Standard Model gives

$$B = \frac{1}{2} + \frac{3}{110} n_h \ . \tag{56}$$

This is inconsistent with the unification hypothesis by a large margin. But perhaps an interesting scheme for physics beyond the Standard Model could fill this gap and allow a unification of the known gauge couplings.

2.6 The special role of the top quark

In the previous section, we discussed the role of the quarks and leptons in the energy region above 1 TeV. However, we ought to give additional consideration to the role of the top quark. This quark is sufficiently heavy that its coupling to the Higgs boson is an important perturbative coupling at very high energies. Thus, even in the simplest models, the top quark plays an important special role in the renormalization group evolution of couplings. It is possible that the top quark has an even more central role in electroweak symmetry breaking, and, in fact, that electroweak symmetry breaking may be *caused* by the strong interactions of the top quark. I will discuss this connection of the top quark to electroweak symmetry breaking later, in the context of specific models. In this section, I would like to prepare for that discussion by analyzing the effects of the large top quark-Higgs boson coupling which is already present in the Minimal Standard Model.

In the minimal Higgs model, the masses of quarks and leptons arise from the perturbative couplings to the Higgs boson written in the third line of (1). These couplings

are most often called the 'Higgs Yukawa couplings'. The top quark mass comes from a Yukawa coupling

$$\Delta\mathcal{L} = -\lambda_t \bar{t}_R \phi \cdot Q_L + \text{h.c.} \ , \tag{57}$$

where $Q_L = (t_L, b_L)$. When the Higgs field acquires a vacuum expectation value of the form (4), this term becomes

$$\Delta\mathcal{L} = -\frac{\lambda_t v}{\sqrt{2}} \ \bar{t}t, \tag{58}$$

and we can read off the relation $m_t = \lambda_t v/\sqrt{2}$. The value of the top quark mass measured at Fermilab is 176 ± 6 GeV for the on-shell mass [9], which corresponds to

$$(m_t)_{\overline{MS}} = 166 \pm 6 \text{ GeV} \ . \tag{59}$$

With the value of v in (8), this implies

$$\lambda_t = 1 \quad \text{or} \quad \alpha_t = \frac{\lambda^2}{4\pi} = (14.0 \pm 0.7)^{-1} \ . \tag{60}$$

In this simplest model, the top quark Yukawa coupling is weak at high energies but still is large enough to compete with QCD.

The large value of λ_t gives rise to two interesting effects. The first of these is an essential modification of the renormalization group equation for the Higgs boson coupling λ given in (33). Let me now rewrite this equation including the one-loop corrections due to λ_t and also to the weak-interaction couplings [10]:

$$\frac{d}{d\log Q}\lambda = \frac{3}{2\pi^2}\left[\lambda^2 - \frac{1}{32}\lambda_t^4 + \frac{g^2}{512}(3 + 2s^2 + s^4)\right] \ , \tag{61}$$

where I have abbreviated $s^2 = \sin^2\theta_w$.

A remarkable property of the formula (61) is that the top quark Yukawa coupling enters the renormalization group equation with a negative sign (which essentially comes from the factor (-1) for the top quark fermion loop). This sign implies that, if the top quark mass is sufficiently large that that λ^4 term dominates, the Higgs coupling λ is driven negative at large Q. This is a dangerous instability which would push the expectation value v of the Higgs field to arbitrarily high values. The presence of this instability gives an upper bound on the top quark mass for fixed m_h, or, equivalently, a lower bound on the Higgs mass for fixed m_t. If we replace λ, λ_t, and g in (61) with the masses of h, t, and W, we find the condition

$$m_h^2 > \frac{1}{2}\left[m_t^2 - \frac{3}{4}m_W^2\right] \ . \tag{62}$$

I should note that finite perturbative corrections shift this bound in a way that is important quantitatively. This effect accounts for the right-hand boundary of the regions shown in Figure 3.

The implications of Figure 3 for the Higgs boson mass are quite interesting. For the correct value of the top quark mass (59), the Minimal Standard Model description of the Higgs boson can be valid only if the mass of the Higgs is larger than about 60 GeV. But for values of the m_h below 100 GeV or above 200 GeV, the Higgs coupling must be sufficiently large that this coupling becomes strong well below the Planck scale. Curiously,

the fit of current precision electroweak data to the Minimal Standard Model (for example, to the more precise version of (23)) gives the value [11]

$$m_h = 124^{+125}_{-71} \text{ GeV} , \tag{63}$$

which actually lies in the region for which the Minimal Standard Model is good to extremely high energies. It is also important to point out that the regions of Figure 3 apply only to the Minimal version of the Standard Model. In models with additional Higgs doublets, with the boundaries giving limits on the lightest Higgs boson, the upper boundary remains qualitatively correct, but the boundary associated with the heavy top quark is usually pushed far to the right.

The second perturbative effect of the top quark Yukawa coupling is its influence back on its own renormalization group evolution. In the same simple one-loop approximation as (61), the renormalization group equation for the top quark Yukawa coupling takes the form

$$\frac{d}{d\log Q}\lambda_t = \frac{\lambda_t}{(4\pi)^2}\left[\frac{9}{2}\lambda_t^2 - 8g_3^2 - \frac{9}{4}g^2\left(1 + \frac{17}{24}s^2\right)\right] . \tag{64}$$

The signs in this equation are not hard to understand. A theory with λ_t and no gauge couplings cannot be asymptotically free, and so λ_t must drive itself to zero at large distances or small Q. On the other hand, the effect of the QCD coupling g_3 is to increase quark masses and also λ_t as Q becomes small.

The two effects of the λ_t and QCD renormalization of λ_t balance at the point

$$\lambda_t = \frac{4}{3}(4\pi\alpha_s)^{1/2} \sim 1.5 , \tag{65}$$

corresponding to $m_t \sim 250$ GeV. This condition was referred to by Hill [12] as the 'quasi-infrared fixed point' for the top quark mass. This 'fixed point' is in fact a line in the (λ_t, α_s) plane. The renormalization group evolution from large Q to small Q carries a general initial condition into this line, as shown in Figure 6; then the parameters flow along the line, with α_s increasing in the familiar way as Q decreases, until we reach $Q \sim m_t$. The effect of this evolution is that theories with a wide range of values for λ_t at a very high unification scale all predict the physical value of m_t to lie close to the fixed-point value (65). This convergence is shown in Figure 7. The fixed point attracts initial conditions corresponding to arbitrarily large values of λ_t at high energy. However, if the initial condition at high energy is sufficiently small, the value of λ_t or m_t might not be able to go up to the fixed point before Q comes down to the value m_t. Thus, there are two possible cases, the first in which the physical value of m_t is very close to the fixed point value, the second in which the physical value of m_t lies at an arbitrary point below the fixed-point value.

In the Minimal Standard Model, the observed top quark mass (59) must correspond to the second possibility. However, in models with two Higgs doublet fields, the quantity which is constrainted to a fixed point is $m_t/\cos\beta$, where β is the mixing angle defined in (12). The fixed point location also depends on the full field content of the model. In the supersymmetric models to be discussed in the next section, the fixed-point relation is

$$\frac{m_t}{\cos\beta} \sim 190 \text{ GeV} \tag{66}$$

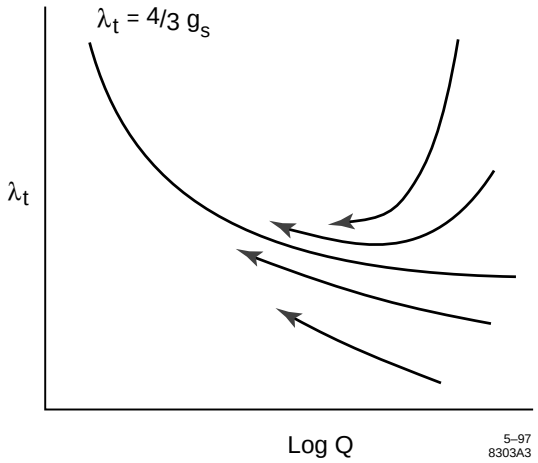

Figure 6: Renormalization-group evolution of the top quark Yukawa coupling λ_t and the strong interaction coupling α_s, from large Q to small Q.

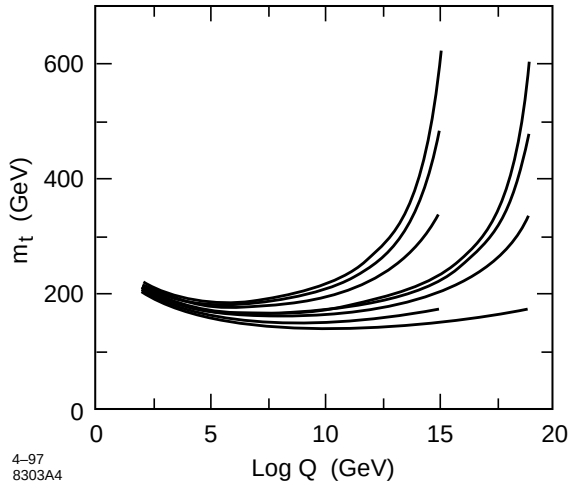

Figure 7: Convergence of predictions for the top quark mass in the Minimal Standard Model, due to renormalization-group evolution, from [12].

for values of $\tan\beta$ that are not too large. In such theories it is quite reasonable that the physical value of the top quark mass could be determined by a fixed point of the renormalization group equation for λ_t.

Now that we understand the implications of the large top quark mass in the simplest Higgs models, we can return to the question of the implications of the large top quark mass in more general models. We have seen that the observed value of m_t can consistently be generated solely by perturbative interactions. We have also seen that, in this case, the coupling λ_t can have important effects on the renormalization group evolution of couplings. But this observation shows that the observed value of m_t is not sufficiently large that it must lead to nonperturbative effects or that it can by itself drive electroweak symmetry breaking. In fact, we now see that m_t or λ_t can be the cause of electroweak symmetry breaking only if we combine these parameters with additional new dynamics that lies outside the Standard Model. I will discuss some ideas which follow this line in Section 5.

2.7 Recapitulation

In this section, I have introduced the major questions for physics beyond the Standard Model by reviewing issues that arise when the Standard Model is extrapolated to very high energy. I have highlighted the issue of electroweak symmetry breaking, which poses an important question for the Standard Model which must be solved at energies close to those of our current accelerators. There are many possibilities, however, for the form of this solution. The new physics responsible for electroweak symmetry breaking might be a new set of strong interactions which changes the laws of particle physics fundamentally at some nearby energy scale. But the analysis we have done tells us that the solution might be constructed in a completely different way, in which the new interactions are weakly coupled for many orders of magnitude above the weak interaction scale but undergoes qualitative changes through the renormalization group evolution of couplings.

The questions we have asked in Section 2.4 and this dichotomy of strong-coupling versus weak-coupling solutions to these questions provide a framework for examining theories of physics beyond the Standard Model. In the next sections, I will consider some explicit examples of such models, and we can see how they illustrate the different possible answers.

3. Supersymmetry: Formalism

The first class of models that I would like to discuss are supersymmetric extensions of the Standard Model. *Supersymmetry* is defined to be a symmetry of Nature that links bosons and fermions. As we will see later in this section, the introduction of supersymmetry into Nature requires a profound generalization of our fundamental theories, including a revision of the theory of gravity and a rethinking of our basic notions of space-time. For many theorists, the beauty of this new geometrical theory is enough to make it compelling. For myself, I think this is quite a reasonable attitude. However, I do not expect you to share this attitude in order to appreciate my discussion.

For the skeptical experimenter, there are other reasons to study supersymmetry. The most important is that supersymmetry is a concrete worked example of physics beyond the Standard Model. One of the virtues of extending the Standard Model using supersymmetry is that the phenomena that we hope to discover at the next energy scale—the new spectrum of particles, and the mechanism of electroweak symmetry breaking—occur in supersymmetric models at the level of perturbation theory, without the need for any new strong interactions. Supersymmetry naturally predicts are large and complex spectrum of new particles. These particles have signatures which are interesting, and which test the capabilities of experiments. Because the theory has weak couplings, these signatures can be worked out directly in a rather straightforward way. On the other hand, supersymmetric models have a large number of undetermined parameters, so they can exhibit an interesting variety of physical effects. Thus, the study of supersymmetric models can give you very specific pictures of what it will be like to experiment on physics beyond the Standard Model and, through this, should aid you in preparing for these experiments. For this reason, I will devote a large segment of these lectures to a detailed discussion of supersymmetry. However, as a necessary corrective, I will devote Section 5 of this article to a review of a model of electroweak symmetry breaking that runs by strong-coupling effects.

This discussion immediately raises a question: Why is supersymmetry relevant to

the major issue that we are focusing on in these lectures, that of the mechanism of electroweak symmetry breaking? A quick answer to this question is that supersymmetry legitimizes the introduction of Higgs scalar fields, because it connects spin-0 and spin-$\frac{1}{2}$ fields and thus puts the Higgs scalars and the quarks and leptons on the same epistemological footing. A better answer to this question is that supersymmetry naturally gives rise to a mechanism of electroweak symmetry breaking associated with the heavy top quark, and to many other properties that are attractive features of the fundamental interactions. These consequences of the theory arise from renormalization group evolution, by arguments similar to those we used to explain the features of the Standard Model that we derived in Sections 2.5 and 2.6. The spectrum of new particles predicted by supersymmetry will also be shaped strongly by renormalization-group effects.

In order to explain these effects, I must unfortunately subject you to a certain amount of theoretical formalism. I will therefore devote this section to describing construction of supersymmetric Lagrangians and the analysis of their couplings. I will conclude this discussion in Section 3.7 by explaining the supersymmetric mechanism of electroweak symmetry breaking. This analysis will be lengthy, but it will give us the tools we need to build a theory of the mass spectrum of supersymmetric particles. With this understanding, we will be ready in Section 4 to discuss the experimental issues raised by supersymmetry, and the specific experiments that should resolve them.

3.1 A little about fermions

In order to write Lagrangians which are symmetric between boson and fermion fields, we must first understand the properties of these fields separately. Bosons are simple, one component objects. But for fermions, I would like to emphasize a few features which are not part of the standard presentation of the Dirac equation.

The Lagrangian of a massive Dirac field is

$$\mathcal{L} = \overline{\psi} i \not{\partial} \psi - m \overline{\psi} \psi \ , \tag{67}$$

where ψ is a 4-component complex field, the Dirac spinor. I would like to write this equation more explicitly by introducing a particular representation of the Dirac matrices

$$\gamma^\mu = \begin{pmatrix} 0 & \sigma^\mu \\ \overline{\sigma}^\mu & 0 \end{pmatrix} \ , \tag{68}$$

where the entries are 2×2 matrices with

$$\sigma^\mu = (1, \vec{\sigma}) \ , \qquad \overline{\sigma}^\mu = (1, -\vec{\sigma}) \ . \tag{69}$$

We may then write ψ as a pair of 2-component complex fields

$$\psi = \begin{pmatrix} \psi_L \\ \psi_R \end{pmatrix} \ . \tag{70}$$

The subscripts indicate left- and right-handed fermion components, and this is justified because, in this representation,

$$\gamma^5 = \begin{pmatrix} -1 & 0 \\ 0 & 1 \end{pmatrix} \ . \tag{71}$$

This is a handy representation for calculations involving high-energy fermions which include chiral interactions or polarization effects, even within the Standard Model [5].

In the notation of (68), (70), the Lagrangian (67) takes the form

$$\mathcal{L} = \psi_L^\dagger i\overline{\sigma}^\mu \partial_\mu \psi_L + \psi_R^\dagger i\sigma^\mu \partial_\mu \psi_R - m\left(\psi_R^\dagger \psi_L + \psi_L^\dagger \psi_R\right) \ . \tag{72}$$

The kinetic energy terms do not couple ψ_L and ψ_R but rather treat them as distinct species. The mass term is precisely the coupling between these components.

I pointed out above (27) that, since the antiparticle of a masssless left-handed particle is a right-handed particle, there is an ambiguity in assigning quantum numbers to fermions. I chose to resolve this ambiguity by considering all left-handed states as particles and all right-handed states as antiparticles. With this philosophy, we would like to trade ψ_R for a left-handed field. To do this, define the 2×2 matrix

$$c = -i\sigma^2 = \begin{pmatrix} 0 & -1 \\ 1 & 0 \end{pmatrix} \ . \tag{73}$$

and let

$$\chi_L = c\psi_R^* \ , \qquad \chi_L^* = c\psi_R \tag{74}$$

Note that $c^{-1} = c^T = -c$, $c^* = c$, so (74) implies

$$\psi_R = -c\chi_L^* \ , \qquad \psi_R^\dagger = \chi_L^T c \ . \tag{75}$$

Also note, by multiplying out the matrices, that

$$c\sigma^\mu c^{-1} = (\overline{\sigma}^\mu)^T \ , \qquad c\overline{\sigma}^\mu c^{-1} = (\sigma^\mu)^T \ . \tag{76}$$

Using these relations, we can rewrite

$$\begin{aligned} \psi_R^\dagger i\sigma^\mu \partial_\mu \psi_R &= \chi_L^T c i\sigma^\mu \partial_\mu (-c)\chi_L^* \\ &= \chi_L^T i(\overline{\sigma}^\mu)^T \partial_\mu \chi_L^* \\ &= -\partial_\mu \chi_L^\dagger i(\overline{\sigma}^\mu)\chi_L \\ &= \chi_L^\dagger i\overline{\sigma}^\mu \partial_\mu \chi_L \ . \end{aligned} \tag{77}$$

The minus sign in the third line came from fermion interchange; it was eliminated in the fourth line by an integration by parts. After this rewriting, the two pieces of the Dirac kinetic energy term have precisely the same form, and we may consider ψ_L and χ_L as two species of the same type of particle.

If we replace ψ_R by χ_L, the mass term in (67) becomes

$$-m\left(\psi_R^\dagger \psi_L + \psi_L^\dagger \psi_R\right) = -m\left(\chi_L^T c\psi_L - \psi_L^\dagger c\chi_L^*\right) \ . \tag{78}$$

Note that

$$\chi_L^T c\psi_L = \psi_L^T c\chi_L \ , \tag{79}$$

with one minus sign from fermion interchange and a second from taking the transpose of c. Thus, this mass term is symmetric between the two species. It is interesting to know

that the most general possible mass term for spin-$\frac{1}{2}$ fermions can be written in terms of left-handed fields ψ_L^a in the form

$$-\frac{1}{2}m^{ab}\psi_L^{aT}c\psi_L^b + \text{h.c.} \ , \tag{80}$$

where m^{ab} is a symmetric matrix. For example, this form for the mass term incorporates all possible different forms of the neutrino mass matrix, both Dirac and Majorana.

From here on, through the end of Section 4, all of the fermions that appear in these lectures will be 2-component left-handed fermion fields. For this reason, there will be no ambiguity if I now drop the subscript L in my equations.

3.2 Supersymmetry transformations

Now that we have a clearer understanding of fermion fields, I would like to explore the possible symmetries that could connect fermions to bosons. To begin, let us try to connect a free massless fermion field to a free massless boson field. Because the scalar product (79) of two chiral fermion fields is complex, this connection will not work unless we take the boson field to be complex-valued. Thus, we should look for symmetries of the Lagrangian

$$\mathcal{L} = \partial_\mu\phi^*\partial^\mu\phi + \psi^\dagger i\overline{\sigma}\cdot\partial\psi \tag{81}$$

which mix ϕ and ψ.

To build this transformation, we must introduce a symmetry parameter with spin-$\frac{1}{2}$ to combine with the spinor index of ψ. I will introduce a parameter ξ which also transforms as a left-handed chiral spinor. Then a reasonable transformation law for ϕ is

$$\delta_\xi\phi = \sqrt{2}\xi^T c\psi \ . \tag{82}$$

A fermion field has the dimensions of $(\text{mass})^{3/2}$, while a boson field has the dimensions of $(\text{mass})^1$; thus, xi must carry the dimensions $(\text{mass})^{-1/2}$ or $(\text{length})^{1/2}$. This means that, in order to form a dimensionally correct transformation law for ψ, we must include a derivative. A sensible formula is

$$\delta_\xi\psi = \sqrt{2}i\sigma\cdot\partial\phi c\xi^* \ . \tag{83}$$

It is not difficult to show that the transformation (82), (83) is a symmetry of (81). Inserting these transformations, we find

$$\delta_\xi\mathcal{L} = \partial_\mu\phi^*\partial^\mu(\sqrt{2}\xi^T c\psi) + (\sqrt{2}i\xi^T c\sigma\cdot\partial\phi)i\overline{\sigma}\cdot\partial\psi + (\xi^*) \ . \tag{84}$$

The term in the first set of parentheses is the right-hand side of (82). The term in the second set of parentheses is the Hermitian conjugate of the right-hand side of (83). The last term refers to terms proportional to ξ^* arising from the variation of ϕ^* and ψ. To manipulate (84), integrate both terms by parts and use the identity

$$\sigma\cdot\partial\overline{\sigma}\cdot\partial = \partial^2 \tag{85}$$

which can be verified directly from (69). This gives

$$\delta_\xi\mathcal{L} = -\phi^*\partial^2(\sqrt{2}\xi^T c\psi) - \sqrt{2}i\xi^T c\cdot i\partial^2\psi + (\xi^*) \ . \tag{86}$$

The two terms shown now cancel, and the ξ^* terms cancel similarly. Thus, $\delta_\xi \mathcal{L} = 0$ and we have a symmetry.

The transformation (83) appears rather strange at first sight. However, this formula takes on a bit more sense when we work out the algebra of supersymmetry transformations. Consider the commutator

$$\begin{aligned}
(\delta_\eta \delta_\xi - \delta_\xi \delta_\eta)\phi &= \delta_\eta(\sqrt{2}\xi^T c\psi) - (\eta \leftrightarrow \xi) \\
&= \sqrt{2}\xi^T c(\sqrt{2}i\sigma^\mu \partial_\mu \phi c\eta^*) - (\eta \leftrightarrow \xi) \\
&= 2i\xi^T c\sigma^\mu c\eta^* \partial_\mu \phi - (\eta \leftrightarrow \xi) \\
&= -2i\xi^T (\overline{\sigma}^\mu)^T \eta^* \partial_\mu \phi - (\eta \leftrightarrow \xi) \\
&= 2i[\eta^\dagger \overline{\sigma}^\mu \xi - \xi^\dagger \overline{\sigma}^\mu \eta]\, \partial_\mu \phi \ . \qquad (87)
\end{aligned}$$

To obtain the fourth line, I have used (76); in the passage to the next line, a minus sign appears due to fermion interchange. In general, supersymmetry transformations have the commutation relation

$$(\delta_\eta \delta_\xi - \delta_\xi \delta_\eta) A = 2i[\eta^\dagger \overline{\sigma}^\mu \xi - \xi^\dagger \overline{\sigma}^\mu \eta]\, \partial_\mu A \qquad (88)$$

on every field A of the theory.

To clarify the significance of this commutation relation, let me rewrite the transformations δ_ξ as the action of a set of operators, the supersymmetry charges Q. These charges must also be spin-$\frac{1}{2}$. To generate the supersymmetry transformation, we contract them with the spinor parameter ξ; thus

$$\delta_\xi = \xi^T c Q - Q^\dagger c \xi^* \ . \qquad (89)$$

At the same time, we may replace $(i\partial_\mu)$ in (88) by the operator which generates spatial translations, the energy-momentum four-vector P^μ. Then (88) becomes the operator relation

$$\left\{ Q_a^\dagger \ , \ Q_b \right\} = (\overline{\sigma}^\mu)_{ab} P_\mu \qquad (90)$$

which defines the *supersymmetry algebra*. This anticommutation relation has a two-fold interpretation. First, it says that the square of the supersymmetry charge Q is the energy-momentum. Second, it says that the square of a supersymmetry transformation is a spatial translation. The idea of a square appears here in the same sense as we use when we say that the Dirac equation is the square root of the Klein-Gordon equation.

We started this discussion by looking for symmetries of the trivial theory (81), but at this stage we have encountered a structure with deep connections. So it is worth looking back to see whether we were forced to come to high level or whether we could have taken another route. It turns out that, given our premises, we could not have ended in any other place [13]. We set out to look for an operator Q that was a symmetry of Nature which carried spin-$\frac{1}{2}$. From this property, the quantity on the left-hand side of (90) is a Lorentz four-vector which commutes with the Hamiltonian. In principle, we could have written a more general formula

$$\left\{ Q_a^\dagger \ , \ Q_b \right\} = (\overline{\sigma}^\mu)_{ab} R_\mu \ , \qquad (91)$$

where R^μ is a conserved four-vector charge different from P^μ. But energy-momentum conservation is already a very strong restriction on particle scattering processes, since

it implies that the only degree of freedom in a two-particle reaction is the scattering angle in the center-of-mass system. A second vector conservation law, to the extent that it differs from energy-momentum conservation, places new requirements that contradict these restrictions except at particular, discrete scattering angles. Thus, it is not possible to have an interacting relativistic field theory with an additional conserved spin-1 charge, or with any higher-spin charge, beyond standard momentum and angular momentum conservation [14]. For this reason, (90) is actually the most general commutation relation that can be obeyed by supersymmetry charges.

The implications of the supersymmetry algebra (90) are indeed profound. If the square of a supersymmetry charge is the total energy-momentum of everything, then *supersymmetry must act on every particle and field in Nature*. We can exhibit this action explicitly by writing out the $a = 1, b = 1$ component of (90),

$$\left\{Q_1^\dagger \ , \ Q_1\right\} = P^0 + P^3 = P^+ \ . \tag{92}$$

On states with $P^+ \neq 0$ (which we can arrange for any particle state by a rotation), define

$$a = \frac{Q_1}{\sqrt{P^+}} \ , \qquad a^\dagger = \frac{Q_1^\dagger}{\sqrt{P^+}} \ . \tag{93}$$

These operators obey the algebra

$$\{a^\dagger \ , \ a\} = 1 \tag{94}$$

of fermion raising and lowering operators. They raise and lower J^3 by $\frac{1}{2}$ unit. Thus, in a supersymmetric theory, every state of nonzero energy has a partner of opposite statistics differing in angular momentum by $\Delta J^3 = \pm\frac{1}{2}$.

On the other hand, for any operator Q, the quantity $\{Q^\dagger, Q\}$ is a Hermitian matrix with eigenvalues that are either positive or zero. This matrix has zero eigenvalues for those states that satisfy

$$Q\,|0\rangle = Q^\dagger\,|0\rangle = 0 \ , \tag{95}$$

that is, for supersymmetric states. In particular, if supersymmetry is not spontaneously broken, the vacuum state is supersymmetric and satisfies (95). Since the vacuum also has zero three-momentum, we deduce

$$\langle 0|\,H\,|0\rangle = 0 \tag{96}$$

as a consequence of supersymmetry. Typically in a quantum field theory, the value of the vacuum energy density is given by a complicated sum of vacuum diagrams. In a supersymmetric theory, these diagrams must magically cancel [15]. This is the first of a number of magical cancellations of radiative corrections that we will find in supersymmetric field theories.

3.3 Supersymmetric Lagrangians

At this point, we have determined the general formal properties of supersymmetric field theories. Now it is time to be much more concrete about the form of the Lagrangians which respect supersymmetry. In this section, I will discuss the particle content of supersymmetric theories and present the most general renormalizable supersymmetric Lagrangians for spin-0 and spin-$\frac{1}{2}$ fields.

We argued from (92) that all supersymmetric states of nonzero energy are paired. In particular, this applies to single-particle states, and it implies that supersymmetric models contain boson and fermion fields which are paired in such a way that the particle degrees of freedom are in one-to-one correspondence. In the simple example (81), I introduced a complex scalar field and a left-handed fermion field. Each leads to two sets of single-particle states, the particle and the antiparticle. I will refer to this set of states—a left-handed fermion, its right-handed antiparticle, a complex boson, and its conjugate—as a *chiral supermultiplet*.

Another possible pairing is a a massless vector field and a left-handed fermion, which gives a *vector supermultiplet*—two transversely polarized vector boson states, plus the left-handed fermion and its antiparticle. In conventional field theory, a vector boson obtains mass from the Higgs mechanism by absorbing one degree of freedom from a scalar field. In supersymmetry, the Higgs mechanism works by coupling a vector supermultiplet to a chiral supermultiplet. This coupling results in a massive vector particle, with three polarization states, plus an extra scalar. At the same time, the left-handed fermions in the two multiplets combine through a mass term of the form (78) to give a massive Dirac fermion, with two particle and two antiparticle states. All eight states are degenerate if supersymmetry is unbroken.

More complicated pairings are possible. One of particular importance involves the graviton. Like every other particle in the theory, the graviton must be paired by supersymmetry. Its natural partner is a spin-$\frac{3}{2}$ field called the *gravitino*. In general relativity, the graviton is the gauge field of local coordinate invariance. The gravitino field can also be considered as a gauge field. Since it carries a vector index plus the spinor index carried by ξ or Q, it can have the transformation law

$$\delta_\xi \psi_\mu = \frac{1}{2\pi G_N} \partial_\mu \xi(x) + \cdots \tag{97}$$

which makes it the gauge field of local supersymmetry. This gives a natural relation between supersymmetry and space-time geometry and emphasizes the profound character of this generalization of field theory.

I will now present the most general Lagrangian for chiral supermultiplets. As a first step, we might ask whether we can give a mass to the fields in (81) consistently with supersymmetry. This is accomplished by the Lagrangian

$$\begin{aligned} \mathcal{L} &= \partial_\mu \phi^* \partial^\mu \phi + \psi^\dagger i\overline{\sigma} \cdot \partial \psi + F^\dagger F \\ &\quad + m(\phi F - \frac{1}{2} \psi^T c \psi) + \text{h.c.} \ . \end{aligned} \tag{98}$$

In this expression, I have introduced a new complex field F. However, F has no kinetic energy and does not lead to any new particles. Such an object is called an *auxiliary field*. If we vary the Lagrangian (98) with respect to F, we find the field equations

$$F^\dagger = -m\phi \ , \qquad F = -m\phi^* \ . \tag{99}$$

Thus F carries only the degrees of freedom that are already present in ϕ. We can substitute this solution back into (98) and find the Lagrangian

$$\mathcal{L} = \partial_\mu \phi^* \partial^\mu \phi - m^2 \phi^* \phi + \psi^\dagger i\overline{\sigma} \cdot \partial \psi - \frac{1}{2} m(\psi^T c \psi - \psi^\dagger c \psi^*) \ , \tag{100}$$

which has equal, supersymmetric masses for the bosons and fermions.

It is not difficult to show that the Lagrangian (98) is invariant to the supersymmetry transformation

$$\begin{aligned} \delta_\xi \phi &= \sqrt{2}\xi^T c\psi \\ \delta_\xi \psi &= \sqrt{2} i\sigma\cdot\partial\phi c\xi^* + \xi F \\ \delta_\xi F &= -\sqrt{2} i\xi^\dagger\overline{\sigma}\cdot\partial\psi \ . \end{aligned} \tag{101}$$

The two lines of (98) are invariant separately. For the first line, the proof of invariance is a straightforward generalization of (86). For the second line, we need

$$\begin{aligned} \delta_\xi(\phi F - \frac{1}{2}\psi^T c\psi) &= (\sqrt{2}\xi^T c\psi)F + \phi(-\sqrt{2}i\xi^\dagger\overline{\sigma}\cdot\partial\psi) - \psi^T c(\sqrt{2}i\sigma\cdot\partial\phi c\xi^* + \xi F) \\ &= \sqrt{2}i\xi^\dagger\overline{\sigma}\cdot\partial\psi - \sqrt{2}i\psi^T c\sigma\cdot\partial\phi c\xi^* \\ &= 0 \ . \end{aligned} \tag{102}$$

The first and last terms in the second line cancel by the use of (79); the terms in the third line cancel after an integration by parts and a rearrangement similar to that in (87) in the second term. Thus, (101) is an invariance of (98). With some effort, one can show that this transformation obeys the supersymmetry algebra, in the sense that the commutators of transformations acting on ϕ, ψ, and F follow precisely the relation (88).

The introduction of the auxiliary field F allows us to write a much more general class of supersymmetric Lagrangians. Let ϕ_j, ψ_j, F_j be the fields of a number of chiral supermultiplets indexed by j. Assign each multiplet the supersymmetry transformation laws (101). Then it can be shown by a simple generalization of the discussion just given that the supersymmetry transformation leaves invariant Lagrangians of the general form

$$\begin{aligned} \mathcal{L} &= \partial_\mu\phi_j^*\partial^\mu\phi_j + \psi_j^\dagger i\overline{\sigma}\cdot\partial\psi_j + F_j^\dagger F_j \\ &\quad + (F_j\frac{\partial W}{\partial\phi_j} - \frac{1}{2}\psi_j^T c\psi_k\frac{\partial^2 W}{\partial\phi_j\partial\phi_k}) + \text{h.c.} \ , \end{aligned} \tag{103}$$

where $W(\phi)$ is an analytic function of the complex fields ϕ_j which is called the *superpotential*. It is important to repeat that $W(\phi)$ can have arbitrary dependence on the ϕ_j, but it must not depend on the ϕ_j^*. The auxiliary fields F_j obey the equations

$$F^\dagger = -\frac{\partial W}{\partial\phi_j} \ . \tag{104}$$

If W is a polynomial in the ϕ_j, the elimination of the F_j by substituting (104) into (103) produces polynomial interactions for the scalar fields.

The free massive Lagrangian (98) is a special case of (103) for one supermultiplet with the superpotential

$$W = \frac{1}{2}m\phi^2 \ . \tag{105}$$

A more interesting model is obtained by setting

$$W = \frac{1}{3}\lambda\phi^3 \ . \tag{106}$$

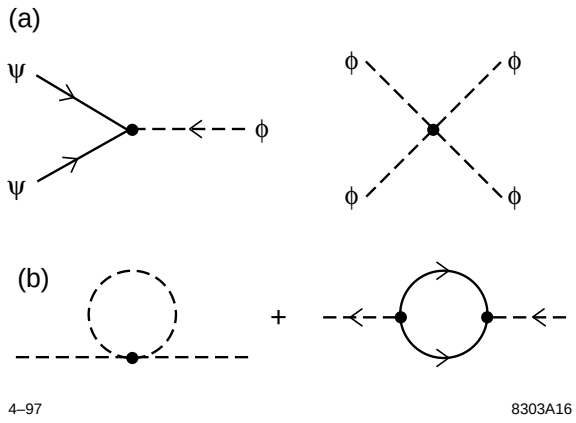

Figure 8: (a) Yukawa and four-scalar couplings arising from the supersymmetric Lagrangian with superpotential (106); (b) Diagrams which give the leading radiative corrections to the scalar field mass term.

In this case, W leads directly to a Yukawa coupling proportional to λ, while substituting for F from (104) yields a four scalar coupling proportional to λ^2:

$$\mathcal{L} = \partial_\mu \phi^* \partial^\mu \phi + \psi^\dagger i \overline{\sigma} \cdot \partial \psi - \lambda^2 |\phi^2|^2 - \lambda[\psi^T c \psi \phi - \phi^* \psi^\dagger c \psi^*] \ . \tag{107}$$

These two vertices are shown in Figure 8(a). Their sizes are such that the two leading diagrams which contribute to the scalar field mass renormalization, shown in Figure 8(b), are of the same order of magnitude. In fact, it is not difficult to compute these diagrams for external momentum $p = 0$. The first diagram has the value

$$-4\lambda^2 i \cdot \int \frac{d^4k}{(2\pi)^4} \frac{i}{k^2} = 4\lambda^2 \int \frac{d^4k}{(2\pi)^4} \frac{1}{k^2} \ . \tag{108}$$

To compute the second diagram, note that the standard form of the fermion propagator is $\left\langle \psi \psi^\dagger \right\rangle$, and be careful to include all minus signs resulting from fermion reordering. Then you will find

$$\begin{aligned} &\frac{1}{2}(-2i\lambda)(2i\lambda) \int \frac{d^4k}{(2\pi)^4} \, \mathrm{tr} \left[\frac{i\sigma \cdot k}{k^2} c (\frac{-i\sigma \cdot k}{k^2})^T c \right] \\ &\qquad = -2\lambda^2 \int \frac{d^4k}{(2\pi)^4} \frac{\mathrm{tr}[\sigma \cdot k \overline{\sigma} \cdot k]}{k^4} \ . \end{aligned} \tag{109}$$

Using (85), the trace gives $2k^2$, and the two diagrams cancel precisely. Thus, the choice (106) presents us with an interacting quantum field theory, but one with exceptional cancellations in the scalar field mass term.

In this simple model, it is not difficult to see that the scalar field mass corrections must vanish as a matter of principle. The theory with superpotential (106) is invariant under the symmetry

$$\phi \to e^{2i\alpha} \phi \ , \qquad \psi \to e^{-i\alpha} \psi \ . \tag{110}$$

This symmetry is inconsistent with the appearance of a fermion mass term $m \psi^T c \psi$, as in (100). The symmetry does not prohibit the appearance of a scalar mass term, but if

the theory is to remain supersymmetric, the scalar cannot have a different mass from the fermion. However, the cancellation of radiative corrections in models of the form (103) is actually much more profound. It can be shown that, in a general model of this type, the only nonvanishing radiative corrections to the potential terms are field rescalings. If a particular coupling—the mass term, a cubic interaction, or any other—is omitted from the original superpotential, it cannot be generated by radiative corrections [16, 17].

For later reference, I will write the potential energy associated with the most general system with a Lagrangian of the form (103). This is

$$V = -F_j^\dagger F_j - F_j \frac{\partial W}{\partial \phi_j} - F_j^\dagger \left(\frac{\partial W}{\partial \phi_j} \right)^* \quad . \tag{111}$$

Substituting for F_j from (104), we find

$$V = \sum_j \left| \frac{\partial W}{\partial \phi_j} \right|^2 \quad . \tag{112}$$

This simple result is called the *F-term* potential. It is minimized by setting all of the F_j equal to zero. If this is possible, we obtain a vacuum state with $\langle H \rangle = 0$ which is also invariant to supersymmetry, in accord with the discussion of (96). On the other hand, supersymmetry is spontaneously broken if for some reason it is not possible to satisfy all of the conditions $F_j = 0$ simultaneously. In that case, we obtain a vacuum state with $\langle H \rangle > 0$.

3.4 Coupling constant unification

At this point, we have not yet completed our discussion of the structure of supersymmetric Lagrangians. In particular, we have not yet written the supersymmetric Lagrangians of vector fields, beyond simply noting that a vector field combines with a chiral fermion to form a vector supermultiplet. Nevertheless, it is not too soon to try to write a supersymmetric generalization of the Standard Model.

I will first list the ingredients needed for this generalization. For each of the $SU(3) \times SU(2) \times U(1)$ gauge bosons, we need a chiral fermion λ^a to form a vector supermultiplet. These new fermions are called *gauginos*. I will refer the specific partners of specific gauge bosons with a tilde. For example, the fermionic partner of the gluon will be called $\widetilde{g}$, the *gluino*, and the fermionic partners of the W^+ will be called $\widetilde{w}^+$, the *wino*.

None of these fermions have the quantum numbers of quarks and leptons. So we need to add a complex scalar for each chiral fermion species to put the quarks and leptons into chiral supermultiplets. I will use the labels for left-handed fermion multiplets in (27) also to denote the quark and lepton supermultiplets. Hopefully, it will be clear from context whether I am talking about the supermultiplet or the fermion. The scalar partners of quarks and leptons are called *squarks* and *sleptons*. I will denote these with a tilde. For example, the partner of $e_L^- = L^-$ is the selectron $\widetilde{e}_L^-$ or $\widetilde{L}^-$. The partner of $\overline{e}^* = e_R^-$ is a distinct selectron which I will call $\widetilde{e}_R^-$. The Higgs fields must also belong to chiral supermultiplets. I will denote the scalar components as h_i and the left-handed fermions as $\widetilde{h}_i$. We will see in a moment that at least two different Higgs multiplets are required.

Although we need a bit more formalism to write the supersymmetric generalization of the Standard Model gauge couplings, it is already completely straightforward to write

the supersymmetric generalization of the Yukawa couplings linking quarks and leptons to the Higgs sector. The generalization of the third line of (1) is given by writing the superpotential

$$W = \lambda_u^{ij} \overline{u}^i h_2 \cdot Q^j + \lambda_d^{ij} \overline{d}^i h_1 \cdot Q^j + \lambda_\ell^{ij} \overline{e}^i h_1 \cdot L^j \tag{113}$$

Note that, where in (1) I wrote ϕ and ϕ^*, I am forced here to introduce two different Higgs fields h_1 and h_2. The hypercharge assignments of $\overline{u}$ and Q require for the first term a Higgs field with $Y = +\frac{1}{2}$; for the next two terms, we need a Higgs field with $Y = -\frac{1}{2}$. Since W must be an analytic function of supermultiplet fields, as I explained below (103), replacing h_1 by $(h_2)^*$ gives a Lagrangian which is not supersymmetric. There is another, more subtle, argument for a second Higgs doublet. Just as in the Standard Model, triangle loop diagrams involving the chiral fermions of the theory contain terms which potentially violate gauge invariance. These anomalous terms cancel when one sums over the chiral fermions of each quark and lepton generation. However, the chiral fermion $\widetilde{h}_2$ leads to a new anomaly term which violates the conservation of hypercharge. This contribution is naturally cancelled by the contribution from $\widetilde{h}_1$.

We still need several more ingredients to construct the full supersymmetric generalization of the Standard Model, but we have now made a good start. We have introduced the minimum number of new particles (unfortunately, this is not a small number), and we have generated new couplings for them without yet introducing new parameters beyond those of the Standard Model.

In addition, we already have enough information to study the unification of forces using the formalism of Section 2.5. To begin, we must extend the formulae (39), (40) to supersymmetric models. For $SU(N)$ gauge theories, the gauginos give a contribution $(-\frac{2}{3}N)$ to the right-hand side of (39). In (40), there is no contribution either from the gauge bosons or from their fermionic partners. We should also group together the contributions from matter fermions and scalars. Then we can write the renormalization group coefficient b_N for $SU(N)$ gauge theories with n_f chiral supermultiplets in the fundamental representation as

$$b_N = 3N - \frac{1}{2} n_f \ . \tag{114}$$

Similarly, the renormalization group coefficient for $U(1)$ gauge theories is now

$$b_1 = -\sum_f t_f^2 \ , \tag{115}$$

where the sum runs over chiral supermultiplets.

Evaluating these expressions for $SU(3) \times SU(2) \times U(1)$ gauge theories with n_g quark and lepton generations and n_h Higgs fields, we find

$$\begin{aligned} b_3 &= 9 - 2n_g \\ b_2 &= 6 - 2n_g - \frac{1}{2} n_h \\ b_1 &= \quad - 2n_g - \frac{3}{10} n_h \ . \end{aligned} \tag{116}$$

Now insert these expressions into (54); for $n_h = 2$, we find

$$B = \frac{5}{7} = 0.714 \ , \tag{117}$$

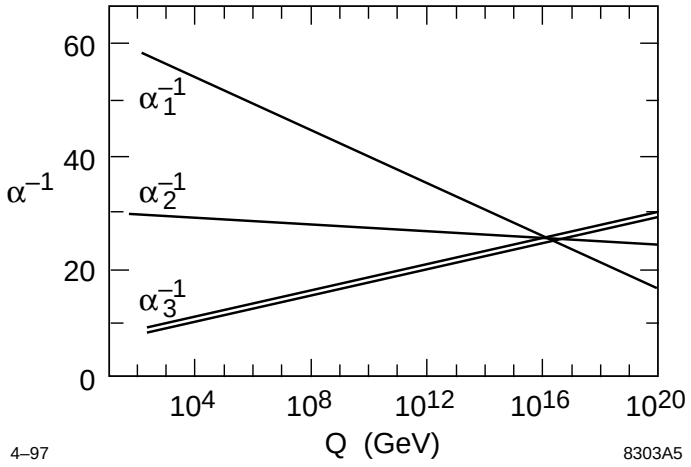

Figure 9: Evolution of the $SU(3) \times SU(2) \times U(1)$ gauge couplings to high energy scales, using the one-loop renormalization group equations of the supersymmetric generalization of the Standard Model.

in excellent agreement with the experimental value (55). Apparently, supersymmetry repairs the difficulty that the Standard Model has in linking in a simple way to grand unification. The running coupling constants extrapolated from the experimental values (52) using the supersymmetric renormalization group equations are shown in Figure 9.

Of course it is not difficult to simply make up a model that agrees with any previously given value of B. I hope to have convinced you that the value (117) arises naturally in grand unified theories based on supersymmetry. By comparing this agreement to the error bars for B quoted in (55), you can decide for yourself whether this agreement is fortuitous.

3.5 The rest of the supersymmetric Standard Model

I will now complete the Lagrangian of the supersymmetric generalization of the Standard Model. First, I must write the Lagrangian for the vector supermultiplet and then I must show how to couple that multiplet to matter fields. After this, I will discuss some general properties of the resulting system.

The vector multiplet (A^a_μ, λ^a) containing the gauge bosons of a Yang-Mills theory and their partners has the supersymmetric Lagrangian

$$\mathcal{L} = -\frac{1}{4}\left(F^a_{\mu\nu}\right)^2 + \lambda^{\dagger a} i\overline{\sigma}^\mu D_\mu \lambda^a + \frac{1}{2}(D^a)^2 \ , \tag{118}$$

where $D_\mu = (\partial_\mu - igA^a_\mu t^a)$ is the gauge-covariant derivative, with t^a the gauge group generator. In order to write the interactions of this multiplet in the simplest form, I have introduced a set of auxiliary real scalar fields, called D^a. (The name is conventional; please do not confuse them with the covariant derivatives.) The gauge interactions of a chiral multiplet are then described by generalizing the first line of (103) to

$$\begin{aligned} \mathcal{L} \ &= \ D_\mu \phi_j^* D^\mu \phi_j + \psi_j^\dagger i\overline{\sigma}^\mu D_\mu \psi_j + F_j^\dagger F_j \\ &\quad -\sqrt{2} ig \left(\phi_j \lambda^{Ta} t^a c \psi_j - \psi^\dagger t^a c \lambda^{*a} \phi_j\right) + g D^a \phi^\dagger t^a \phi \ . \end{aligned} \tag{119}$$

Eliminating the auxiliary fields using their field equation

$$D^a = -g \sum_j \phi^\dagger t^a \phi \tag{120}$$

gives a second contribution to the scalar potential, which should be added to the F-term (112). This is the *D-term*

$$V = \frac{g^2}{2} \left(\sum_j \phi^\dagger t^a \phi \right)^2 \ . \tag{121}$$

As with the F-term, the ground state of this potential is obtained by setting all of the D^a equal to zero, if it is possible. In that case, one obtains a supersymmetric vacuum state with $\langle H \rangle = 0$.

The full supersymmetric generalization of the Standard Model can be written in the form

$$\mathcal{L} = \mathcal{L}_{\rm gauge} + \mathcal{L}_{\rm kin} + \mathcal{L}_{\rm Yukawa} + \mathcal{L}_\mu \ . \tag{122}$$

The first term is the kinetic energy term for the gauge multiplets of $SU(3) \times SU(2) \times U(1)$. The second term is the kinetic energy term for quark, lepton, and Higgs chiral multiplets, including gauge couplings of the form (119). The third term is the Yukawa and scalar interactions given by the second line of (103) using the superpotential (113). The last term is that following from an additional gauge-invariant term that we could add to the superpotential,

$$\Delta W = \mu h_1 \cdot h_2 \ . \tag{123}$$

This term contributes a supersymmetric mass term to the Higgs fields and to their fermions partners. This term is needed on phenomenological grounds, as I will discuss in Section 4.4. The parameter μ is the only new parameter that we have added so far to the Standard Model.

This Lagrangian does not yet describe a realistic theory. It has exact supersymmetry. Thus, it predicts charged scalars degenerate with the electron and massless fermionic partners for the photon and gluons. On the other hand, it has some very attrative properties. For the reasons explained below (110), there is no quadratically divergent renormalization of the Higgs boson masses, or of any other mass in the theory. Thus, the radiative correction (26), which was such a problem for the Standard Model, is absent in this generalization. In fact, the only renormalizations in the theory are renormalizations of the $SU(3) \times SU(2) \times U(1)$ gauge couplings and rescalings of the various quark, lepton, and Higgs fields. In the next section, I will show that we can modify (122) to maintain this property while making the mass spectrum of the theory more realistic.

The Lagrangian (122) conserves the discrete quantum number

$$R = (-1)^{L+Q+2J} \ , \tag{124}$$

where L is the lepton number, $Q = 3B$ is the quark number, and J is the spin. This quantity is called *R-parity*, and it is constructed precisely so that $R = +1$ for the conventional gauge boson, quark, lepton, and Higgs states while $R = -1$ for their supersymmetry partners. If R is exactly conserved, supersymmetric particles can only be produced in pairs,

and the lightest supersymmetric partner must be absolutely stable. On the other hand, R-parity can be violated only by adding terms to $\mathcal{L}$ which violate baryon- or lepton-number conservation.

It is in fact straightforward to write a consistent R-parity-violating supersymmetric theory. The following terms which can be added to the superpotential are invariant under $SU(3) \times SU(2) \times U(1)$ but violate baryon or lepton number:

$$\Delta W = \lambda_B^{ijk} \overline{u}^i \overline{d}^j \overline{d}^k + \lambda_L^{ijk} Q^i \cdot L^j \overline{d}^k + \lambda_e^{ijk} L^i \cdot L^j \overline{e}^k + \mu_L^i L^i \cdot h_2 \ . \tag{125}$$

A different phenomenology is produced if one adds the baryon-number violating couplings λ_B, or if one adds the other couplings written in (125), which violate lepton number. If one were to add both types of couplings at once, that would be a disaster, leading to rapid proton decay.

For a full exploration of the phenomenology of supersymmetric theories, we should investigate both models in which R-parity is conserved, in which the lightest superpartner is stable, and models in which R-parity is violated, in which the lightest superpartner decays through B- or L- violating interactions. In these lectures, since my plan is to present illustrative examples rather than a systematic survey, I will restrict my attention to models with conserved R-parity.

3.6 How to describe supersymmetry breaking

Now we must address the question of how to modify the Lagrangian (122) to obtain a model that could be realistic. Our problem is that the supersymmetry on which the model is based is not manifest in the spectrum of particles we see in Nature. So now we must add new particles or interactions which cause supersymmetry to be spontaneously broken.

It would be very attractive if there were a simple model of supersymmetry breaking that we could connect to the supersymmetric Standard Model. Unfortunately, models of supersymmetry breaking are generally not simple. So most studies of supersymmetry do not invoke the supersymmetry breaking mechanism directly but instead try to treat its consequences phenomenologically. This can be done by adding to (122) terms which violate supersymmetry but become unimportant at high energy. Some time ago, Grisaru and Girardello [18] listed the terms that one can add to a supersymmetric Lagrangian without disturbing the cancellation of quadratic divergences in the scalar mass terms. These terms are

$$\mathcal{L}_{\text{soft}} = -M_j^2 \, |\phi_j|^2 - m_a \lambda^{Ta} c \lambda^a + B\mu h_1 \cdot h_2 + AW(\phi) \ , \tag{126}$$

where W is the superpotential (113), plus other possible analytic terms cubic in the scalar fields ϕ_j. These terms give mass to the squarks and sleptons and to the gauginos, moving the unobserved superpartners to higher energy. Note that terms of the structure $\phi^* \phi \phi$ and the mass term $\psi^T c \psi$ do not appear in (126) because they can regenerate the divergences of the nonsupersymmetric theory. All of the coefficients in (126) have the dimensions of (mass) or (mass)^2. These new terms in (126) are called *soft supersymmetry-breaking terms*. We can build a phenomenological model of supersymmetry by adding to (122) the various terms in $\mathcal{L}_{\text{soft}}$ with coefficients to be determined by experiment.

It is not difficult to understand that it is the new, rather than the familiar, half of the spectrum of the supersymmetric model that obtains mass from (126). In Section 2.5, I argued that the particles we see in high-energy experiments are visible only because they are protected from acquiring very large masses by some symmetry principle . In that discussion, I invoked only the Standard Model gauge symmetries. In supersymmetric models, we have a more complex situation. In each supermultiplet, one particle is protected from acquiring mass, as before, by $SU(2) \times U(1)$. However, their superpartners—the squarks, sleptons, and gauginos—are protected from obtaining mass only by the supersymmetry relation to their partner. Thus, if supersymmetry is spontaneously broken, all that is necessary to generate masses for these partners is a coupling of the supersymmetry-breaking expectation values to the Standard Model supermultiplets.

This idea suggests a general structure for a realistic supersymmetric model. All of the phenomena of the model are driven by supersymmetry breaking. First, supersymmetry is broken spontaneously in some new sector of particles at high energy. Then, the coupling between these particles and the quarks, leptons, and gauge bosons leads to soft supersymmetry-breaking terms for those supermultiplets. It is very tempting to speculate further that those terms might then give rise to the spontaneous breaking of $SU(2) \times U(1)$ and so to the masses for the W and Z and for the quarks and leptons. I will explain in the next section how this might happen.

The size of the mass terms in (126) depends on two factors. The first of these is the mass scale at which supersymmetry is broken. Saying for definiteness that supersymmetry breaking is due to the nonzero value of an F auxiliary field, we can denote this scale by writing $\langle F \rangle$, which has the dimensions of (mass)^2. The second factor is the mass of the bosons or fermions which couple the high-energy sector to the particles of the Standard Model and thus communicate the supersymmetry breaking. I will call this mass $\mathcal{M}$, the *messenger scale*. Then the mass parameters that appear in (126) should be of the order of

$$m_S = \frac{\langle F \rangle}{\mathcal{M}} \ . \tag{127}$$

If supersymmetry indeed gives the mechanism of electroweak symmetry breaking, then m_S should be of the order of 1 TeV. A case that is often discussed in the literature is that in which the messenger is supergravity. In that case, $\mathcal{M}$ is the Planck mass $m_{\rm Pl}$, equal to 10^{19} GeV, and $\langle F \rangle \sim 10^{11}$ (GeV)^2. Alternatively, both $\langle F \rangle$ and $\mathcal{M}$ could be of the order of a few TeV.

The detailed form of the soft supersymmetry-breaking terms depends on the underlying model that has generated them. If one allows these terms to have their most general form (including arbitrary flavor- and CP-violating interactions, they contain about 120 new parameters. However, any particular model of supersymmetry breaking generates a specific set of these soft terms with some observable regularities. One of our goals in Section 4 of these lectures will be to understand how to determine the soft parameters experimentally and thus uncover the patterns which govern their construction.

3.7 Electroweak symmetry breaking from supersymmetry

There is a subtlety in trying to determine the pattern of the soft parameters experimentally. Like all other coupling constants in a supersymmetric theory, these parameters run under the influence of the renormalization group equations. Thus, the true underlying

pattern might not be seen directly at the TeV energy scale. Rather, it might be necessary to extrapolate the measured values of parameters to higher energy to look for regularities.

The situation here is very similar to that of the Standard Model coupling constants. The underlying picture which leads to the values of the $SU(3) \times SU(2) \times U(1)$ coupling constants is not very obvious from the data (52). Only when these data are extrapolated to very high energy using the renormalization group do we see evidence for their unification. Obviously, such evidence must be indirect. On the other hand, the discovery of supersymmetric particles, and the discovery that these particles showed other unification relations—with the same unification mass scale—would give powerful support to this picture.

I will discuss general systematics of the renormalization-group running of the soft parameters in Section 4.2. But there is one set of renormalization group equations that I would like to call your attention to right away. These are the equations for the soft mass of the Higgs boson and the squarks which are most strongly coupled to it. We saw in Section 2.6 that the top quark Yukawa coupling was sufficiently large that it could have an important effect in renormalization group evolution. Let us consider, then, the evolution equations for the three scalars that interact through this coupling, the Higgs boson h_2, the scalar top $\widetilde{Q}_t = \widetilde{t}_L$, and the scalar top $\widetilde{t}_R$. The most important terms in these equations are the following:

$$\begin{aligned}
\frac{d}{d\log Q} M_h^2 &= \frac{1}{(4\pi)^2} \left\{ 3\lambda_t^2 (M_h^2 + M_Q^2 + M_t^2) + \cdots \right\} \\
\frac{d}{d\log Q} M_Q^2 &= \frac{1}{(4\pi)^2} \left\{ 2\lambda_t^2 (M_h^2 + M_Q^2 + M_t^2) - \frac{32}{3} g_3^2 m_3^2 \cdots \right\} \\
\frac{d}{d\log Q} M_t^2 &= \frac{1}{(4\pi)^2} \left\{ 3\lambda_t^2 (M_h^2 + M_Q^2 + M_t^2) - \frac{32}{3} g_3^2 m_3^2 + \cdots \right\} ,
\end{aligned} \tag{128}$$

where g_3 is the QCD coupling, m_3 is the mass of the gluino, and the omitted terms are of electroweak strength. The last two equations exhibit the competition between the top quark Yukawa coupling and QCD renormalizations which we saw earlier in (61) and (64). The supersymmetric QCD couplings cause the masses of the $\widetilde{Q}_t$ and $\widetilde{t}_R$ to increase at low energies, while the effect of λ_t causes all three masses to decrease.

Indeed, if the $\widetilde{Q}_t$ and $\widetilde{t}_R$ masses stay large, the equations (128) predict that M_h^2 should go down through zero and become negative [19]. Thus, if all scalar mass parameters are initially positive at high energy scales, these equations imply that the Higgs boson h_2 will acquire a negative parameter and thus an instability to electroweak symmetry breaking. An example of the solution to the full set of renormalization group equations, exhibiting the instability in M_h^2, is shown in Figure 10 [20].

At first sight, it might have been any of the scalar fields in the theory whose potential would be unstable by renormalization group evolution. But the Higgs scalar h_2 has the strongest instability if the top quark is heavy. In this way, the supersymmetric extension of the Standard Model naturally contains the essential feature that we set out to find, a physical mechanism for electroweak symmetry breaking. As a bonus, we find that this mechanism is closely associated with the heaviness of the top quark.

If you have been patient through all of the formalism I have presented in this section, you now see that your patience has paid off. It was not obvious when we started that

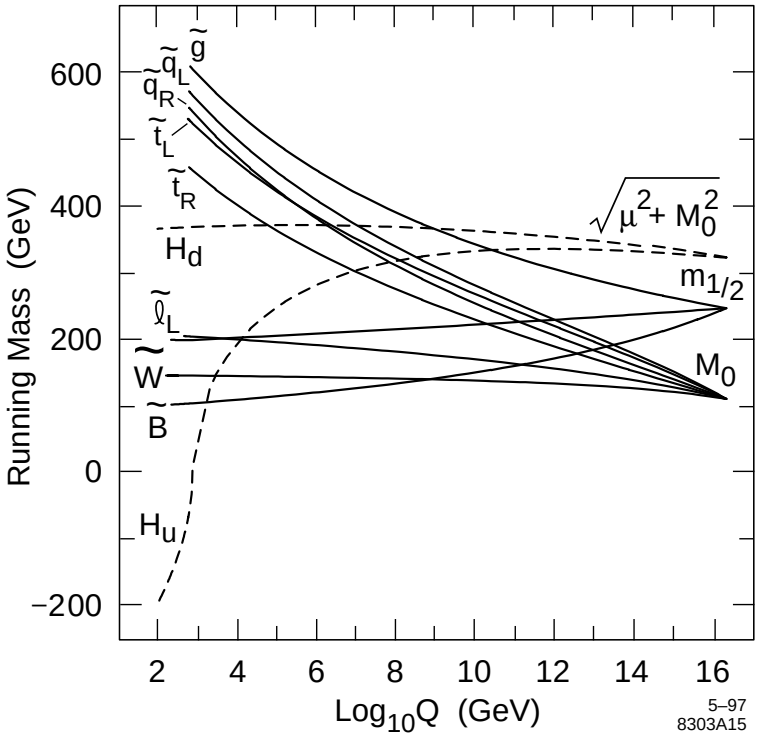

Figure 10: Example of the evolution of the soft supersymmetry-breaking mass terms from the grand unification scale to the weak interaction scale, from [20]. The initial conditions for the evolution equations at the grand unification scale are taken to be the universal among species, in a simple pattern presented in Section 4.2.

supersymmetry would give the essential ingredients of a theory of electroweak symmetry breaking. But it turned out to be so. In the next section, I will present more details of the physics of supersymmetric models and present a program for their experimental exploration.

4. Supersymmetry: Experiments

In the previous section, I have presented the basic formalism of supersymmetry. I have also explained that supersymmetric models have several features that naturally answer questions posed by the Standard Model. At the beginning of Section 3, I told you that supersymmetry might be considered a worked example of physics beyond the Standard Model. Though I doubt you are persuaded by now that physics beyond the Standard Model must be supersymmetric, I hope you see these models as reasonable alternatives that can be understood in very concrete terms.

Now I would like to analyze the next step along this line of reasoning. What if, at LEP 2 or at some higher-energy machine, the superpartners appear? This discovery would change the course of experimental high-energy physics and shape it along a certain direction. We should then ask, what will be the important issues in high-energy physics, and how will we resolve these issues experimentally? In this section, I will give a rather detailed answer to this question.

I emphasize again that I am not asking you to become a believer in supersymmetry. A different discovery about physics beyond the Standard Model would change the focus

of high-energy physics in a different direction. But we will learn more by choosing a particular direction and studying its far-reaching implications than by trying to reach vague but general conclusions. I will strike off in a different direction in Section 5.

On the other hand, I hope you are not put off by the complexity of the supersymmetric Standard Model. It is true that this model has many ingredients and a very large content of new undiscovered particles. On the other hand, the model develops naturally from a single physical idea. I argued in Section 2.2 that this structure, a complex phenomenology built up around a definite principle of physics, is seen often in Nature. It leads to a more attractive solution to the problems of the Standard Model than a model whose only virtue is minimality.

It is true that, in models with complex consequences, it may not be easy to see the underlying structure in the experimental data. This is the challenge that experimenters will face. I will now discuss how we can meet this challenge for the particular case in which the physics beyond the Standard Model is supersymmetric.

4.1 More about soft supersymmetry breaking

As we discussed in Section 3.6, a realistic supersymmetric theory has a Lagrangian of the form

$$\mathcal{L} = \mathcal{L}_{\rm gauge} + \mathcal{L}_{\rm kin} + \mathcal{L}_{\rm Yukawa} + \mathcal{L}_{\mu} + \mathcal{L}_{\rm soft} \ . \tag{129}$$

Of the various terms listed here, the first three contain only couplings that are already present in the Lagrangian of the Standard Model. The fourth term contains one new parameter μ. The last term, however, contains a very large number of new parameters.

I have already explained that one should not be afraid of seeing a large number of undetermined parameters here. The same proliferation of parameters occurs in any theory with a certain level of complexity when viewed from below. The low-energy scattering amplitudes of QCD, for example, contain many parameters which turn out to be the masses and decay constants of hadronic resonances. If it is possible to measure these parameters, we will obtain a large amount of new information.

In thinking about the values of the soft supersymmetry-breaking parameters, there are two features that we should take into account. The first is that the soft parameters obey renormalization group equations. Thus, they potentially change significantly from their underlying values at the messenger scale defined in (127) to their physical values observable at the TeV scale. We have seen in Section 3.7 that these changes can have important physical consequences. In the next section, I will describe the renormalization group evolution of the supersymmetry-breaking mass terms in more detail, and we will use our understanding of this evolution to work out some general predictions for the superparticle spectrum.

The second feature is that there are strong constraints on the flavor structure of soft supersymmetry breaking terms which come from constraints on flavor-changing neutral current processes. In (126), I have written independent mass terms for each of the scalar fields. In principle, I could also have written mass terms that mixed these fields. However, if we write the scalars in the basis in which the quark masses are diagonalized, we must not find substantial off-diagonal terms. A mixing

$$\Delta\mathcal{L} = \Delta M_d^2 \overline{s}^\dagger \overline{d} \ , \tag{130}$$

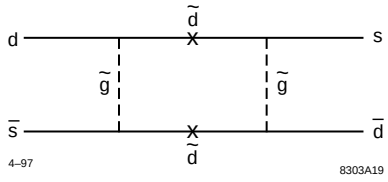

Figure 11: A potentially dangerous contribution of supersymmetric particles to flavor-changing neutral current processes.

for example, would induce an excessive contribution to the K_L–K_S mass difference through the diagram shown in Figure 11 unless

$$\frac{\Delta M_d^2}{M_d^2} < 10^{-2} \left(\frac{M_d}{300 \text{ GeV}} \right)^2 \ . \tag{131}$$

Similar constraints arise from D–$\overline{D}$ mixing, B–$\overline{B}$ mixing, $\mu \to e\gamma$ [21].

The strength of the constraint (131) suggests that the physical mechanism that generates the soft supersymmetry breaking terms contains a natural feature that suppresses such off-diagonal terms. One possibility is that equal soft masses are generated for all scalars with the same $SU(2) \times U(1)$ quantum numbers. Then the scalar mass matrix is proportional to the matrix **1** and so is diagonal in any basis [22, 23]. Another possibility is that, by virtue of discrete flavor symmetries, the scalar mass matrices are approximately diagonal in the same basis in which the quark mass matrix is diagonal [24]. These two solutions to the potential problem of supersymmetric flavor violation are called, respectively, 'universality' and 'alignment'. A problem with the alignment scenario is that the bases which diagonalize the u and d quark mass matrices differ by the weak mixing angles, so it is not possible to completely suppress the mixing both for the u and d partners. This scenario then leads to a prediction of D–$\overline{D}$ mixing near the current experimental bound.

4.2 The spectrum of superparticles—concepts

We are now ready to discuss the expectations for the mass spectrum of supersymmetric partners. Any theory of this spectrum must have two parts giving , first, the generation of the underlying soft parameters at the messenger scale and , second, the modification of these parameters through renormalization group evolution. In this section, I will make the simplest assumptions about the underlying soft parameters and concentrate on the question of how these parameters are modified by the renormalization group. In the next section, we will confront the question of how these simple assumptions can be tested.

Let us begin by considering the fermionic partners of gauge bosons, the gauginos. If the messenger scale lies above the scale of grand unification, the gauginos associated with the $SU(3) \times SU(2) \times U(1)$ gauge bosons will be organized into a single representation of the grand unification group and thus will have a common soft mass term. This gives a very simple initial condition for renormalization group evolution.

The renormalization group equation for a gaugino mass m_i is

$$\frac{d}{d \log Q} m_i = -\frac{1}{(4\pi)^2} \cdot 2b_i \cdot m_i \ , \tag{132}$$

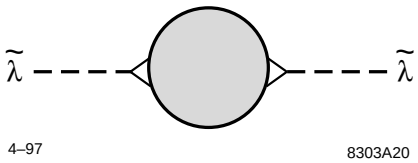

Figure 12: A simple radiative correction giving gaugino masses in the pattern of 'gaugino unification'.

where $i = 3, 2, 1$ for the gauginos of $SU(3) \times SU(2) \times U(1)$ and b_i is the coefficient in the equation (38) for the coupling constant renormalization. Comparing these two equations, we find that $m_i(Q)$ and $\alpha_i(Q)$ have the same renormalization group evolution, and so their ratio is constant as a function of Q. This relation is often written

$$\frac{m_i(Q)}{\alpha_i(Q)} = \frac{m_{1/2}}{\alpha_U} \ , \tag{133}$$

where α_U is the unification value of the coupling constant ($\alpha_U^{-1} = 24$), and $m_{1/2}$ is the underlying soft mass parameter. As the α_i flow from their unified value at very large scales to their observed values at $Q = m_Z$, the gaugino masses flow along with them. The result is that the grand unification of gaugino masses implies the following relation among the observable gaugino masses:

$$\frac{m_1}{\alpha_1} = \frac{m_2}{\alpha_2} = \frac{m_3}{\alpha_3} \ . \tag{134}$$

I will refer to this relation as *gaugino unification*. It implies that, for the values at the weak scale,

$$\frac{m_1}{m_2} = 0.5 \ , \qquad \frac{m_3}{m_2} = 3.5 \ . \tag{135}$$

I caution you that these equations apply to a perturbative (for example, $\overline{MS}$) definition of the masses. For the gluino mass m_3, the physical, on-shell, mass may be larger than the $\overline{MS}$ mass by 10–20%, due to a radiative correction which depends on the ratio of the masses of the gluon and quark partners [25].

Though gaugino unification is a consequence of the grand unification of gaugino masses, it does not follow uniquely from this source. On the contrary, this result can also follow from models in which gaugino masses arise from radiative corrections at lower energy. For example, in a model of Dine, Nelson, Nir, and Shirman [26], gaugino masses are induced by the diagram shown in Figure 12, in which a supersymmetry-breaking expectation value of F couples to some new supermultiplets of mass roughly 100 TeV, and this influence is then tranferred to the gauginos through their Standard Model gauge couplings. As long as the mass pattern of the heavy particles is sufficiently simple, we obtain gaugino masses m_i proportional to the corresponding α_i, which reproduces (134).

Now consider the masses of the squarks and sleptons, the scalar partners of quarks and leptons. We saw in Section 3.4 that, since the left- and right-handed quarks belong to different supermultiplets Q, $\overline{u}$, $\overline{d}$, each has its own scalar partners. The same situation applies for the leptons. In this section, I will assume for maximum simplicity that the underlying values of the squark and slepton mass parameters are completely universal, with the value M_0. This is a stronger assumption than the prediction of grand unification,

and one which does not necessarily have a fundamental justification. Nevertheless, there are two effects that distort this universal mass prediction into a complex particle spectrum.

The first of these effects comes from the D-term potential (121). Consider the contributions to this potential from the Higgs fields h_1, h_2 and from a squark or slepton field $\tilde{f}$. Terms contributing to the $\tilde{f}$ mass comes from the D^a terms associated with the $U(1)$ and the neutral $SU(2)$ gauge bosons,

$$\begin{aligned} V &= \frac{g'^2}{2}\left(h_1^*(-\frac{1}{2})h_1 + h_2^*(\frac{1}{2})h_2 + \tilde{f}^* Y \tilde{f}\right)^2 \\ &\quad + \frac{g^2}{2}\left(h_1^*\tau^3 h_1 + h_2^*\tau^3 h_2 + \tilde{f}^* I^3 \tilde{f}\right)^2 \ . \end{aligned} \tag{136}$$

The factors in the first line are the hypercharges of the fields h_1, h_2. Now replace these Higgs fields by their vacuum expectation values

$$\langle h_1 \rangle = \frac{1}{\sqrt{2}}\begin{pmatrix} v\cos\beta \\ 0 \end{pmatrix} \qquad \langle h_2 \rangle = \frac{1}{\sqrt{2}}\begin{pmatrix} 0 \\ v\sin\beta \end{pmatrix} \tag{137}$$

and keep only the cross term in each square. This gives

$$\begin{aligned} V &= 2\frac{g'^2}{2}\frac{v^2}{2}\left(-\frac{1}{2}\cos^2\beta + \frac{1}{2}\sin^2\beta\right)\tilde{f}^* Y \tilde{f} + 2\frac{g^2}{2}\frac{v^2}{2}\left(+\frac{1}{2}\cos^2\beta - \frac{1}{2}\sin^2\beta\right)\tilde{f}^* I^3 \tilde{f} \\ &= -c^2 m_Z^2(\sin^2\beta - \cos^2\beta)\tilde{f}^*(I^3 - \frac{s^2}{c^2}Y)\tilde{f} \\ &= -m_Z^2(\sin^2\beta - \cos^2\beta)\tilde{f}^*(I^3 - s^2 Q)\tilde{f} \ . \end{aligned} \tag{138}$$

Thus, this term gives a contribution to the scalar mass

$$\Delta M_f^2 = -m_Z^2 \frac{\tan^2\beta - 1}{\tan^2\beta + 1}(I^3 - s^2 Q) \ . \tag{139}$$

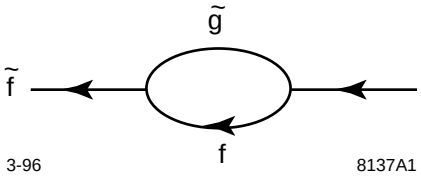

Figure 13: Renormalization of the soft scalar mass due to the gaugino mass.

The second effect is the renormalization group running of the scalar mass induced by the gluino mass through the diagram shown in Figure 13. The renormalization group equation for the scalar mass M_f is

$$\frac{d}{d\log Q}M_f = -\frac{1}{(4\pi)^2}\cdot 8 \cdot \sum_i C_2(r_i) g_i^2 m_i^2 \ , \tag{140}$$

where

$$C_2(r_i) = \begin{cases} \frac{3}{5}Y^2 & U(1) \\ 0, \ \frac{3}{4} & \text{singlets, doublets of } SU(2) \\ 0, \ \frac{4}{3} & \text{singlets, triplets of } SU(3) \end{cases} \ . \tag{141}$$

In writing this equation, I have ignored the Yukawa couplings of the flavor f. This is a good approximation for light flavors, but we have already seen that it is not a good approximation for the top squarks, and it may fail also for the b and τ partners if $\tan\beta$ is large. In those cases, one must add further terms to the renormalization group equations, such as those given in (128).

To integrate the equation (140), we need to know the behavior of the gaugino masses as a function of Q. Let me assume that this is given by gaugino unification according to (133). Then

$$\frac{g_i^2 m_i^2}{4\pi} = \alpha_i(Q) \cdot \frac{\alpha_i^2(Q) m_i(\mathcal{M})}{\alpha_{i\mathcal{M}}^2} = \alpha_i^3(Q) \cdot \frac{m_2}{\alpha_2^2} \ . \tag{142}$$

where $\alpha_{i\mathcal{M}}$ is the value of α_i at the messenger scale, and the quantities at the extreme right are to be evaluated at the weak interaction scale. If we inserting this expression into (140) and taking the evolution of $\alpha_i(Q)$ to be given by (51), the right-hand side of (140) is given as an explicit function of Q. To integrate the equation from messenger scale to the weak scale, we only need to evaluate

$$\begin{aligned} \int_{m_Z}^{\mathcal{M}} d\,\log Q\, \alpha_i^3(Q) &= \int_{m_Z}^{\mathcal{M}} d\,\log Q \frac{\alpha_{i\mathcal{M}}^3}{(1+(b_i/2\pi)\alpha_{i\mathcal{M}}\log(Q/\mathcal{M}))^3} \\ &= \frac{2\pi}{b_i\alpha_{i\mathcal{M}}} \frac{\alpha_{i\mathcal{M}}^3}{(1+(b_i/2\pi)\alpha_{i\mathcal{M}}\log(Q/\mathcal{M}))^2}\Big|_{m_Z}^{\mathcal{M}} \\ &= \frac{2\pi}{b_i}(\alpha_i^2 - \alpha_{i\mathcal{M}}^2) \end{aligned} \tag{143}$$

Then, assembling the renormalization group and D-term contributions, the physical scalar mass at the weak interaction scale is given by

$$M_f^2 = M_0^2 + \sum_i \frac{2}{b_i} C_2(r_i)\, \frac{\alpha_i^2 - \alpha_{i\mathcal{M}}^2}{\alpha_2^2}\, m_2^2 + \Delta M_f^2 \ . \tag{144}$$

The term in (144) induced by the renormalization group effect is not simple, but it is also not so difficult to understand. It is amusing that it is quite similar in form to the formula one would find for a one-loop correction from a diagram of the general structure shown in Figure 13. Indeed, in the model of Dine, Nelson, Nir, and Shirman referred to above, for which the messenger scale is quite close to the weak interaction scale, the computation of radiative corrections gives the simple result

$$M_f^2 = \sum_i 2C_2(r_i) \frac{\alpha_i^2}{\alpha_2^2} m_2^2 + \Delta M_f^2 \ , \tag{145}$$

where, in this formula, the quantity m_2/α_2 is simply the mass scale of the messenger particles. The formulae (144) and (145) do differ quantitatively, as we will see in the next section.

The equations (133) and (144) give a characteristic evolution from the large scale $\mathcal{M}$ down to the weak interaction scale. The colored particles are carried upward in mass by a large factor, while the masses of color-singlet sleptons and gauginos change by a smaller amount. The effects of the top Yukawa coupling discussed in Section 3.7 add to these mass shifts, lowering the masses of the top squarks and sending the (mass)^2 of the Higgs field h_2 down through zero. These observations explain all of the basic qualitative features of the evolution which we saw illustrated in Figure 10.

4.3 The spectrum of superparticles—diagnostics

Now that we understand the various effects that can contribute to the superpartner masses, we can try to analyze the inverse problem: Given a set of masses observed experimentally, how can we read the pattern of the underlying mass parameters and determine the value of the messenger scale? In this section, I will present some general methods for addressing this question.

This question of the form of the underlying soft-supersymmetry breaking parameters requires careful thought. If supersymmetric particles are discovered at LEP 2 or LHC, this will become the most important question in high-energy physics. It is therefore important not to trivialize this question or to address it only in overly restrictive contexts. In reading the literature on supersymmetry experiments at colliders, it is important to keep in mind the broadest range of possibilities for the spectrum of superparticles. Be especially vigilant for code-words such as 'the minimal SUGRA framework' [27] or 'the Monte Carlo generator described in [93]' [28] which imply the restriction to the special case in which M_0 is universal and $\mathcal{M}$ is close to the Planck mass.

Nevertheless, in this section, I will make some simplifying assumptions. If the first supersymmetric partners are not found a LEP 2, the D-term contribution (139) is a small correction to the mass formula. In any event, I will ignore it from here on. Since this term is model-independent, it can in principle be computed and subtracted if the value of $\tan\beta$ is known. (It is actually not so easy to measure $\tan\beta$; a collection of methods is given in [29].) In addition, I will ignore the effects of weak-scale radiative corrections. These are sometimes important and can distort the overall pattern unless they are subtracted correctly [30].

I will also assume, in my description of the spectrum of scalars, that the spectrum of gauginos is given in terms of m_2 by gaugino unification. As I have explained in the previous section, gaugino unification is a feature of the simplest schemes for generating the soft supersymmetry-breaking masses both when $\mathcal{M}$ is very large and when it is relatively small. However, there are many more complicated possibilities. The assumption of gaugino unification can be tested experimentally, as I will explain in Section 4.5. This is an essential part of any experimental investigation of the superparticle spectrum. If the assumption is not valid, that also affects the interpretation of the spectrum of scalar particles. In particular, the renormalization effects included in the various curves shown in this section must be recomputed using the correct mass relations among the three gauginos.

Once the gaugino masses are determined, we can ask about the relation between the mass spectrum of gauginos and that of scalars. To analyze this relation, it is useful to form the 'Dine-Nelson plot', that is, the plot of

$$\frac{M_f}{m_2} \quad \text{against} \quad C \equiv \left[\sum_i C_2(r_i) \frac{\alpha_i^2}{\alpha_2^2} \right]^{1/2} , \tag{146}$$

suggested by (145). Some sample curves on this plot are shown in Figure 14. The quantity C takes on only five distinct values, given by the $SU(3) \times SU(2) \times U(1)$ quantum numbers of $\overline{e}$, L, $\overline{d}$, $\overline{u}$, and Q. These are indicated in the figure as vertical dashed lines. (The values of C for $\overline{d}$ and $\overline{u}$ are almost identical. The dot-dash line is the prediction of (145). The solid lines are the predictions of the renormalization group term in (144) for $\mathcal{M} = 100$ TeV, 2×10^{16} GeV (the grand unification scale), and 10^{18} GeV (the superstring scale).

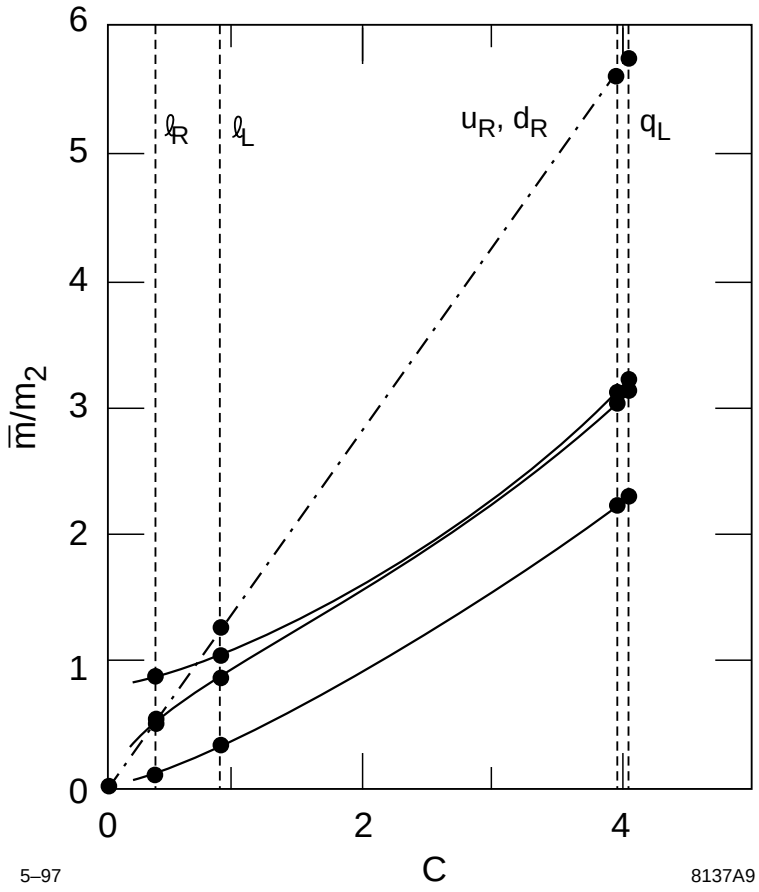

Figure 14: The simplest predictions for the mass spectrum of squarks and sleptons, expressed on the Dine-Nelson plot (146). The dot-dashed curve is the prediction of (145); the solid curves show the effect of renormalization-group evolution with (from bottom to top) $\mathcal{M} = 10^5$ GeV, 2×10^{16} GeV, 10^{18} GeV.

With this orientation, it is interesting to ask how a variety of models of supersymmetry breaking appear in this presentation. In Figure 15, I show the Dine-Nelson plot for a collection of models from the literature discussed in [31]. The highest solid curve from Figure 14 has been retained for reference. The model in the upper left-hand corner is the 'minimal SUGRA' model with a universal M_0 at the Planck scale. In this case, the dashed curve lies a constant distance in m^2 above the solid curve. The model in the upper right-hand corner is that of [26] with renormalization-group corrections properly included. The model in the bottom right-hand corner gives an example of the alignment scenario of [24]. The plot is drawn in such a way as to suggest that, the underlying soft scalar masses tend to zero for the first generation of quarks and leptons. This behavior could be discovered experimentally with the analysis I have suggested here.

It is interesting that the various models collected in Figure 15 look quite different to the eye in this presentation. This fact gives me confidence that, if we could actually measure the mass parameters needed for this analysis, those data would provide us with incisive information on the physics of the very large scales of unification and supersymmetry breaking.

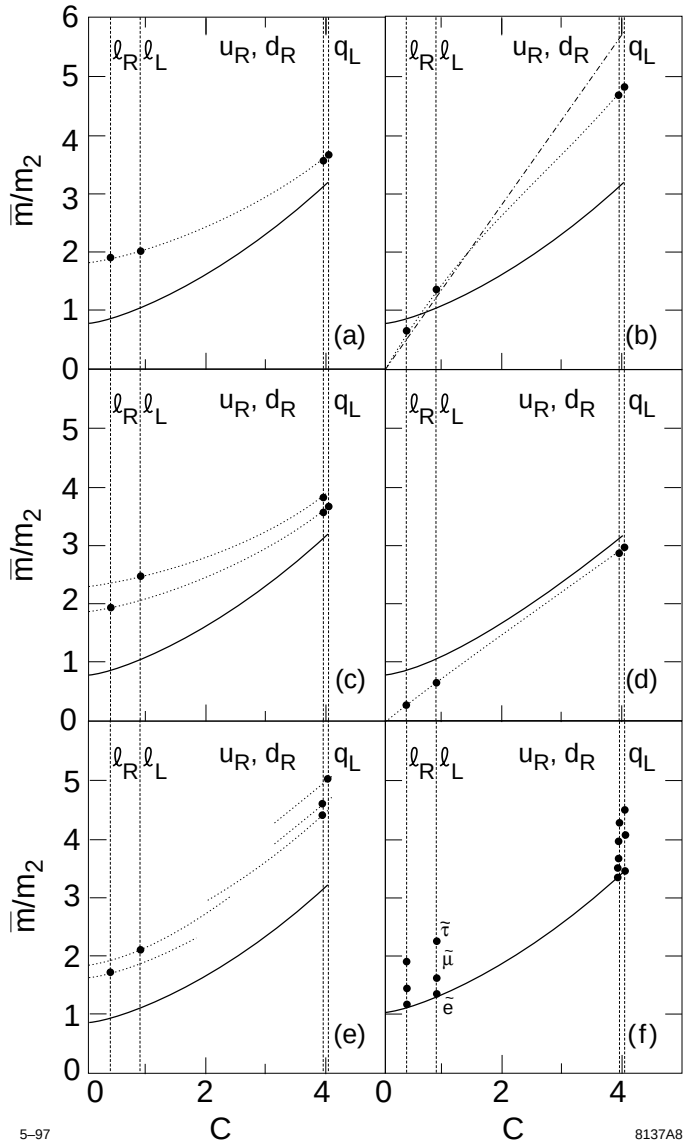

Figure 15: Scalar spectrum predicted in a number of theoretical models of supersymmetry breaking, as displayed on the Dine-Nelson plot, from [31].

4.4 The superpartners of W and Higgs

Now that we have framed the problem of measuring the mass spectrum of superparticles, we must address the question of how this can be done. What are the signatures of the presence of supersymmetric particles, and how can we translate from the characteristics of observable processes to the values of the parameters of which determine the supersymmetry spectrum?

I will discuss the signatures and decay schemes for superparticles in the next section. First, though, we must discuss a complication which needs to be taken into account in this phenomenology.

After $SU(2) \times U(1)$ symmetry-breaking, any two particles with the same color, charge, and spin can mix. Thus, the spin-$\frac{1}{2}$ supersymmetric partners of the W bosons and the charged Higgs bosons can mix with one another. Similarly, the partners of the γ, Z^0, h_1^0, and h_2^0 enter into a 4×4 mixing problem.

Consider first the mixing problem of the charged fermions. The mass terms for these fermions arise from the gaugino-Higgs coupling in (119), the soft gaugino mass term in (126), and the fermion mass term arising from the superpotential (123). The relevant terms from the Lagrangian are

$$\begin{aligned} \Delta\mathcal{L} &= -\sqrt{2} i \frac{g}{2} \left(h_2^0 \widetilde{w}^{-T} c \widetilde{h}_2^+ - \widetilde{h}_1^{-T} c \widetilde{w}^+ h_1^0 \right) \\ &\quad - m_2 \widetilde{w}^{-T} c \widetilde{w}^+ + \mu \widetilde{h}_1^{-T} c \widetilde{h}_2^+ \ . \end{aligned} \tag{147}$$

If we replace h_1^0 and h_2^0 by their vacuum expectation values in (137), these terms take the form

$$\Delta\mathcal{L} = -\left(\widetilde{w}^- \quad i\widetilde{h}_1^- \right)^T c \, \mathbf{m} \begin{pmatrix} \widetilde{w}^+ \\ i\widetilde{h}_2^+ \end{pmatrix} \ , \tag{148}$$

where $\mathbf{m}$ is the mass matrix

$$\mathbf{m} = \begin{pmatrix} m_2 & \sqrt{2} m_W \sin\beta \\ \sqrt{2} m_W \cos\beta & \mu \end{pmatrix} \tag{149}$$

The physical massive fermions are the eigenstates of this mass matrix. They are called *charginos*, $\widetilde{\chi}_{1,2}^{\pm}$, where 1 labels the lighter state. More precisely, the charginos $\widetilde{\chi}_1^+$, $\widetilde{\chi}_2^+$ are the linear combinations that diagonalize the matrix $\mathbf{m}^\dagger\mathbf{m}$, and $\widetilde{\chi}_1^-$, $\widetilde{\chi}_2^-$ are the linear combinations that diagonalize the matrix $\mathbf{m}\mathbf{m}^\dagger$.

The diagonalization of the matrix (149) is especially simple in the limit in which the supersymmetry parameters m_2 and μ are large compared to m_W. In the region $\mu > m_2 \gg m_W$, $\widetilde{\chi}_1^+$ is approximately $\widetilde{w}^+$, with mass $m_1 \approx m_2$, while $\widetilde{\chi}_2^+$ is approximately $\widetilde{h}_2^+$, with mass $m_2 \approx \mu$. For $m_2 > \mu \gg m_W$, the content of $\widetilde{\chi}_1^+$ and $\widetilde{\chi}_2^+$ reverses. More generally, we refer to the region of parameters in which $\widetilde{\chi}_1^+$ is mainly $\widetilde{w}^+$ as the *gaugino region*, and that in which $\widetilde{\chi}_1^+$ is mainly $\widetilde{h}_2^+$ as the *Higgsino region*. If charginos are found are LEP 2, it is quite likely that they may be mixtures of gaugino and Higgsino; however, the region of parameters in which the charginos are substantially mixed decreases as the mass increases. The contours of constant $\widetilde{\chi}_1^+$ mass in the (μ, m_2) plane, for $\tan\beta = 4$ are shown in Figure 16.

An analysis similar to that leading to (149) gives the mass matrix of the neutral fermionic partners. This is a 4×4 matrix acting on the vector $(\widetilde{b}, \widetilde{w}^3, i\widetilde{h}_1^0, i\widetilde{h}_2^0)$, where $\widetilde{b}$

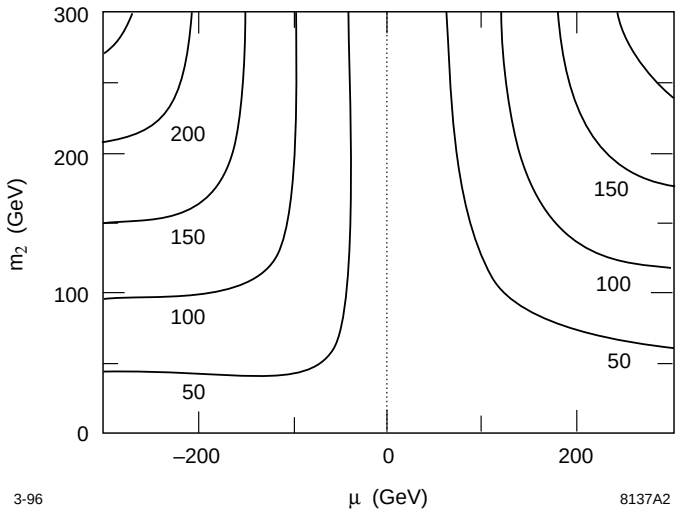

Figure 16: Contours of fixed chargino mass in the plane of the mass parameters (μ, m_2), computed for $\tan\beta = 4$.

and $\widetilde{w}^3$ are the partners of the $U(1)$ and the neutral $SU(2)$ gauge boson. In this basis, the mass matrix takes the form

$$\mathbf{m} = \begin{pmatrix} m_1 & 0 & -m_Z s\cos\beta & m_Z s\sin\beta \\ 0 & m_2 & m_Z c\cos\beta & -m_Z c\sin\beta \\ -m_Z s\cos\beta & m_Z c\cos\beta & 0 & -\mu \\ m_Z s\sin\beta & -m_Z c\sin\beta & -\mu & 0 \end{pmatrix} . \qquad (150)$$

The linear combinations which diagonalize this matrix are called *neutralinos*, $\widetilde{\chi}_1^0$ through $\widetilde{\chi}_4^0$ from lowest to highest mass. The properties of these states are similar to those of the charginos. For example, in the gaugino region, $\widetilde{\chi}_1^0$ is mainly $\widetilde{b}$ with mass m_1, and $\widetilde{\chi}_2^0$ is mainly $\widetilde{w}^3$, with mass m_2.

Note that, when $\mu = 0$, the neutralino mass matrix (150) has an eigenvector with zero eigenvalue $(0, 0, \sin\beta, \cos\beta)$. In addition, the vector $(0, 0, \cos\beta, -\sin\beta)$ has a relatively small mass $m_\chi \sim m_Z^2/m_2$. This situation is excluded by the supersymmetry searches at LEP 1, for example, [32]. Thus, we are required on phenomenological grounds to include the superpotential (123) with a nonzero value of μ. It is also important to note that, with the 'minimal SUGRA' assumptions used in many phenomenological studies, it is easiest to arrange electroweak symmetry breaking through the renormalization group mechanism discussed in Section 3.7 if μ is of order $m_3 \approx 3.5 m_2$. Thus, this set of assumptions typically leads to the gaugino region of the chargino-neutralino physics.

4.5 Decay schemes of superpartners

With this information about the mass eigenstates of the superpartners, we can work out their decay schemes and, from this, their signatures. As I have explained at the end of Section 3.5, I restrict this discussion to the situation in which R-parity, given by (124), is conserved and so the lightest supersymmetric partner is stable. In most of this discussion, I will assume that this stable particle is the lightest neutralino $\widetilde{\chi}_1^0$. The neutralino is a massive but weakly-interacting particle. It would not be observed directly

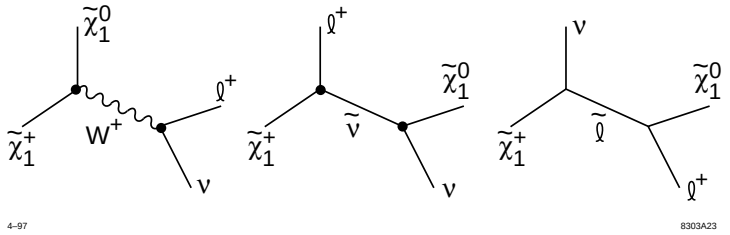

Figure 17: Diagrams leading to the decay of the chargino $\widetilde{\chi}_1^+$ to the 3-body final state $\ell^+\nu\widetilde{\chi}_1^0$. The chargino can decay to $u\overline{d}\widetilde{\chi}_1^0$ by similar processes.

in a detector at a high-energy collider but rather would appear as missing energy and unbalanced momentum.

In this context, we can discuss the decays of specific superpartners. Clearly, the lighter superpartners will have the simplest decays, while the heavier superpartners will decay to the lighter ones. Since heavy squarks and sleptons often decay to charginos and neutralinos, it is convenient to begin with these.

The decay pattern of the lighter chargino depends on its field content and, in particular, on whether its parameters lie in the gaugino region or the Higgsino region. In the gaugino region, the lighter chargino is mainly $\widetilde{w}^+$, with mass m_2. The second neutralino is almost degenerate, but the first neutralino has mass $m_1 = 0.5m_2$, assuming gaugino unification. If $m_2 > 2m_W$, the decay $\widetilde{\chi}_1^+ \to W^+\widetilde{\chi}_1^0$ typically dominates. If m_2 is smaller, the chargino decays to 3-body final states through the diagrams shown in Figure 17, and through the analogous diagrams involving quarks. The last two diagrams involve virtual sleptons. If the slepton mass is large, the branching ratio to quarks versus leptons is the usual color factor of 3. However, if the sleptons are light, the branching ratio to leptons may be enhanced.

In the Higgsino region, the chargino $\widetilde{\chi}_1^+$ and the two lightest neutralinos $\chi 1$, $\chi 2$ are all roughly degenerate at the mass μ. The first diagram in Figure 17 dominates in this case, but leads to only a small visible energy in the $\ell^+\nu$ or $u\overline{d}$ system.

The decay schemes of the second neutralino $\widetilde{\chi}_2^0$ are similar to those of the chargino. Since supersymmetry models typically have a light neutral Higgs boson h^0, the decay $\widetilde{\chi}_2^0 \to \widetilde{\chi}_1^0 h^0$ may be important. If neither this process nor the on-shell decay to Z^0 are allowed, the most important decays are the 3-body processes such as $\widetilde{\chi}_2^0 \to \widetilde{\chi}_1^0 q\overline{q}$. The process $\widetilde{\chi}_2^0 \to \widetilde{\chi}_1^0 \ell^+\ell^-$ is particularly important at hadron colliders, as we will see in Section 4.8.

Among the squarks and sleptons, we see from Figure 15 that the $\widetilde{e}_R^-$ of each generation is typically the lightest. This particle couples to $U(1)$ but not $SU(2)$ and so, in the gaugino region, it decays through $\widetilde{e}_R^- \to e\widetilde{\chi}_1^0$. On the other hand, the partners $\tilde{L}$ of the left-handed leptons prefer to decay to $\ell\widetilde{\chi}_2^0$ or $\nu\widetilde{\chi}_1^+$ if these modes are open.

It is a typical situation that the squarks are heavier than the gluino. For example, the renormalization group term in (144), with $\mathcal{M}$ of the order of the unification scale, already gives a contribution equal to $3m_2$. In that case, the squarks decay to the gluino, $\widetilde{q} \to q\widetilde{g}$. If the gluinos are heavier, then, in the gaugino region, the superpartners of the right-handed quarks decay dominantly to $q\widetilde{\chi}_1^0$, while the partners of the left-handed quarks

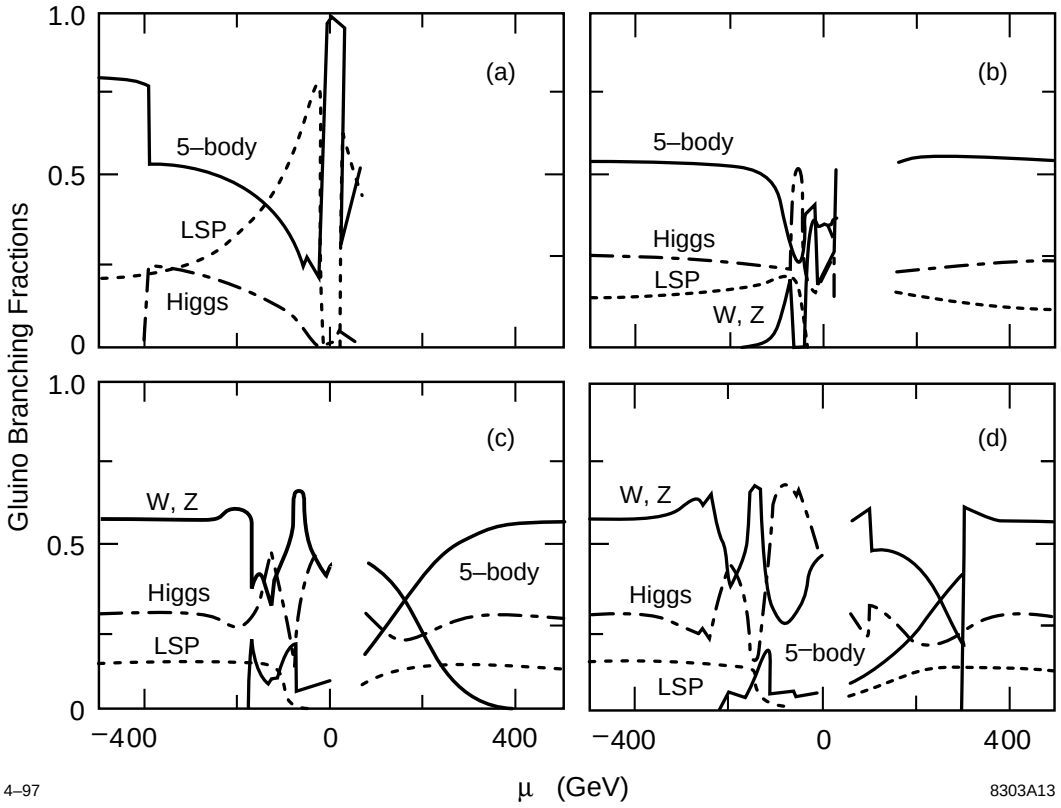

Figure 18: Branching fractions for gluino decay in the various classes of final states possible for $m(\tilde{g}) < m(\tilde{q})$, from [34]. The four graphs correspond to the gluino masses (a) 120 GeV, (b) 300 GeV, (c) 700 GeV, (d) 1000 GeV. The branching fractions are given as a function of μ with m_2 determined from the gluino mass by the gaugino unification relation (133).

prefer to decay to $q\widetilde{\chi}_2^0$ or $q\widetilde{\chi}_1^+$.

If the squarks and gluinos are much heavier than the color-singlet superpartners, their decays can be quite complex, including cascades through heavy charginos, neutralinos, and Higgs bosons [33, 34, 35]. Figure 18 shows the branching fractions of the gluino as a function of μ, assuming gaugino unification and the condition that the squarks are heavier than the gluino. The boundaries apparent in the figure correspond to the transition from the gaugino region (at large $|\mu|$) to the Higgsino region. The more complex decays indicated in the figure can be an advantage in hadron collider experiments, because they lead to characteristic signatures such as multi-leptons or direct Z^0 production in association with missing transverse momentum. On the other hand, as the dominant gluino decay patterns become more complex, the observed inclusive cross sections depend more indirectly on the underlying supersymmetry parameters.

Up to now, I have been assuming that the lightest superpartner is the $\widetilde{\chi}_1^0$. However, there is an alternative possibility that is quite interesting to consider. According to Goldstone's theorem, when a continuous symmetry is spontaneously broken, a massless particle appears as a result. In the most familiar examples, the continuous symmetry transforms the internal quantum numbers of fields, and the massless particle is a Goldstone boson. If the spontaneously broken symmetry is coupled to a gauge boson, the

Goldstone boson combines with the gauge boson to form a massive vector boson; this is the Higgs mechanism. Goldstone's theorem also applies to the spontaneous breaking of supersymmetry, but in this case the massless particle is a Goldstone fermion or *Goldstino*. Then it would seem that the Goldstino should be the lightest superpartner into which all other superparticles decay?

To analyze this question, we need to know two results from the theory of the Goldstino. Both have analogues in the usual theory of Goldstone bosons. I have already pointed out in (97) that the gravitino, the spin-$\frac{3}{2}$ supersymmetric partner of the graviton, acts as the gauge field of local supersymmetry. This particle can participate in a supersymmetric version of the Higgs mechanism. If supersymmetry is spontaneously broken by the expectation value of an F term, the gravitino and the Goldstino combine to form a massive spin-$\frac{3}{2}$ particle with mass

$$m_\psi = \frac{\langle F \rangle}{\sqrt{3} m_{\text{ Pl}}} \ , \tag{151}$$

where $m_{\text{ Pl}}$ is the Planck mass. Notice that, if the messenger scale $\mathcal{M}$ is of the order of $m_{\text{ Pl}}$, this mass scale is of the order of the scale m_S of soft supersymmetry-breaking mass terms given in (127). In fact, in this case, the massive gravitino is typically heavier than the $\widetilde{\chi}_1^0$. On the other hand, if $\mathcal{M}$ is of order 100 TeV, with $\langle F \rangle$ such that the superparticle masses are at the weak interaction scale, m_ψ is of order 10^{-2} eV and so is much lighter than any of the superpartners we have discussed above.

The second result bears on the probability for producing Goldstinos. The methods used to analyze pion physics in QCD generalize to this case and predict that the Goldstino $\widetilde{G}$ is produced through the effective Lagrangian

$$\Delta\mathcal{L} = \frac{1}{\langle F \rangle} j_\mu^T c \partial^\mu \widetilde{G} \tag{152}$$

where $\langle F \rangle$ is the supersymmetry-breaking vacuum expectation value in (151) and j_μ is the conserved current associated with supersymmetry. Integrating by parts, this gives a coupling for the vertex $\widetilde{f} \to f \widetilde{G}$ proportional to

$$\frac{\Delta m}{\langle F \rangle} \ , \tag{153}$$

where Δm is the supersymmetry-breaking mass difference between f and $\widetilde{f}$. If the Goldstino becomes incorporated into a massive spin-$\frac{3}{2}$ field, this does not affect the production amplitude, as long as the Goldstinos are emitted at energies large compared to their mass. I will discuss this point for the more standard case of a Goldstone boson in Section 5.3. This result tells us that, if the messenger scale $\mathcal{M}$ is of order $m_{\text{ Pl}}$ and $\langle F \rangle$ is connected with $\mathcal{M}$ through (127), the rate for the decay of any superpartner to the Goldstino is so slow that it is irrelevant in accelerator experiments. On the other hand, if $\mathcal{M}$ is less than 100 TeV, decays to the Goldstino can become relevant.

For the case of the coupling of the $\widetilde{b}$, the superpartner of the $U(1)$ gauge boson, to the photon and Z^0 fields, the effective Lagrangian (152) takes the more explicit form

$$\Delta\mathcal{L} = \frac{m_1}{\langle F \rangle} \widetilde{b}^\dagger \sigma^{\mu\nu} (c F_{\mu\nu} - s Z_{\mu\nu}) \widetilde{G} \ . \tag{154}$$

This interaction leads to the decay $\widetilde{b} \to \gamma\widetilde{G}$ with lifetime [36]

$$c\tau = (0.1 \text{ mm}) \left(\frac{100 \text{ GeV}}{m_1}\right)^5 \left(\frac{\langle F \rangle^{1/2}}{100 \text{ TeV}}\right)^4 . \tag{155}$$

It is difficult to estimate whether the value of $c\tau$ resulting from (155) should be meters or microns. But this argument does predict that, if the $\widetilde{\chi}_1^0$ is the lightest superpartner of Standard Model particles, all decay chains should end with the decay of the $\widetilde{\chi}_1^0$ to $\gamma\widetilde{G}$. If the lifetime (155) is short, each $\widetilde{\chi}_1^0$ momentum vector, which we visualized above as missing energy, should be realized instead as missing energy plus a direct photon.

It is also possible in this case of small $\langle F \rangle$ that the lightest sleptons $\widetilde{e}_R^-$ could be lighter than the $\widetilde{\chi}_1^0$. If these particles are the lightest superparticles, they lead to an unacceptable cosmological abundance of stable charged matter. This problem disappears, however, if they can decay to the Goldstino. In that case, all supersymmetric decay chains terminate with leptons and missing energy, for example,

$$\widetilde{\chi}_1^0 \to \ell^- \widetilde{\ell}_R^+ \to \ell^- \ell^+ \widetilde{G} . \tag{156}$$

From here on, I will concentrate on the most straightforward case in which the $\widetilde{\chi}_1^0$ is the lightest superparticle and is stable over the time scales observable in collider experiments. However, it is important to keep these alternative phenomenologies in mind when you are actually looking for superparticle signatures in the data.

4.6 The mass scale of supersymmetry

At last, we have all the background we require to discuss the experiments which will detect and study supersymmetric particles at colliders. In this section, I would like to recapitulate the general ideas that we have formulated for this study. I will also note the implication of the these idea for the mass range of supersymmetric particles. If the picture of supersymmetry that I have constructed here is correct, the supersymmetric particles should be discovered at planned, or even at the present, accelerators.

Although the mass scale of supersymmetry depends on many parameters and is in principle adjustible over a large range, there is a good reason to expect to find supersymmetric particles relatively near at hand. As I have discussed in Section 3.7, supersymmetry provides a mechanism for electroweak symmetry breaking. If we assume that this indeed is the mechanism of supersymmetry breaking, the W and Z masses must be masses characteristic of the scale of soft supersymmetry-breaking parameters. Alternatively, m_W can only be much less than m_S in (127) by virtue of an unnatural cancellation or fine-tuning of parameters. This possibility has been studied quantitatively in a number of theoretical papers [37, 38, 39], with the conclusion that the relation between m_W and m_S is natural (by the authors' definitions) only when

$$m_2 < 3m_W . \tag{157}$$

Of course, it is possible that the mechanism of electroweak symmetry breaking does not involve supersymmetry. In that case, there might still be supersymmetry at a very high scale (to satisfy aesthetic arguments or to aid in the quantization of gravity), but in this case supersymmetry would not be relevant to experimental high-energy physics.

The schemes for the supersymmetric mass spectrum discussed in Sections 4.2 and 4.3 give a definite expectation for the ordering of states. The gaugino unification relation predicts that the gluino is the heaviest of the gauginos, with the on-shell gluino mass satisfying

$$m(\tilde{g}) \sim 4m_2 \ . \tag{158}$$

Our results were much less definitive about the mass relations of the squarks and sleptons. Roughly, though,

$$m(\tilde{q}) \sim (2-6) \cdot m(\tilde{\ell}) \ , \quad \text{and} \quad m(\tilde{\ell}) \sim m_2 \ , \tag{159}$$

in the models discussed in Section 4.3.

The relations (157)–(159) predict that we should find charginos below 250 GeV in mass and gluinos below 1 TeV. This mass region is not very far away. The LEP 2 and Tevatron experimental programs will cover almost half of this parameter space in the next five years. The LHC can probe for supersymmetric particles up to masses about a factor 3 beyond the region predicted by the relations above, and an e^+e^- linear collider with up to 1.5 TeV in the center of mass would have a roughly equivalent reach.

Search strategies for supersymmetric particles depend on the detailed properties of the model. But in general, assuming R-parity conservation and the identification of $\widetilde{\chi}_1^0$ as the lightest superparticle, the basic signature of supersymmetry is new particle production associated with missing energy. In collider experiments, we would typically be looking for a multi-jet or multi-lepton final state, together with the characteristic missing transverse momentum or acoplanarity.

Because I would like to continue in a somewhat different direction, I will not describe in detail the techniques and strategies for the discovery of supersymmetry at these colliders. The search strategies for various supersymmetric particles at LEP 2 are described in [40]. Experimental strategies for discovering supersymmetry at the Tevatron are reviewed in [41], together with an estimation of the reach in the mass spectrum.

It is important to point out, though, that if the phenomenology of supersymmetry follows the general lines I have laid out here, it will be discovered, at the latest, by the LHC. The cross sections for LHC signatures of supersymmetry involving multiple leptons and direct Z^0 production associated with missing transverse energy are shown in Figure 19 [35]. These cross sections are very large, of order 100 fb, for example, for the like-sign dilepton signal, at a collider that is designed to produce an event sample of 100 fb^{-1} per year per detector. Supersymmetry can also be seen by looking for events with large jet activity and missing transverse momentum. A sample comparison of signal and background for an observable that measures the jet activity is shown in Figure 20 [42]. The authors of this analysis conclude that, at the LHC, the major backgrounds to supersymmetry reactions do not come from Standard Model background processes but rather from other supersymmetry reactions.

That prospect is enticing, but it is only the beginning of an experimental research program on supersymmetry. We have seen that the theory of the supersymmetry spectrum is complex and subtle. The investigation of supersymmetry should allow us to measure this spectrum. That in turn will give us access to the soft supersymmetry-breaking parameters, which are generated at very short distances and which therefore should hold information about the very deep levels of fundamental physics. So it is important to investigate to

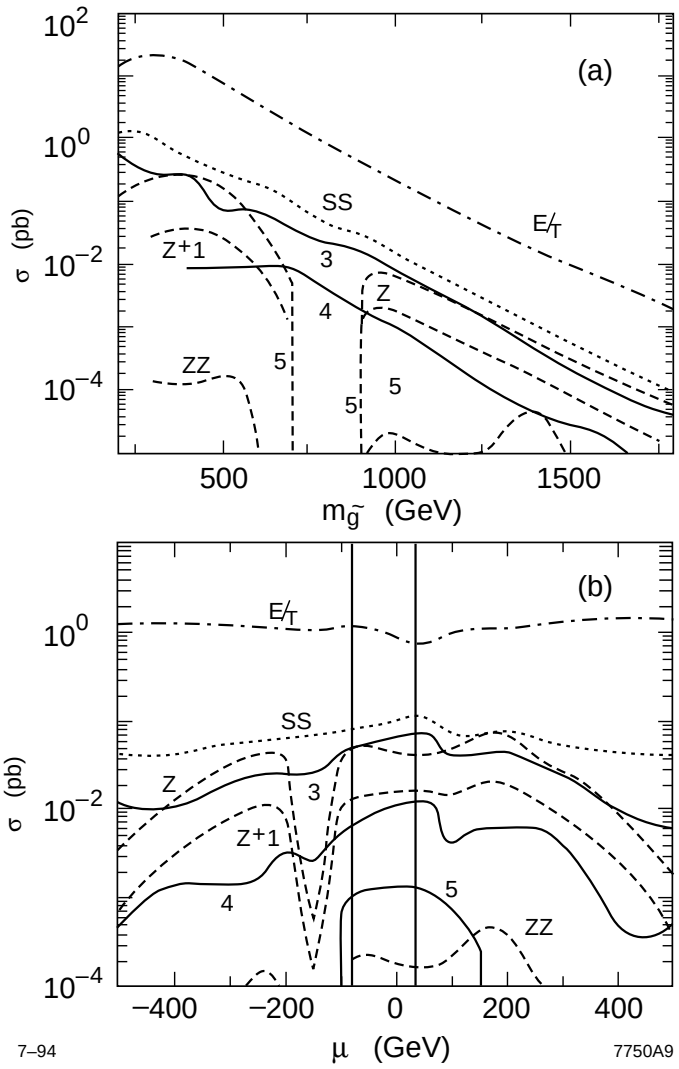

Figure 19: Cross sections for various signatures of supersymmetric particle production at the LHC, from from [35]. The observables studied are, from top to bottom, missing E_T, like-sign dileptons, multi-leptons, and $Z+$ leptons. The top graph plots the cross sections as a function of $m(\tilde{g})$ for $m(\tilde{q}) = 2m(\tilde{g})$, and $\mu = -150$ GeV, and m_2 given by gaugino unification. The bottom graph, plotted for $m(\tilde{g}) = 750$ GeV as a function of μ, shows the model-dependence of the cross sections.

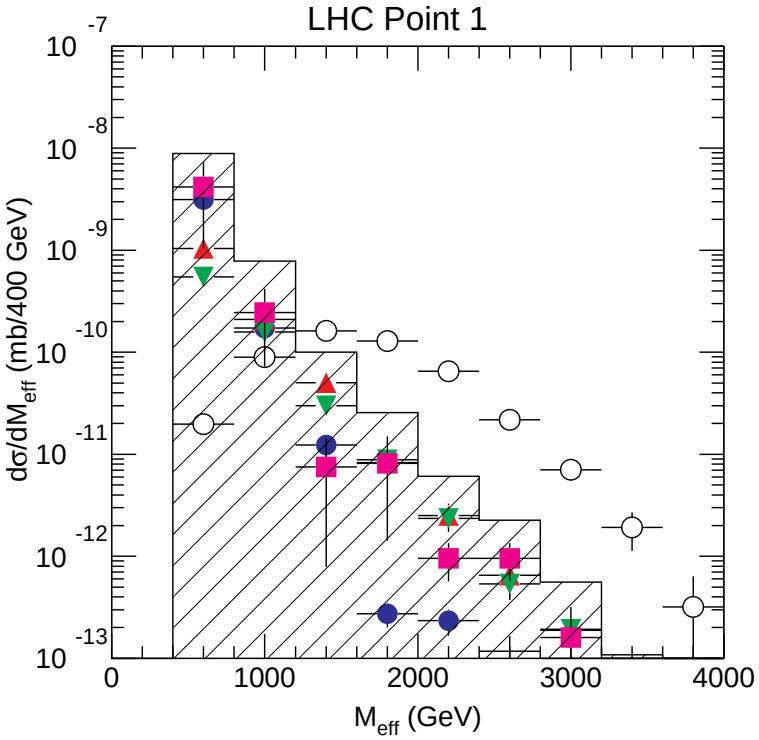

Figure 20: Simulation of the observation of supersymmetric particle production at the LHC, from [42], at a point in parameter space with $m(\tilde{g}) = 1$ TeV. The observable M_{eff} is given by the sum of the missing E_T and the sum of the E_T values for the four hardest jets. The supersymmetry signal is shown as the open circles. Among the backgrounds, the squares are due to QCD processes, and the other points shown are due to W, Z, and t production.

what extent these experimental measurements are actually feasible using accelerators that we can foresee.

In discussing this question, I will assume, pessimistically, that the scale of supersymmetry is relatively high, and so I will concentrate on experiments for the high-energy colliders of the next generation, the LHC and the e^+e^- linear collider discussed in the introduction. As a byproduct, this approach will illustrate the deep analytic power that both of these machines can bring to bear on new physical phenomena.

4.7 Superspectroscopy at e^+e^- colliders

I will start this discussion of supersymmetry measurements from the side of e^+e^- colliders. It is intuitively clear that, if we had an e^+e^- collider operating in the energy region appropriate to supersymmetric particle production, some precision measurements could be made. But I have stressed that the soft supersymmetry-breaking Lagrangian can contain a very large number of parameters which become intertwined in the mass spectrum. Thus, it is important to ask, is there a set of measurements which extracts and disentangles these parameters? I will explain now how to do that.

I do not wish to imply, with this approach, that precision supersymmetry measurements are possible only at e^+e^- colliders. In fact, the next section will be devoted to precision information that can be obtained from hadron collider experiments. And, indeed,

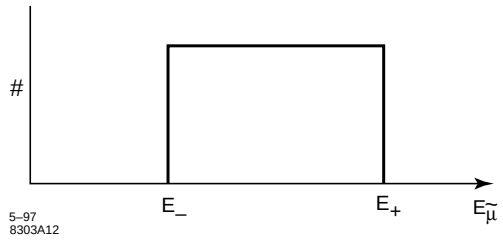

Figure 21: Schematic energy distribution in a slepton or squark decay, allowing a precision supersymmetry mass measurement at an e^+e^- collider.

to justify the construction of an e^+e^- linear collider, it is necessary to show that the e^+e^- machine adds significantly to the results that will be available from the LHC. Nevertheless, it has pedagogical virtue to begin from the e^+e^- side, because the e^+e^- experiments allow a completely systematic approach to the issues of parameter determination. I will return to the question of comparing e^+e^- and pp colliders in Section 4.9.

To begin, let me review some of the parameters of future e^+e^- colliders. Cross sections for e^+e^- annihilation decreases with the center-of-mass energy as $1/E^2_{\rm CM}$. Thus, to be effective, a future collider must provide a data sample of 20-50 fb^{-1}/year at an center of mass energy of 500 GeV, and a data sample increasing from this value as $E^2_{\rm CM}$ at higher energies. The necessary luminosities are envisioned in the machine designs [43]. Though new sources of machine-related background appear, the experimental environment is anticipated to be similar to that of LEP [44]. An important feature of the experimental arrangement not available at LEP is an expected 80–90% polarization of the electron beam. We will see in a moment that this polarization provides a powerful physics analysis tool.

The simplest supersymmetry analyses at e^+e^- colliders involve e^+e^- annihilation to slepton pairs. Let $\tilde\mu_R$ denote the second-generation $\tilde e^-_R$. This particle has a simple decay $\tilde\mu_R \to \mu\tilde\chi^0_1$, so pair-production of $\tilde\mu_R$ results in a final state with $\mu^+\mu^-$ plus missing energy. The production process is simple s-channel annihilation through a vitual γ and Z^0; thus, the cross section and polarization asymmetry are characteristic of the standard model quantum numbers of the $\tilde\mu_R$ and are independent of the soft supersymmetry-breaking parameters.

It is straightforward to measure the mass of the $\tilde\mu_R$, and the method of this analysis can be applied to many other examples. Because the $\tilde\mu_R$ is a scalar, it decays isotropically to its two decay products. When we transform to the lab frame, the distribution of μ energies is flat between the kinematic endpoints, as indicated in Figure 21. The endpoints occur at

$$E_\pm = (1 \pm \beta)\gamma\mathcal{E} \ , \tag{160}$$

with $\beta = (1 - 4m(\tilde\mu)^2/E^2_{\rm CM})^{1/2}$, $\gamma = E_{\rm CM}/2m(\tilde\mu)$, and

$$\mathcal{E} = \frac{m(\tilde\mu)^2 - m(\tilde\chi^0_1)^2}{2m(\tilde\mu^2)} \ . \tag{161}$$

Given the measured values of $E_\pm$, one can solve algebraically for the mass of the parent $\tilde\mu_R$ and the mass of the missing particle $\tilde\chi^0_1$. Since many particles have two-body decays to the $\tilde\chi^0_1$, this mass can be determined redundantly. For heavy supersymmetric particles, the

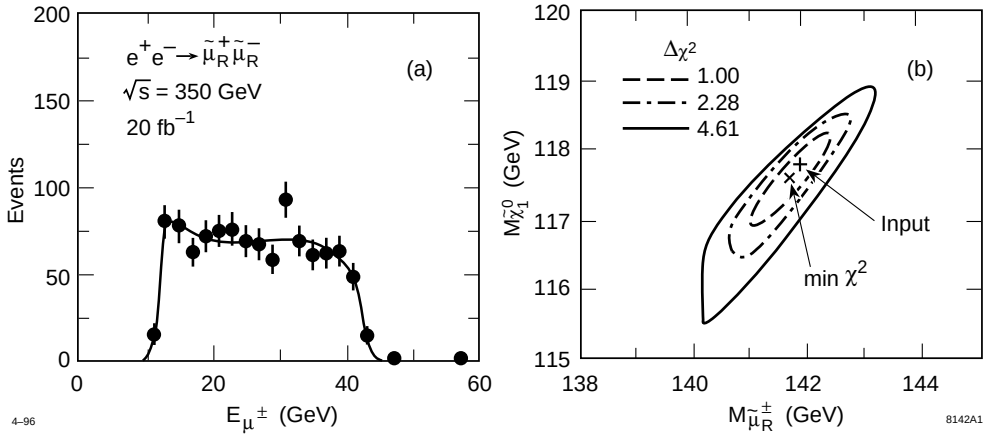

Figure 22: Simulation of the $\tilde{\mu}_R$ mass measurement at an e^+e^- linear collider, from [45]. The left-hand graph gives the event distribution in the decay muon energy. The right-hand graph shows the χ^2 contours as a function of the masses of the parent $\tilde{\mu}_R$ and the daughter $\tilde{\chi}_1^0$.

lower endpoint may sometimes be obscured by background from cascade decays through heavier charginos and neutralinos. So it is also interesting to note that, once the mass of the $\tilde{\chi}_1^0$ is known, the mass of the parent particle can be determined from the measurement of the higher endpoint only.

A simulation of the $\tilde{\mu}_R$ mass measurement done by the JLC group [45] is shown in Figure 22. The simulation assumes 95% right-handed electron polarization, which essentially eliminates the dominant background $e^+e^- \to W^+W^-$, but even with 80% polarization the endpoint discontinuities are clearly visible. The measurement gives the masses of $\tilde{\mu}_R$ and $\tilde{\chi}_1^0$ to about 1% accuracy. As another example of this technique, Figure 23 shows a simulation by the NLC group [44] of the mass measurement of the $\tilde{\nu}$ in $\tilde{\nu} \to e^-\tilde{\chi}_1^+$.

To go beyond the simple mass determinations, we can look at processes in which the production reactions are more complex. Consider, for example, the pair-production of the first-generation $\tilde{e}_R^-$. The production goes through two Feynman diagrams, which are shown in Figure 24. Because the $\tilde{\chi}_1^0$ is typically light compared to other superparticles, it is the second diagram that is dominant, especially at small angles. By measuring the forward peak in the cross section, we obtain an additional measurement of the lightest neutralino mass, and a measurement of its coupling to the electron. We have seen in (119) that the coupling of $\tilde{b}$ to $e^+\tilde{e}_R^-$ is proportional to the standard model $U(1)$ coupling g'. Thus, this information can be used to determine one of the neutralino mixing angles. Alternatively, if we have other diagnostics that indicate that the neutralino parameters are in the gaugino region, this experiment can check the supersymmmetry relation of couplings. For a 200 GeV $\tilde{e}_R^-$, with a 100 fb^{-1} data sample at 500 GeV, the ratio of couplings can be determined to 1% accuracy [46].

Notice that the neutralino exchange diagram in Figure 24 is present only for $e_R^-e_L^+ \to \tilde{e}_R^-\tilde{e}_R^+$, since $\tilde{e}_R^-$ is the superpartner of the right-handed electron. On the other hand, with the initial state $e_L^-e_R^+$, we have the analogous diagram producing the superpartner of the left-handed electron $\tilde{L}^-$. In the gaugino region, the process $e_L^-e_R^+ \to \tilde{L}^-\tilde{L}^+$ has large contributions both from $\tilde{\chi}_1^0$ ($\tilde{b}$) exchange and from $\tilde{\chi}_2^0$ ($\tilde{w}^3$) exchange. The reaction $e_L^-e_L^+ \to$

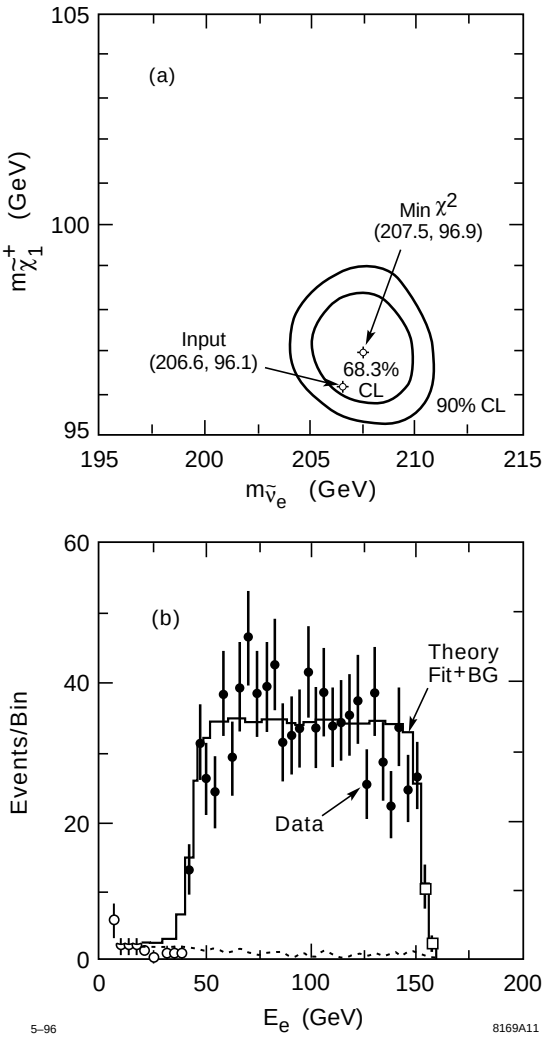

Figure 23: Simulation of the $\widetilde{\nu}$ mass measurement at an e^+e^- linear collider, from [44]. The bottom graph gives the event distribution in the decay electron energy. The top graph shows the χ^2 contours as a function of the masses of the parent $\widetilde{\nu}$ and the daughter $\widetilde{\chi}_1^+$.

$\widetilde{L}^-\widetilde{e}_R^+$ is also mediated by neutralino exchange and contains additional useful information.

Along with the sleptons, the chargino $\widetilde{\chi}_1^+$ is expected to be a relatively light particle which is available for precision measurements at an e^+e^- collider. The dominant decays of the chargino are $\widetilde{\chi}_1^+ \to q\overline{q}\widetilde{\chi}_1^0$ and $\widetilde{\chi}_1^+ \to \ell^+\nu\widetilde{\chi}_1^0$, leading to events with quark jets, leptons, and missing energy. In mixed hadron-lepton events, one chargino decay can be analyzed as a two-body decay into the observed $q\overline{q}$ system plus the unseen neutral particle $\widetilde{\chi}_1^0$; then the mass measurement technique of Figure 21 can be applied. The simulation of a sample measurement, using jet pairs restricted to an interval around 30 GeV in mass, is shown in Figure 25 [44]. The full data sample (50 fb^{-1} at 500 GeV) gives the $\widetilde{\chi}_1^+$ mass to an accuracy of 1% [47].

The diagrams for chargino pair production are shown in Figure 26. The cross section depends strongly on the initial-state polarization. If the $\widetilde{\nu}$ is very heavy, it is permissible to ignore the second diagram; then the first diagram leads to a cross section roughly ten times larger for e_L^- than for e_R^-. If the $\widetilde{\nu}$ is light, this diagram interferes destructively to

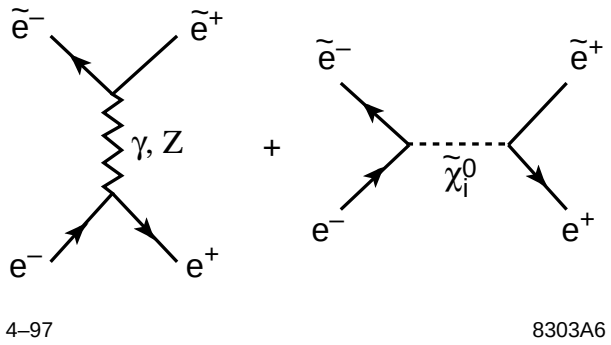

Figure 24: Feynman diagrams for the process of selectron pair production.

lower the cross section.

For a right-handed electron beam, the second diagram vanishes. Then there is an interesting connection between the chargino production amplitude and the values of the chargino mixing angles [45]. Consider first the limit of very high energy, $E^2_{\rm CM} \gg m_Z^2$. In this limit, we can ignore the Z^0 mass and consider the virtual gauge bosons in the first diagram to be the $U(1)$ and the neutral $SU(2)$ bosons. But the e_R^- does not couple to the $SU(2)$ gauge bosons. On the other hand, the W^+ and $\tilde{w}^+$ have zero hypercharge and so do not couple to the $U(1)$ boson. Thus, at high energy, the amplitude for $e_R^- e^+ \to \tilde{\chi}_1^+ \tilde{\chi}_1^-$ is nonzero only if the charginos have a Higgsino component and is, in fact, proportional to the chargino mixing angles. Even if we do not go to asymptotic energies, this polarized cross section is large in the Higgsino region and small in the gaugino region, as shown in Figure 27. This information can be combined with the measurement of the forward-backward asymmetry to determine both of the chargino mixing angles in a manner independent of the other supersymmetry parameters [48].

If the study with e_R^- indicates that the chargino parameters are in the gaugino region, measurement of the differential cross section for $e_L^- e^+ \to \tilde{\chi}_1^+ \tilde{\chi}_1^-$ can be used to determine the magnitude of the second diagram in Figure 26. The value of this diagram can be used to estimate the $\tilde{\nu}$ mass or to test another of the coupling constant relations predicted by supersymmetry. With a 100 fb^{-1} data sample, the ratio between the $\tilde{w}^+ \tilde{\nu} e_L^-$ coupling and the $W^+ \nu e_L^-$ coupling can be determined to 25% accuracy if $m(\tilde{\nu})$ must also be determined by the fit, and to 5% if $m(\tilde{\nu})$ is known from another measurement.

These examples demonstrate how the e^+e^- collider experiments can determine superpartner masses and the mixing angle of the charginos and neutralinos. The experimental program is systematic and does not depend on assumptions about the values of other supersymmetry parameters. It only demands the basic requirement that the color-singlet superpartners are available for study at the energy at which the collider can run. If squarks can be pair-produced at these energies, they can also be studied in this systematic way. Not only can their masses be measured, but polarization observables can be used to measure the small mass differences predicted by (144) and (145) [49].

4.8 Superspectroscopy at hadron colliders

At the end of Section 4.6, I explained that it should be relatively straightforward to identify the signatures of supersymmetry at the LHC. However, it is a challenging problem

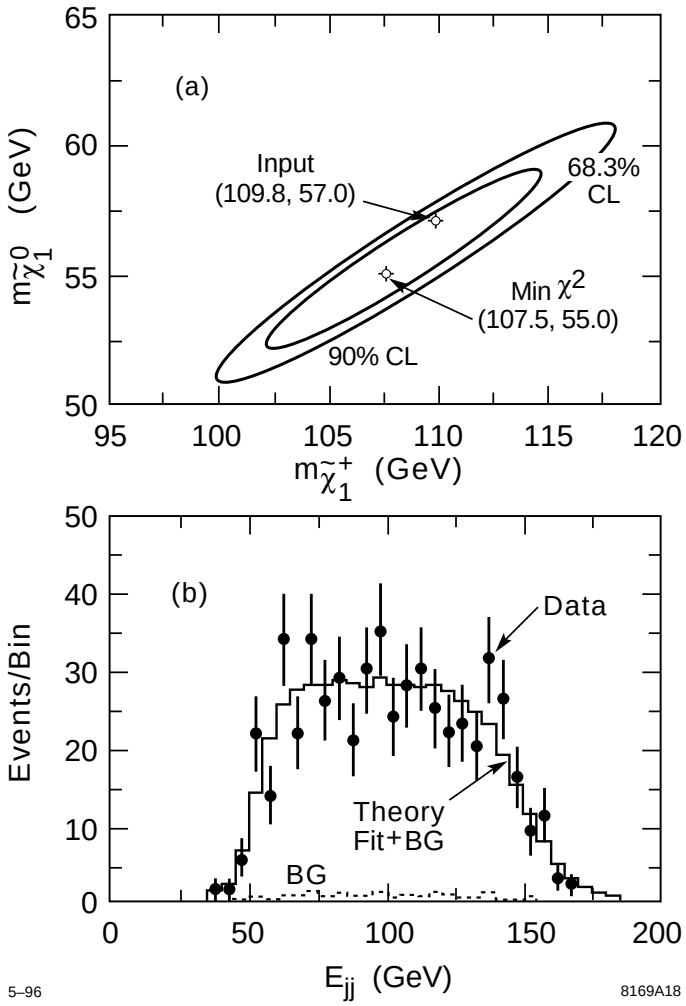

Figure 25: Simulation of the $\widetilde{\chi}_1^+$ mass measurement at an e^+e^- linear collider, from [44]. The bottom graph gives the event distribution in the energy of the $\overline{q}q$ pair emitted in a $\widetilde{\chi}_1^+$ hadronic decay. The hadronic system is restricted to a bin in mass around 30 GeV. The bottom graph shows the χ^2 contours as a function of the masses of the parent $\widetilde{\chi}_1^+$ and the daughter $\widetilde{\chi}_1^0$.

there to extract precision information about the underlying supersymmetry parameters. For a long time, it was thought that this information would have to come from cross sections for specific signatures whose origin is complex and model-dependent. However, it has been realized more recently that the LHC can, in certain situations, offer ways to determine supersymmetry mass parameters kinematically.

Let me briefly describe the parameters of the LHC [50]. This is a pp collider with 14 TeV in the center of mass. The design luminosity corresponds to a data sample, per experiment, of 100 fb^{-1} per year. A simpler experimental environment, without multiplet hadronic collisions per proton bunch crossing, is obtained by running at a lower luminosity of 10 fb^{-1} per year, and this is probably what will be done initially. If the supersymmetric partners of Standard Model particles indeed lie in the region defined by our estimates (157)–(159), this low luminosity should already be sufficient to begin detailed exploration

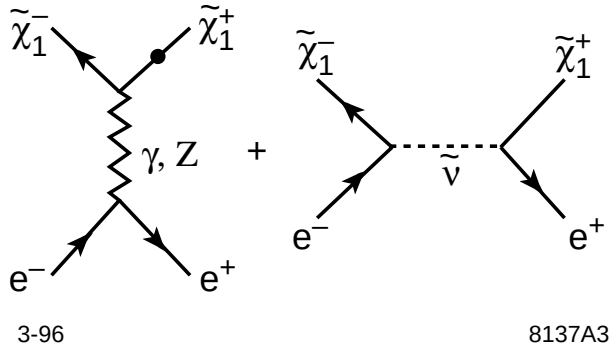

Figure 26: Feynman diagrams for the process of chargino pair production.

of the supersymmetry mass spectrum.

Before we discuss methods for direct mass measurement, I should point out that the many signatures available at the LHC which do not give explicit kinematic reconstructions do offer a significant amount of information. For example, the ATLAS collaboration [28, 51] has suggested comparing the cross-sections for like-sign dilepton events with $\ell^+\ell^+$ versus $\ell^-\ell^-$. The excess of events with two positive leptons comes from the process in which two u quarks exchange a gluino and convert to $\tilde{u}$, making use of the fact that the proton contains more u than d quarks. The contribution of this process peaks when the squarks and gluinos have roughly equal masses, as shown in Figure 28. Thus, this measurement allows one to estimate the ration of the squark and gluino masses. Presumably, if the values of μ, m_1, and m_2 were known from the e^+e^- collider experiments, it should be possible to make a precise theory of multi-lepton production and to use the rates of these processes to determine $m(\tilde{g})$ and $m(\tilde{q})$.

In some circumstances, however, the LHC provides direct information on the superparticle spectrum. Consider, for example, decay chains which end with the decay $\tilde{\chi}_2^0 \to \ell^+\ell^-\tilde{\chi}_1^0$ discussed in Section 4.5. The dilepton mass distribution has a discontinuity at the kinematic endpoint where

$$m(\ell^+\ell^-) = m(\tilde{\chi}_2^0) - m(\tilde{\chi}_1^0) \ . \tag{162}$$

The sharpness of this kinematic edge is shown in Figure 29, taken from a study of the process $q\overline{q} \to \tilde{\chi}_1^+\tilde{\chi}_2^0$ [52]. Under the assumptions of gaugino unification plus the gaugino region of parameter space, the mass difference in (162) equals $0.5m_2$. Thus, if we have some independent evidence for these assumptions, the position of this edge can be used to give the overall scale of superparticle masses. Also, if the gluino mass can be measured, the ratio of that mass to the mass difference (162) provides a test of these assumptions.

At a point in parameter space studied for the ATLAS Collaboration in [42], it is possible to go much further. We need not discuss why this particular point in the 'minimal SUGRA' parameter space was chosen for special study, but it turned out to have a number of advantageous properties. The value of the gluino mass was taken to be 300 GeV, leading to a very large gluino production cross section, equal to 1 nb, at the LHC. The effect of Yukawa couplings discussed in Section 3.7 lowers the masses of the superpartners of t_L and b_L, in particular, making $\tilde{b}_L$ the lightest squark. Then a major decay chain for the $\tilde{g}$

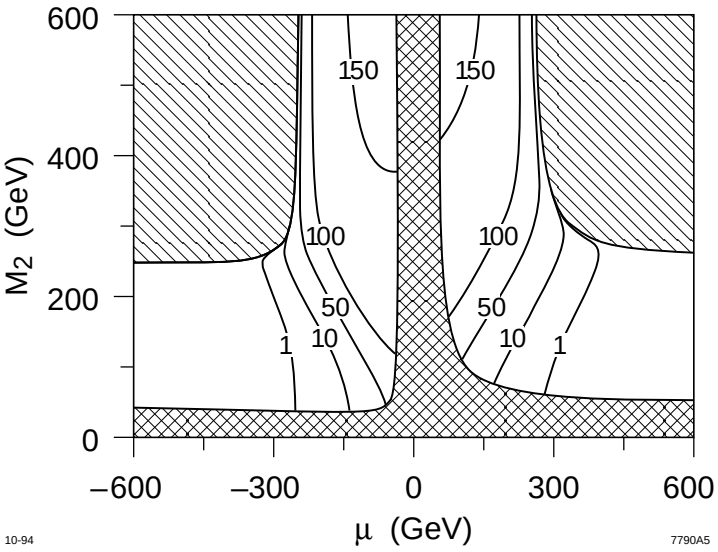

Figure 27: Contours of constant cross section, in fb, for the reaction $e_R^- e^+ \to \widetilde{\chi}_1^+ \widetilde{\chi}_1^-$ at $E_{\rm CM} = 500$ GeV, from [48]. The plot shows how the value of this cross section maps to the position in the (μ, m_2) plane. The boundaries of the indicated regions are the curves on which the $\widetilde{\chi}_1^+$ mass equals 50 GeV and 250 GeV.

would be

$$\widetilde{g} \to \widetilde{b}_L \overline{b} \to b \overline{b} \widetilde{\chi}_2^0 \ , \tag{163}$$

which could be followed by the dilepton decay of the $\widetilde{\chi}_2^0$.

Since the number of events expected at this point is very large, we can select events in which the $\ell^+\ell^-$ pair falls close to its kinematic endpoint. For these events, the dilepton pair and the daughter $\widetilde{\chi}_1^0$ are both at rest with respect to the parent $\widetilde{\chi}_2^0$. Then, if we are also given the mass of the $\widetilde{\chi}_1^0$, the energy-momentum 4-vector of the $\widetilde{\chi}_2^0$ is determined. This mass might be obtained from the assumptions listed below (162), from a more general fit of the LHC supersymmetry data to a model of the supersymmetry mass spectrum, or from a direct measurement at an e^+e^- collider. In any event, once the momentum vector of the $\widetilde{\chi}_2^0$ is determined, there is no more missing momentum in the decay chain. It is now possible to successively add b jets to reconstruct the $\widetilde{b}_L$ and then the $\widetilde{g}$. The mass peaks for these states obtained from the simulation results of [42] are shown in Figure 30. For a fixed $m(\widetilde{\chi}_1^0)$, the masses of $\widetilde{b}_L$ and $\widetilde{g}$ are determined to 1% accuracy.

It may seem that this example uses many special features of the particular point in parameter space which was chosen for the analysis. At another point, the spectrum might be different in a way that would compromise parts of this analysis. For example, the $\widetilde{\chi}_2^0$ might be allowed to decay to an on-shell Z^0, or the gluino might lie below the $\widetilde{b}_L$. On the other hand, the method just described can be extended to any superpartner with a three-body becay involving one unobserved neutral. In [42], other examples are discussed which apply these ideas to decay chains that end with $\widetilde{q} \to \widetilde{\chi}_1^0 h^0 q$ and $\widetilde{t} \to \widetilde{\chi}_1^0 W^+ b$.

To properly evaluate the capability of the LHC to perform precision supersymmetry measurements, we must remember that Nature has chosen (at most) one point in the supersymmetry parameter space, and that every point in parameter space is special in its

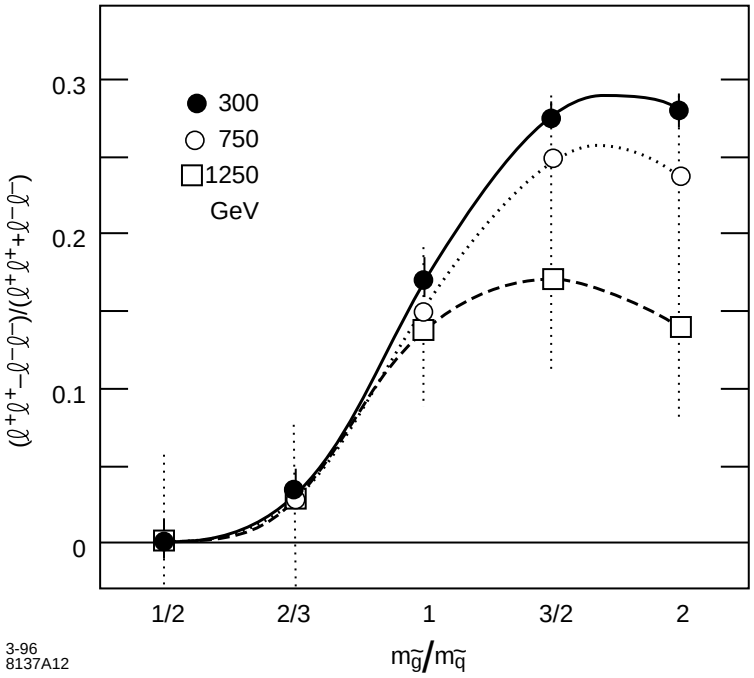

Figure 28: The asymmetry between the cross sections for dilepton events with $\ell^+\ell^+$ and those with $\ell^-\ell^-$ expected at the LHC, plotted as a function of the ratio of the gluino to the squark mass, from [28]. The three curves refer to the idicated values of the lighter of the squark and gluino masses.

own way. It is not likely that we will know, in advance, which particular trick that will be most effective. However, we have now only begun the study of strategies to determine the superparticle spectrum from the kinematics of LHC reactions. There are certainly many more tricks to be discovered.

4.9 Recapitulation

If physics beyond the Standard Model is supersymmetric, I am optimistic about the future prospects for experimental particle physics. At the LHC, if not before, we will discover the superparticle spectrum. This spectrum encodes information about physics at the energy scale of supersymmetry breaking, which might be as high as the grand unification or even the superstring scale. If we can measure the basic parameters that determine this spectrum, we can uncover the patterns that will let us decode this information and see much more deeply into fundamental physics.

It is not clear how much of this program can already be done at the LHC and how much must be left to the experimental program of an e^+e^- linear collider. For adherents of the linear collider, the worst case would be that Nature has chosen a minimal parameter set and also some special mass relations that allow the relevant three or four parameters to be determined at the LHC. Even in this case, the linear collider would have a profoundly interesting experimental program. In this simple scenario, the LHC experimenters will be able to fit their data to a small number of parameters, but the hadron collider experiments cannot verify that this is the whole story. To give one example, it is not known how, at a hadron collider, to measure the mass of the $\tilde{\chi}_1^0$, the particle that provides the basic quan-

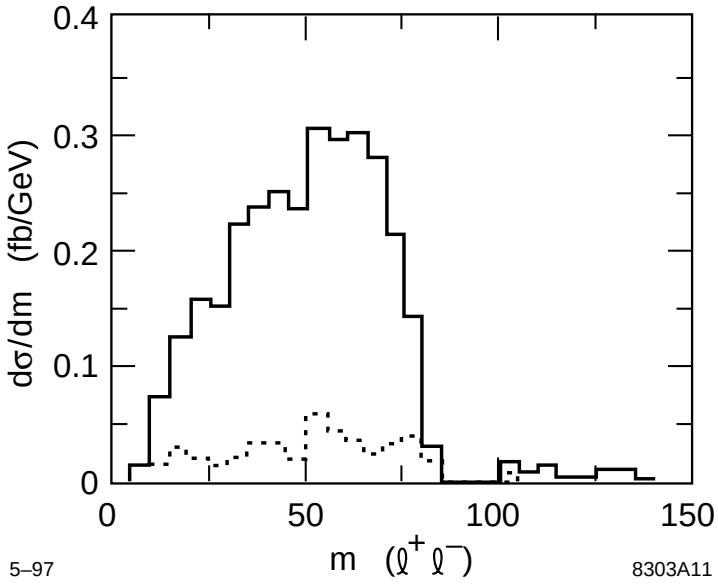

Figure 29: Distribution of the dilepton mass in the process $p\overline{p} \to \widetilde{\chi}_1^+ \widetilde{\chi}_2^0 + X$, with the $\widetilde{\chi}_2^0$ decaying to $\ell^+\ell^-\widetilde{\chi}_1^0$, from [52].

tum of missing energy-momentum used to build up the supersymmetry mass spectrum. The LHC experiments may give indirect determinations of $m(\widetilde{\chi}_1^0)$. The linear collider can provide a direct precision measurement of this particle mass. If the predicted value were found, that would be an intellectual triumph comparable to the direct discovery of the W boson in $p\overline{p}$ collisions.

I must also emphasize that there is an important difference between the study of the supersymmetry spectrum and that of the spectrum of weak vector bosons. In the latter case, the spectrum was predicted by a coherent theoretical model, the $SU(2) \times U(1)$ gauge theory. In the case of supersymmetry, as I have emphasized in Section 4.3, the minimal parametrization is just a guess—and one guess among many. Thus, it is a more likely outcome that a simple parametrization of the supersymmetry spectrum would omit crucial details. To discover these features, one would need the model-independent approach to supersymmetry parameter measurements that the e^+e^- experiments can provide.

In this more general arena for the construction and testing of supersymmetry model, the most striking feature of the comparison of colliders is how much each facility adds to the results obtainable at the other. From the e^+e^- side, we will obtain a precision understanding of the color-singlet portion of the supersymmetry spectrum. We will measure parameters which determine what decay chains the colored superparticles will follow. From the pp side, we will observe some of these decay chains directly and obtain precise inclusive cross sections for the decay products. This should allow us to analyze these decay chains back to their origin and to measure the superspectrum parameters of heavy colored superparticles. Thus, if the problem that Nature poses for us is supersymmetry, these two colliders together can solve that problem experimentally.

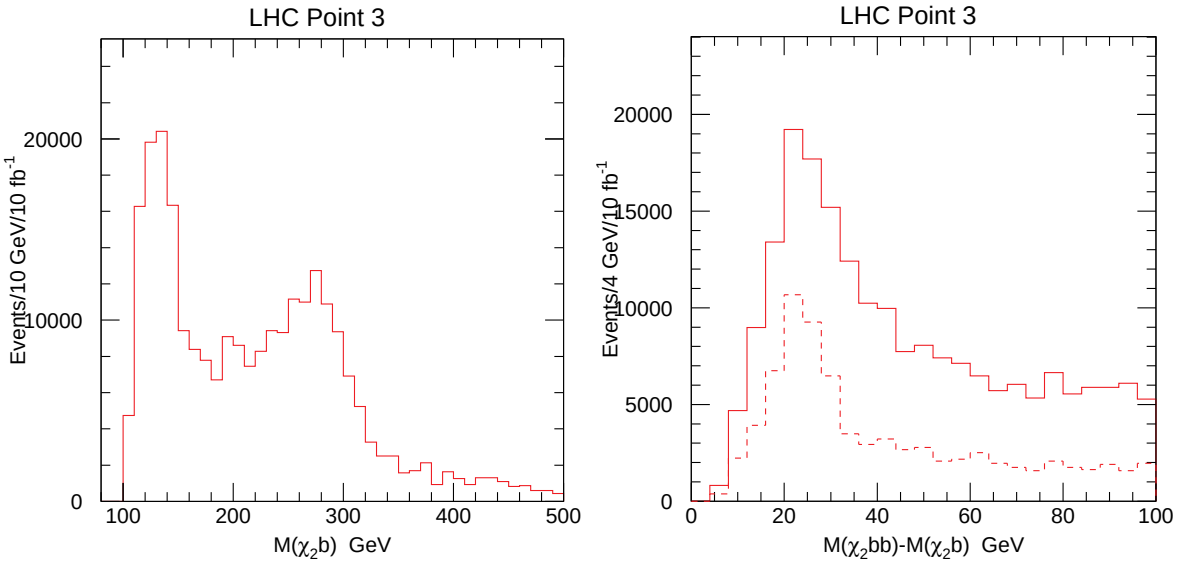

Figure 30: Reconstruction of the mass of the $\widetilde{b}$ and the $\widetilde{g}$ at the LHC, at a point in supersymmetry parameter space studied in [42]. In the plot on the left, the peak near 300 GeV shows the reconstructed $\widetilde{b}$. The plot on the right shows the event distribution in the variable $m(\widetilde{g}) - m(\widetilde{b})$. The dashed distribution shows the values for the events lying between 230 GeV and 330 GeV in the left-hand figure.

5. Technicolor

In the previous two sections, I have given a lengthy discussion of the theoretical structure of models of new physics based on supersymmetry. I have explained how supersymmetry leads to a solution to the problem of electroweak symmetry breaking. I have explained that the ramifications of supersymmetry are quite complex and lead to a rich variety of phenomena that can be studied experimentally at colliders.

This discussion illustrated one of the major points that I made at the beginning of these lectures. In seeking an explanation for electroweak symmetry breaking, we could just write down the minimal Lagrangian available. However, for me, it is much more attractive to look for a theory in which electroweak symmetry breaking emerges from a definite physical idea. If the idea is a profound one, it will naturally lead to new phenomena that we can discover in experiments.

Supersymmetry is an idea that illustrates this picture, but it might not be the right idea. You might worry that this example was a very special one. Therefore, if I am to provide an overview of ideas on physics beyond the Standard Model, I should give at least one more example of a physical idea that leads to electroweak symmetry breaking, and one assumptions of a very different kind. Therefore, in this section, I will discuss models of electroweak symmetry breaking based on the postulate of new strong interactions at the electroweak scale. We will see that this idea leads to a different set of physical predictions but nevertheless implies a rich and intriguing experimental program.

5.1 The structure of technicolor models

The basic structure of a model of electroweak symmetry breaking by new strong interactions is that of the Weinberg-Susskind model discussed at the end of Section 2.2. This model was based on a strong-interaction model that was essentially a scaled up

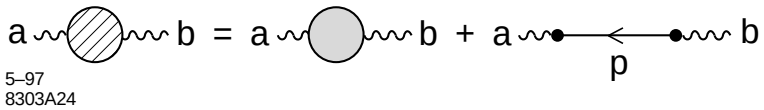

Figure 31: Contributions to the vacuum polarization of the W boson from technicolor states.

version of QCD. From here on, I will refer to the new strong interaction gauge symmetry as 'technicolor'. In this section, I will discuss more details of this model, and also add features that are necessary to provide for quark and lepton mass generation.

In Section 2.2, I pointed out that the Weinberg-Susskind model leads to a vacuum expectation value which breaks $SU(2)\times U(1)$. To understand this model better, we should first try to compute the W and Z boson mass matrix that comes from this symmetry breaking.

QCD with two massless flavors has the global symmetry $SU(2) \times SU(2)$; independent $SU(2)$ symmetries can rotate the doublets $q_L = (u_L, d_L)$ and $q_R = (u_R, d_R)$. When the operator $\overline{q}q$ obtains vacuum expectation values as in (16), the two $SU(2)$ groups are locked together by the pairing of quarks with antiquarks in the vacuum. Then the overall $SU(2)$ is unbroken; this is the manifest isospin symmetry of QCD. The second $SU(2)$ is that associated with the axial vector currents

$$J^{\mu 5a} = \overline{q}\gamma^\mu\gamma^5\tau^a q \ . \tag{164}$$

This symmetry is spontaneously broken. By Goldstone's theorem, the symmetry breaking leads to a massless boson for each spontaneously broken symmetry, one created or annihilated by each broken symmetry current. These three particles are identified with the pions of QCD. The matrix element between the axial $SU(2)$ currents and the pions can be parametrized as

$$\langle 0|J^{\mu 5a}|\pi^b(p)\rangle = if_\pi p^\mu \delta^{ab} \ . \tag{165}$$

By recognizing that $J^{\mu 5a}$ is a part of the weak interaction current, we can identify f_π as the pion decay constant, $f_\pi = 93$ MeV. The assumption of Weinberg and Susskind is that the same story is repeated in technicolor. However, since the technicolor quarks are assumed to be massless, the pions remain precisely massless at this stage of the argument.

If the system with spontaneously broken symmetry and massless pions is coupled to gauge fields, the gauge boson should obtain mass through the Higgs mechanism. To compute the mass term, consider the gauge boson vacuum polarization diagram shown in Figure 31.

Let us assume first that we couple only the weak interaction $SU(2)$ bosons to the techniquarks. The coupling is

$$\Delta\mathcal{L} = gA^a_\mu J^a_{L\mu} \ . \tag{166}$$

Then the matrix element (165) allows a pion to be annihilated and a gauge boson created, with the amplitude

$$ig\cdot(-\frac{1}{2})\cdot if_\pi p_\mu \delta^{ab} \ ; \tag{167}$$

the second factor comes from $J^a_{L\mu} = \frac{1}{2}(J^a_\mu - J^{a5}_\mu)$. Using this amplitude, we can evaluate the amplitude for a process in which a gauge boson converts to a Goldstone boson and then

converts back. This corresponds to the diagram contributing to the vacuum polarization shown as the second term on the right-hand side of Figure 31. The value of this diagram is

$$\left(\frac{gf_\pi p_\mu}{2}\right)\frac{1}{p^2}\left(-\frac{gf_\pi p_\nu}{2}\right) \ . \tag{168}$$

The full vacuum polarization amplitude $i\Pi^{ab}_{\mu\nu}(p)$ consists of this term plus more complicated terms with massive particles or multiple particles exchanged. These are indicated as the shaded blob in Figure 31. If there are no massless particles in the symmetry-breaking sector other than the pions, (168) is the only term with a $1/p^2$ singularity near $p = 0$. Now recognize that the gauge current $J^a_{L\mu}$ is conserved, and so the vacuum polarization must satisfy

$$p^\mu\,\Pi^{ab}_{\mu\nu}(p) = 0 \ . \tag{169}$$

These two requirements are compatible only if the vacuum polarization behaves near $p = 0$ as

$$\Pi^{ab}_{\mu\nu} = \left(\frac{gf_\pi}{2}\right)^2\left(g_{\mu\nu} - \frac{p_\mu p_\nu}{p^2}\right)\delta^{ab} \ . \tag{170}$$

This is a mass term for the vector boson, giving

$$m_W = g\frac{v}{2} \ , \quad \text{with} \quad v = f_\pi \ . \tag{171}$$

This is the result that I promised above (18).

Now add to this structure the $U(1)$ gauge boson B_μ coupling to hypercharge. Repeating the same arguments, we find the mass matrix

$$m^2 = \left(\frac{f_\pi}{2}\right)^2\begin{pmatrix} g^2 & & & \\ & g^2 & & \\ & & g^2 & -gg' \\ & & -gg' & (g')^2 \end{pmatrix} \ , \tag{172}$$

acting on $(A^1_\mu, A^2_\mu, A^3_\mu, B_\mu)$. This has just the form of (21). The eigenvalues of this matrix give the vector boson masses (7), with $v = 246$ GeV $= f_\pi$. This is the result promised above (18). More generally, in a model with N_D technicolor doublets, we require,

$$v^2 = N_D f_\pi^2 \ . \tag{173}$$

Thus, a larger technicolor sector lies lower in energy and is closer to the scale of present experiments.

In my discussion of (21), I pointed out that this equation calls for the presence of an unbroken $SU(2)$ global symmetry of the new strong interactions, called *custodial* $SU(2)$, in addition to the spontaneously broken weak interaction $SU(2)$ symmetry. This global $SU(2)$ symmetry requires that the first three diagonal entries in (172) are equal, giving the mass relation $m_W/m_Z = \cos\theta_w$. Custodial $SU(2)$ symmetry also acts on the heavier states of the new strong interaction theory and will play an important role in our analysis of the experimental probes of this sector.

The model I have just described gives mass the the W and Z bosons, but it does not yet give mass to quarks and leptons. In order to accomplish this, we must couple the

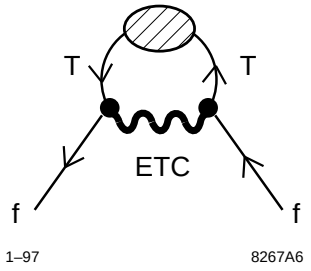

Figure 32: ETC generation of quark and lepton masses.

quarks and leptons to the techniquarks. This is done by introducing further gauge bosons called *Extended Technicolor* (ETC) bosons [53, 54]. If we imagine that the ETC bosons connect light fermions to techniquarks, and that they are very heavy, a typical coupling induced by these bosons would have the form

$$\begin{aligned} i\Delta\mathcal{L} &= (ig_E\overline{u}_L\gamma^\mu U_L)\frac{-i}{-m_E^2}(ig_E\overline{U}_R\gamma_\mu u_R) \\ &= -i\frac{g_E^2}{m_E^2}\overline{u}_L\gamma^\mu U_L\overline{U}_R\gamma_\mu u_R \end{aligned} \tag{174}$$

Now replace $U_L\overline{U}_R$ by its vacuum expectation value due to dynamical techniquark mass generation:

$$\left\langle U_L\overline{U}_R\right\rangle = -\frac{1}{4}\left\langle\overline{U}U\right\rangle = \frac{1}{4}\Delta \ , \tag{175}$$

where m_E and g_E are the ETC mass and coupling, Δ is as in (16) and the unit matrix is in the space of Dirac indices. Inserting (175) into (174), we find a fermion mass term

$$m_u = \frac{g_E^2}{m_E^2}\Delta \ . \tag{176}$$

The origin of this term is shown diagrammatically in Figure 32. In principle, masses could be generated in this way for all of the quarks and leptons.

From (176), we can infer the mass scale required for the ETC interactions. Estimating with $g_E \approx 1$, and $\Delta \sim 4\pi f_\pi^3$ (which gives $\langle\overline{u}u\rangle = (300\ \text{MeV})^3$ in QCD), we find

$$m_E = g_E\left(\frac{4\pi f_\pi^3}{m_f}\right)^{1/2} = \begin{cases} 43\ \text{TeV} & f = s \\ 1.0\ \text{TeV} & f = t \end{cases} \ , \tag{177}$$

using the s and t quark masses as reference points in the fermion mass spectrum.

The detailed structure of the ETC exchanges must be paired with a suitable structure of the techiquark sector. We might call 'minimal technicolor' the theory with precisely one weak interaction $SU(2)$ doublet of techniquarks. In this case, all of the flavor structure must appear in the ETC group. In particular, some ETC bosons must be color triplets to give mass to the quarks through the mechanism of Figure 32. Another possibility is that the technicolor sector could contain techniquarks with the $SU(3) \times SU(2) \times U(1)$ quantum numbers of a generation of quarks and leptons [55]. Then the ETC bosons could all be color singlets, though they would still carry generation quantum numbers. In this

case also, (173) would apply with $N_D = 4$, putting $f_\pi = 123$ GeV. More complex cases in which ETC bosons can be doublets of $SU(2)$ have also been discussed in the literature [56].

5.2 Experimental constraints on technicolor

The model that I have just described makes a number of characteristic physical predictions that can be checked in experiments at energies currently available. Unfortunately, none of these predictions checks experimentally. Many theorists view this as a repudiation of the technicolor program. However, others point to the fact that we have built up the technicolor model assuming that the dynamics of the technicolor interactions exactly copies that of QCD. By modifying the pattern or the explicit energy scale of chiral symmetry breaking, it is possible to evade these difficulties. Nevertheless, it is important to be aware of what the problems are. In this section, I will review the three major experimental problems with technicolor models and then briefly examine how they may be avoided through specific assumptions about the strong interaction dynamics.

The first two problems are not specifically associated with technicolor but rather with the ETC interactions that couple techniquarks to the Standard Model quarks and leptons. If two matrices of the ETC group link quarks with techniquarks, the commutator of these matrices should link quarks with quarks. This implies that there should be ETC bosons which create new four-quark interactions with coefficients of order g_E^2/m_E^2. In the Standard Model, there are no flavor-changing neutral current couplings at the tree level. Such couplings are generated by weak interaction box diagrams and other loop effects, but the flavor-changing part of these interactions is suppressed to the level observed experimentally by the GIM cancellation among intermediate flavors [57]. This cancellation follows from the fact that the couplings of the various flavors of quarks and leptons to the W and Z depend only on their $SU(2) \times U(1)$ quantum numbers. For ETC, however, either the couplings or the boson masses must depend strongly on flavor in order to generate the observed pattern of quark and lepton masses. Thus, generically, one expects large flavor-changing neutral current effects. It is possible to suppress these couplings to a level at which they do not contribute excessively to the K_L–K_S mass difference, but only by raising the ETC mass scale to $m_E \geq 1000$ TeV. In a similar way, ETC interactions generically give excessive contributions to $K^0 \to \mu^+ e^-$ and to $\mu \to e\gamma$ unless $m_E \geq 100$ TeV [58, 59]. These estimates contradict the value of the ETC boson masses required in (177). There are schemes for natural flavor conservation in technicolor theories, but they require a very large amount of new structure just above 1 TeV [60, 61, 62].

The second problem comes in the value of the top quark mass. If ETC is weakly coupled, the value of any quark mass should be bounded by approximately

$$m_f \leq \frac{g_E^2}{4\pi} \Delta^{1/2} \ , \tag{178}$$

where Δ is the techniquark bilinear expectation value. Estimating as above, this bounds the quark masses at about 70 GeV [63]. To see this problem from another point of view, look back at the mass of the ETC boson associated with the top quark, as given in (177). This is comparable to the mass of the technicolor ρ meson, which we would estimate from (18) to have a value of about 2 TeV. So apparently the top quark's ETC boson must be a particle with technicolor strong interactions. This means that the model described above

is not self-consistent. Since this new strongly-interacting particle generates mass for the t but not the b, it has the potential to give large contributions to other relations that violate weak-interaction isospin. In particular, it can give an unwanted large correction to the relation $m_W = m_Z \cos\theta_w$ in (20).

The third problem relates directly to the technicolor sector itself. This issue arises from the precision electroweak measurments. In principle, the agreement of precision electroweak measurements with the Standard Model is a strong constraint on any type of new physics. The constraint turns out to be especially powerful for technicolor. To explain this point, I would like to present some general formalism and then specialize it to the case of technicolor.

At first sight, new physics can affect the observables of precision electroweak physics through radiative corrections to the $SU(2) \times U(1)$ boson propagators, to the gauge boson vertices, and to 4-fermion box diagrams. Typically, though, the largest effects are those from vacuum polarization diagrams. To see this, recall that almost all precision electroweak observables involve 4-fermion reactions with light fermions only. (An exception is the $Z \to b\bar{b}$ vertex, whose discussion I will postpone to Section 5.7.) In this case, the vertex and box diagrams involve only those new particles that couple directly to the light generations. If the new particles are somehow connected to the mechanism of $SU(2) \times U(1)$ breaking and fermion mass generation, these couplings are necessarily small. The vacuum polarization diagrams, on the other hand, can involve all new particles which couple to $SU(2) \times U(1)$, and can even be enhanced by color or flavor sums over these particles.

The vacuum polarization corrections also can be accounted in a very simple way. It is useful, first, to write the W and Z vacuum polarization amplitudes in terms of current-current expectation values for the $SU(2)$ and electromagnetic currents. Use the relation

$$J_Z = J_3 - s^2 J_Q \ , \tag{179}$$

where J_Q is the electromagnetic current, and $s^2 = \sin^2\theta_w$, $c^2 = \cos^2\theta_w$. Write the weak coupling constants explicitly in terms of e, s^2 and c^2. Then the vacuum polarization amplitudes of γ, W, and Z and the γZ mixing amplitude take the form

$$\begin{aligned} \Pi_{\gamma\gamma} &= e^2 \Pi_{QQ} \\ \Pi_{WW} &= \frac{e^2}{s^2} \Pi_{QQ} \\ \Pi_{ZZ} &= \frac{e^2}{c^2 s^2} (\Pi_{33} - 2s^2 \Pi_{3Q} + s^4 \Pi_{QQ}) \\ \Pi_{Z\gamma} &= \frac{e^2}{cs} (\Pi_{3Q} - s^2 \Pi_{QQ}) \ . \end{aligned} \tag{180}$$

The current-current amplitudes Π_{ij} are functions of (q^2/M^2), where M is the mass of the new particles whose loops contribute to the vacuum polarizations.

If these new particles are too heavy to be found at the Z^0 or in the early stages of LEP 2, the ratio q^2/M^2 is bounded for $q^2 = m_Z^2$. Then it is reasonable to expand the current-current expectation values a power series. In making this expansion, it is important to take into account that any amplitude involving an electromagnetic current will vanish at $q^2 = 0$ by the standard QED Ward identity. Thus, to order q^2, we have six

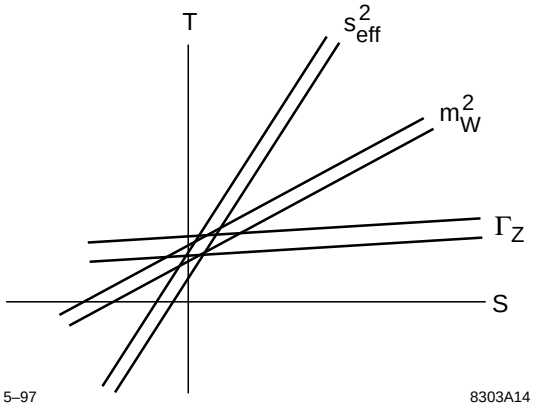

Figure 33: Schematic determination of S and T from precision electroweak measurements. For each observable, the width of the band corresponds to the experimental error in its determination.

coefficients,

$$\begin{aligned} \Pi_{QQ} &= q^2\Pi'_{QQ}(0) + \cdots \\ \Pi_{11} &= \Pi_{11}(0) + q^2\Pi'_{11}(0) + \cdots \\ \Pi_{3Q} &= q^2\Pi'_{3Q}(0) + \cdots \\ \Pi_{33} &= \Pi_{33}(0) + q^2\Pi'_{33}(0) + \cdots \end{aligned} \tag{181}$$

To specify the coupling constants g, g' and the scale v of the electroweak theory, we must measure three parameters. The most accurate reference values come from α, G_F, and m_Z. Three of the coefficients in (181) are absorbed into these parameters. This leaves three independent coefficients which can in principle be extracted from experimental measurements. These are conventionally defined [64] as

$$\begin{aligned} S &= 16\pi[\Pi'_{33}(0) - \Pi'_{3Q}(0)] \\ T &= \frac{4\pi}{s^2c^2m_Z^2}[\Pi_{11}(0) - \Pi_{33}(0)] \\ U &= 16\pi[\Pi'_{33}(0) - \Pi'_{11}(0)] \end{aligned} \tag{182}$$

I include in these parameters only the contributions from new physics. From the definitions, you can see that S measures the overall magnitude of q^2/M^2 effects, and T measures the magnitude of effects that violate the custodial $SU(2)$ symmetry of the new particles. The third parameter U requires both q^2-dependence and $SU(2)$ violation and typically is small in explicit models.

By inserting the new physics contributions to the intermediate boson propagators in weak interaction diagrams, we generate shifts from the Standard Model predictions which are linear in S, T, and U. For example, the effective value of $\sin^2\theta_w$ governing the forward-backward and polarization asymmetries at the Z^0 is shifted from its value $(s^2)_{\rm SM}$, in the Minimal Standard Model, by

$$(s^2)_{\rm eff} - (s^2)_{\rm SM} = \frac{\alpha}{c^2 - s^2}[\frac{1}{4}S - s^2c^2T] \ . \tag{183}$$

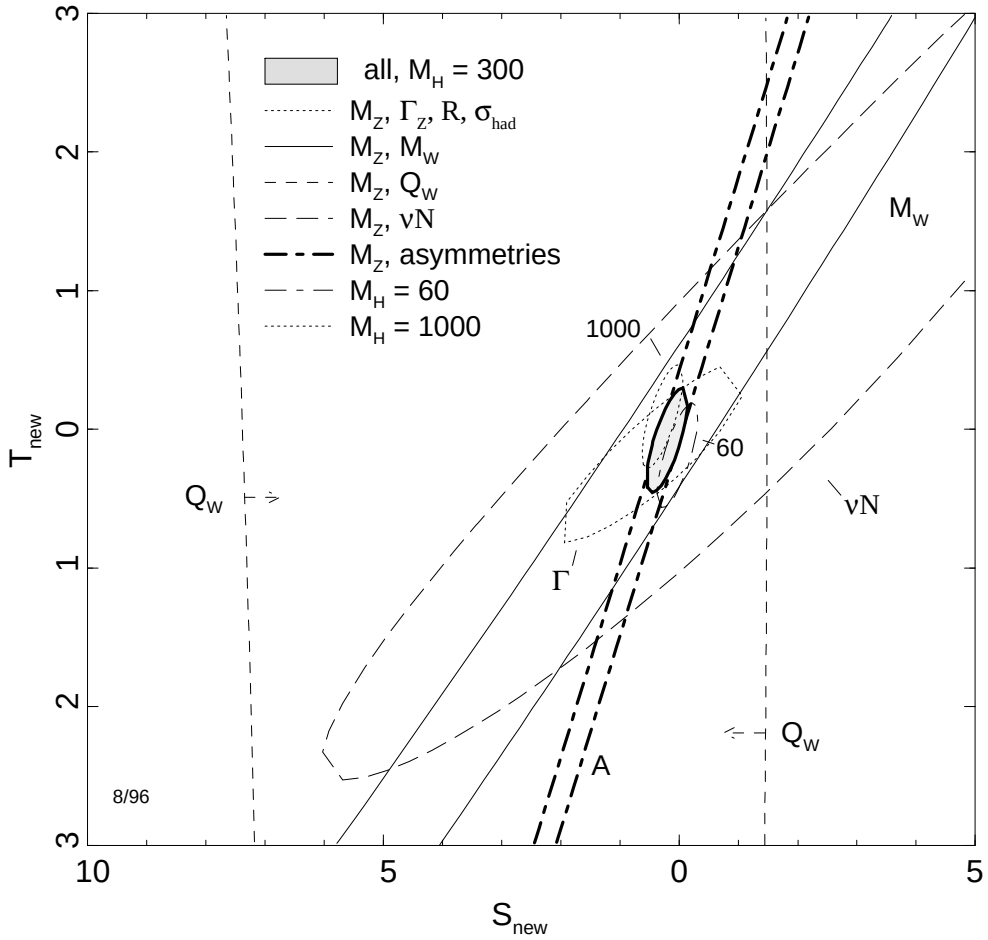

Figure 34: Current determination of S and T by a fit to the corpus of precision electroweak data, from [11]. The various ellipses show fits to a subset of the data, including the values of α, G_F, and m_Z plus those of one or several additional observables.

All of the standard observables except for m_W and Γ_W are independent of U, and since U is in any event expected to be small, I will ignore it from here on. In that case, any precision weak interaction measurement restricts us to the vicinity of the line in the S-T plane. The constraints that come from the measurements of $(s^2)_{\rm eff}$, m_W, and Γ_Z are sketched in Figure 33. If these lines meet, they indicate particular values of S and T which fit the deviations from the Standard Model in the whole corpus of weak interaction data. Figure 34 shows such an S-T fit to the data available in the summer of 1996 [11]. The various curves show fits to α, G_F, m_Z plus a specific subset of the other observables; the varying slopes of these constraints illustrate the behavior shown in Figure 33.

There is one important subtlety in the interpretation of the final values of S and T. In determining the Minimal Standard Model reference values for the fit, it is necessary to specify the value of the top quark mass and also a value for the mass of the Minimal Standard Model Higgs boson. Raising m_t gives the same physical effect as increasing T; raising m_H increases S while slightly decreasing T. Though m_t is known from direct measurements, m_H is not. The analysis of Figure 34 assumed $m_t = 175$ GeV, $m_H = 300$ GeV. In comparing S and T to the predictions of technicolor models, it is most

straightforward to compute the difference between the technicolor contribution to the vacuum polarization and that of a 1 TeV Higgs boson. Shifting to this reference value, we have the experimental constraint

$$S = -0.26 \pm 0.16 \ . \tag{184}$$

The negative sign indicates that there should be a smaller contribution to the W and Z vacuum polarizations than that predicted by a 1 TeV Standard Model Higgs boson. This is in accord with the fact that a lower value of the Higgs boson mass gives the best fit to the Minimal Standard Model, as I have indicated in (63).

In many models of new physics, the contributions to S become small as the mass scale M increases, with the behavior $S \sim m_Z^2/M^2$. This is the case, for example, in supersymmetry. For example, charginos of mass about 60 GeV can contribute to S at the level of of a few tenths of a unit, but heavier charginos have a negligible effect on this parameter. In technicolor models, however, there is a new strong interaction sector with resonances that can appear directly in the W and Z vacuum polarizations. There is a concrete formula which describes these effects. Consider a technicolor theory with $SU(2)$ isospin global symmetry. In such a theory, we can think about producing hadronic resonances through e^+e^- annihilation. In the standard parametrization, the cross section for e^+e^- annihilation to hadrons through a virtual photon is given by the point cross section for $e^+e^- \to \mu^+\mu^-$ times a factor $R(s)$, equal asymptotically to the sum of the squares of the quark charges. Let $R_V(s)$ be the analogous factor for a photon which couples to the isospin current $J^{\mu 3}$ and so creates $I = 1$ vector resonances only, and let $R_A(s)$ be the factor for a photon which couples to the axial isospin current $J^{\mu 53}$. Then

$$S = \frac{1}{3\pi} \int_0^\infty \frac{ds}{s} \left[R_V(s) - R_A(s) - H(s) \right] \ , \tag{185}$$

where $H(s) \approx \frac{1}{4}\theta(s - m_h^2)$ is the contribution of the Standard Model Higgs boson used to compute the reference value in (183). In practice, this $H(s)$ gives a small correction. If one evaluates R_V and R_A using the spectrum of QCD, scaled up appropriately by the factor (18), one finds [64]

$$S = +0.3 N_D \frac{N_{TC}}{3} \ , \tag{186}$$

where N_D is the number of weak doublets and N_{TC} is the number of technicolors. Even for $N_D = 1$ and $N_{TC} = 3$, this is a substantial positive value, one inconsistent with (184) at the 3 σ level. Models with several technicolor weak doublets are in much more serious conflict with the data.

These phenomenological problems of technicolor are challenging for the theory, but they do not necessarily rule it out. Holdom [65] has suggested a specific dynamical scheme which solves the first of these three problems. In estimating the scale of ETC interactions, we assumed that the techniquark condensate falls off rapidly at high momentum, as the quark condensate does in QCD. If the techniquark mass term fell only slowly at high momentum, ETC would have a larger influence at larger values of m_E. Then the flavor-changing direct effect of ETC on light quark physics would be reduced. It is possible that such a difference between technicolor and QCD would also ameliorate the other two problems I have discussed [66]. In particular, if the $J = 1$ spectrum of technicolor models

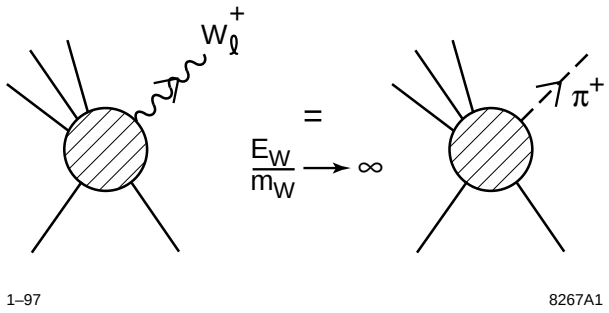

Figure 35: The Goldstone Boson Equivalence Theorem.

is not dominated by the low-lying ρ and a_1 mesons, as is the case in QCD, there is a chance that the vector and axial vector contributions to (185) would cancel to a greater extent.

It is disappointing that theorists are unclear about the precise predictions of technicolor models, but it is not surprising. Technicolor relies on the presence of a new strongly-coupled gauge theory. Though the properties of QCD at strong coupling now seem to be well understood through numerical lattice gauge theory computations, our understanding of strongly coupled field theories is quite incomplete. There is room for quantiatively and even qualitatively different behavior, especially in theories with a large number of fermion flavors. What the arguments in this section show is that technicolor cannot be simply a scaled-up version of QCD. It is a challenge to theorists, though, to find the strong-interaction theory whose different dynamical behavior fixes the problems that extrapolation from QCD would lead us to expect.

5.3 Direct probes of new strong interactions

If the model-dependent constraints on technicolor have led us into a murky theoretical situation, we should look for experiments that have a directly, model-independent interpretation. The guiding principle of technicolor is that $SU(2) \times U(1)$ symmetry breaking is caused by new strong interactions. We should be able to test this idea by directly observing elementary particle reactions involving these new interactions. In the next few sections, I will explain how these experiments can be done.

In order to design experiments on new strong interactions, there are two problems that we must discuss. First, the natural energy scale for technicolor, and also for alternative theories with new strong interactions, is of the order of 1 TeV. Thus, to feel these interactions, we will need to set up parton colllisions with energies of order 1 TeV in the center of mass. This energy range is well beyond the capabilities of LEP 2 and the Tevatron, but it should be available at the LHC and the e^+e^- linear collider. Even for these facilities, the experiments are challenging. For the LHC, we will see that it requires the full design luminosity. For the linear collider, it requires a center-of-mass energy of 1.5 TeV, at the top of the energy range now under consideration.

Second, we need to understand which parton collisions we should study. Among the particles that interact in high-energy collisions, do any carry the new strong interactions? At first it seems that all of the elementary particles of collider physics are weakly coupled. But remember that, in the models we are discussing, the W and Z bosons acquire

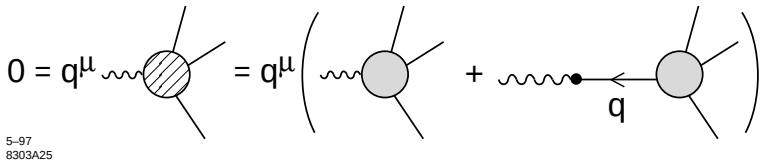

Figure 36: Ward identity used in the proof of the Goldstone Boson Equivalence Theorem.

their mass through their coupling to the new strong interactions. As a part of the Higgs mechanism, these bosons, which are massless and transversely polarized before symmetry breaking, pick up longitudinal polarization states by combining with the Goldstone bosons of the symmetry-breaking sector. It is suggestive, then, that at very high energy, the longitudinal polarization states of the W and Z bosons should show their origin and interact like the pions of the strong interaction theory. In fact, this correspondence can be proved; it is called the Goldstone Boson Equivalence Theorem [67, 68, 69, 70]. The statement of the theorem is shown in Figure 35.

It is complicated to give a completely general proof of this theorem, but it is not difficult to demonstate the simplest case. Consider a process in which one W boson is emitted. Since the W couples to a conserved gauge current, the emission amplitude obeys a Ward identity, shown in Figure 36. We can analyze this Ward identity as we did the analogous diagrammatic identity in Figure 31. The current which creates the W destroys a state of the strong interaction theory; this is either a massive state or a massless state consisting of one pion. Call the vertex from which the W is created directly Γ_W, and call the vertex for the creation of a pion $i\Gamma_\pi$. Then the Ward identity shown in Figure 36 reads

$$q_\mu \Gamma_W^\mu(q) + q_\mu \left(\frac{g f_\pi q^\mu}{2} \right) \frac{i}{q^2} i\Gamma_\pi(q) = 0 \ . \tag{187}$$

Using (171), this simplifies to

$$q_\mu \Gamma_W^\mu = m_W \Gamma_\pi \ . \tag{188}$$

To apply this equation, look at the explicit polarization vector representing a vector boson of longitudinal polarization. For a W boson moving in the $\hat{3}$ direction, $q^\mu = (E, 0, 0, q)$ with $E^2 - q^2 = m_W^2$, the longitudinal polarization vector is

$$\epsilon^\mu = \left(\frac{q}{m_W}, 0, 0, \frac{E}{m_W} \right) \ . \tag{189}$$

This vector satisfies $\epsilon \cdot q = 0$. At the same time, it becomes increasingly close to q^μ / m_W as $E \to \infty$. Because of this, the contraction of ϵ^μ with the first term in the vertex shown in Figure 36 is well approximated by $(q_\mu / m_W)\Gamma_W^\mu$ in this limit, while at the same time the contraction of ϵ^μ with the pion diagram gives zero. Thus, Γ_W is the complete amplitude for emission of a physical W boson. According to (188), it satisfies

$$\epsilon_\mu \Gamma_W^\mu = \Gamma_\pi \tag{190}$$

for $E \gg m_W$. This is the precise statement of Goldstone boson equivalence.

The Goldstone boson equivalence theorem tells us that the longitudinal polarization states of W^+, W^-, and Z^0, studied in very high energy reactions, are precisely the pions of

the new strong interactions. In the simplest technicolor models, these particles would have the scattering amplitudes of QCD pions. However, we can also broaden our description to include more general models. To do this, we simply write the most general theory of pion interactions at energies low compared to the new strong-interaction scale, and then reinterpret the initial and final particles are longitudinally polarized weak bosons.

This analysis is dramatically simplified by the observation we made below (21) that the new strong interactions should contain a global $SU(2)$ symmetry which remains exact when the weak interaction $SU(2)$ is spontaneously broken. I explained there that this symmetry is required to obtain the relation $m_W = m_Z \cos\theta_w$, which is a regularity of the weak boson mass spectrum. This unbroken symmetry shows up in technicolor models as the manifest $SU(2)$ isospin symmetry of the techniquarks.

From here on, I will treat the pions of the new strong interactions as massless particles with an exact isospin $SU(2)$ symmetry. The pions form a triplet with $I = 1$. Then a two-pion state has isospin 0, 1, or 2. Using Bose statistics, we see that the three scattering channels of lowest angular momentum are

$$\begin{aligned} I &= 0 \qquad J = 0 \\ I &= 1 \qquad J = 1 \\ I &= 2 \qquad J = 0 \end{aligned} \tag{191}$$

From here on, I will refer to these channels by their isospin value. Using the analogy to the conventional strong interactions, it is conventional to call a resonance in the $I = 0$ channel a σ and a resonance in the $I = 1$ channel a ρ or techni-ρ.

Now we can describe the pion interactions by old-fashioned pion scattering phenomenology [71]. As long we are at energies sufficiently low that the process $\pi\pi \to 4\pi$ is not yet important, unitarity requires the scattering amplitude in the channel I to have the form

$$\mathcal{M}_I = 32\pi e^{i\delta_I} \sin\delta_I \cdot \begin{cases} 1 & J = 0 \\ 3\cos\theta & J = 1 \end{cases} , \tag{192}$$

where δ_I is the phase shift in the channel I. Since the pions are massless, these can be expanded at low energy as

$$\delta_I = \frac{s}{A_I}\left(1 + \frac{s}{M_I^2} + \cdots\right) , \tag{193}$$

where A_I is the relativistic generalization of the scattering length and M_I similarly represents the effective range. The parameter M_I is given this name because it estimates the position of the leading resonance in the channel I. The limit $M_I \to \infty$ is called the *Low Energy Theorem* (LET) model.

Because the pions are Goldstone bosons, it turns our that their scattering lengths can be predicted in terms of the amplitude (165) [72]. Thus,

$$A_I = \begin{cases} 16\pi f_\pi^2 = (1.7\text{ TeV})^2 & I = 0 \\ 96\pi f_\pi^2 = (4.3\text{ TeV})^2 & I = 1 \\ -32\pi f_\pi^2 & I = 2 \end{cases} . \tag{194}$$

Experiments which involve WW scattering at very high energy should give us the chance to observe these values of A_I and to measure the corresponding values of M_I.

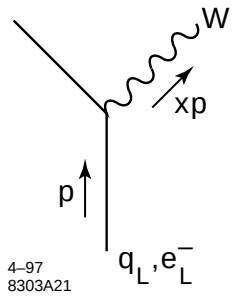

Figure 37: Kinematics for the radiation of a longitudinal W parton.

The values of A_I given in (194) represent the basic assumptions about manifest and spontaneously broken symmetry which are built into our analysis. The values of M_I, on the other hand, depend on the details of the particular set of new strong interactions that Nature has provided. For example, in a technicolor model, the quark model of techicolor interactions predicts that the strongest low-lying resonance should be a ρ ($I = 1$), as we see in QCD. In a model with strongly coupled spin-0 particles, the strongest resonance would probably be a σ, an $I = 0$ scalar bound state. More generally, if we can learn which channels have low-lying resonances and what the masses of these resonances are, we will have a direct experimental window into the nature of the new interactions which break $SU(2) \times U(1)$.

5.4 New strong interactions in WW scattering

How, then, can we create collisions of longitudinal W bosons at TeV center-of-mass energies? The most straightforward method to create high-energy W bosons is to radiate them from incident colliding particles, either quarks at the LHC or electrons and positrons at the linear collider.

The flux of W bosons associated with a proton or electron beam can be computed by methods similar to those used to discuss parton evolution in QCD [5, 73]. We imagine that the W bosons are emitted from the incident fermion lines and come together in a collision process with momentum transfer Q. The kinematics of the emission process is shown in Figure 37. The emitted bosons are produced with a spectrum in longitudinal momentum, parametrized by the quantity x, the *longitudinal fraction*. They also have a spectrum in transverse momentum $p_\perp$. The emitted W boson is off-shell, but this can be ignored to a first approximation if Q is much larger than $(m_W^2 + p_\perp^2)^{1/2}$. In this limit, the distribution of the emitted W bosons is described by relatively simple formulae. Note that an incident d_L or e_L^- can radiate a W^-, while an incident u_L or e_R^+ can radiate a W^+.

The distribution of transversely polarized W^- bosons emitted from an incident d_L or e_L^- is given by

$$\int dx\, f_{e_L^- \to W_{tr}^-}(x, Q) = \int_0^{Q^2} \frac{dp_\perp^2}{p_\perp^2 + m_W^2} \int \frac{dx}{x}\, \frac{\alpha}{4\pi s^2} \frac{1 + (1-x)^2}{x} \ , \qquad (195)$$

where, as before, $s^2 = \sin^2 \theta_w$. The integral over transverse momenta gives an enhancement factor of $\log Q^2/m_W^2$, analogous to the factor $\log s/m_e$ which appears in the formula for radiation of photons in electron scattering processes. The distribution of longitudinally

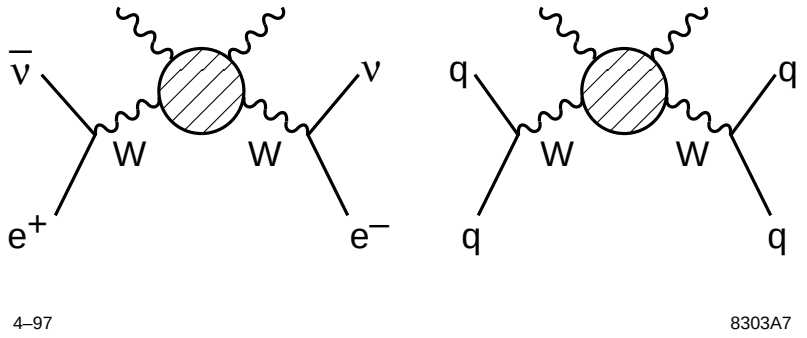

Figure 38: Collider processes which involve WW scattering.

polarized W^- bosons has a somewhat different structure,

$$\begin{aligned}\int dx\, f_{e_L^-\to W_{long}^-}(x,Q) &= \int_0^{Q^2} \frac{dp_\perp^2 m_W^2}{(p_\perp^2+m_W^2)^2} \int \frac{dx}{x}\ \frac{\alpha}{2\pi s^2}\frac{1-x}{x} \\ &= \int \frac{dx}{x}\ \frac{\alpha}{2\pi s^2}\frac{1-x}{x}\ . \end{aligned} \tag{196}$$

This formula does not show the logarithmic distribution in $p_\perp$ seen in (195); instead, it produces longitudinally polarized W bosons at a characteristic $p_\perp$ value of order m_W.

When both beams radiate longitudinally polarized W bosons, we can study boson-boson scattering through the reactions shown in Figure 38. In pp reactions one can in principle study all modes of WW scattering, though the most complete simulations have been done for the especially clean $I = 2$ channel, $W^+W^+ \to W^+W^+$. In e^+e^- collisions, one is restricted to the channels $W^+W^- \to W^+W^-$ and $W^+W^- \to Z^0Z^0$. The diagrams in which a longitudinal Z^0 appears in the initial state are suppressed by the small Z^0 coupling to the electron

$$\frac{g^2(e_L^- \to e_L^- Z^0)}{g^2(e_L^- \to \nu W^-)} = \left(\frac{(\frac{1}{2}-s^2)/cs}{1/\sqrt{2}s}\right)^2 = 0.2\ . \tag{197}$$

The $I = 2$ process $W^-W^- \to W^-W^-$ could be studied in a dedicated e^-e^- collision experiment.

I will now briefly discuss the experimental strategies for observing these reactions in the LHC and linear collider environments and present some simulation results. In the pp reactions, the most important background processes come from the important high transverse momentum QCD processes which, with some probability, give final states that mimic W boson pairs. For example, in the process $gg \to gg$ with a momentum transfer of 1 TeV, each final gluon typically radiates gluons and quarks before final hadronization, to produce a system of hadrons with of order 100 GeV. When the mass of this system happens to be close to the mass of the W, the process has the characteristics of WW scattering. Because of the overwhelming rate for $gg \to gg$, all studies of WW scattering at hadron colliders have restricted themselves to detection of one or both weak bosons in leptonic decay modes. Even with this restriction, the process $gg \to t\bar{t}$ provides a background of isolated lepton pairs at high transverse momentum. This background and a similar one from $q\overline{q} \to W+$ jets, with jets faking leptons, are controlled by requiring some further

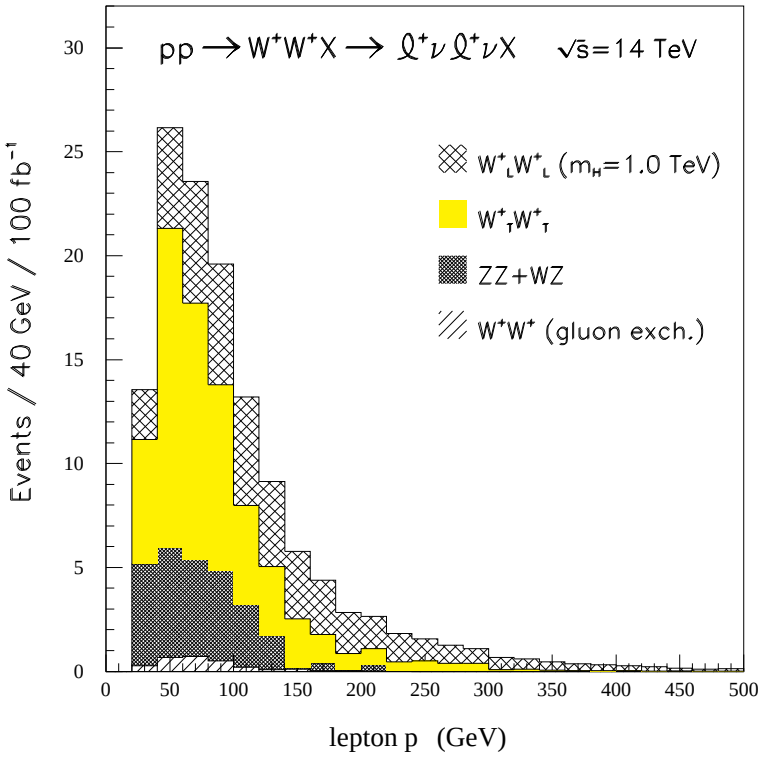

Figure 39: Expected numbers of $W^+W^+ \to (\ell\nu)(\ell\nu)$ events due to signal and background processes, after all cuts, for a 100 fb^{-1} event sample at the LHC, from [28]. The signal corresponds to a Higgs boson of mass 1 TeV.

evidence that the initial W bosons are color-singlet systems radiated from quark lines. To achieve this, one could require a forward jet associated with the quark from which the W was radiated, or a low hadronic activity in the central rapidity region, characteristic of the collision of color-singlet species.

Figure 39 shows a simulation by the ATLAS collaboration of a search for new strong interactions in W^+W^+ scattering [28]. In this study, both W bosons were assumed to be observed in their leptonic decays to e or μ, and a forward jet tag was required. The signal corresponds to a model with a 1 TeV Higgs boson, or, in our more general terminology, a 1 TeV $I = 0$ resonance. The size of the signal is a few tens of events in a year of running at the LHC at high luminosity. Note that the experiment admits a substantial background from various sources of tranversely polarized weak bosons. Though there is a significant excess above the Standard Model expectation, the signal is not distinguished by a resonance peak, and so it will be important to find experimental checks that the backgrounds are correctly estimated. An illuminating study of the other important reaction $pp \to Z^0 Z^0 + X$ is given in [74].

The WW scattering experiment is also difficult at an e^+e^- linear collider. A center of mass energy well above 1 TeV must be used, and again the event rate is a few tens per year at high luminosity. The systematic problems of the measurement are different, however, so that the e^+e^- results might provide important new evidence even if a small effect is first seen at the LHC. In the e^+e^- environment, it is possible to identify the weak bosons in their hadronic decay modes, and in fact this is necessary to provide sufficient

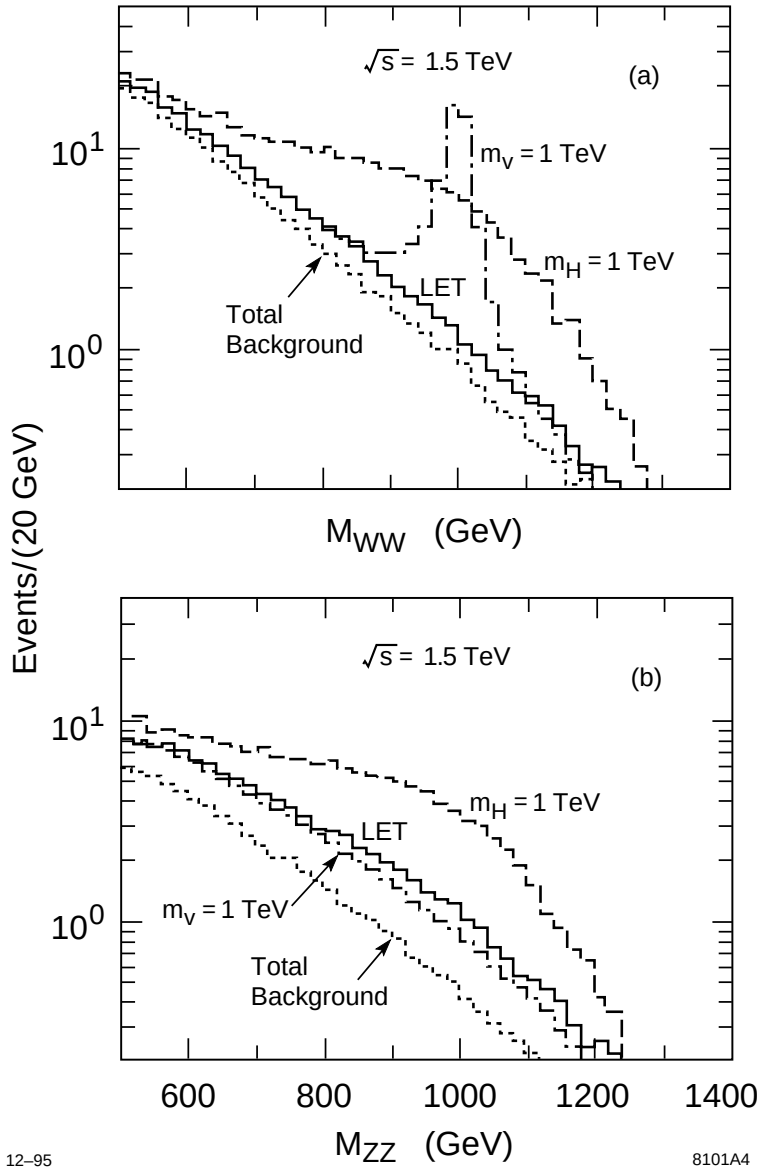

Figure 40: Expected numbers of W^+W^- and $ZZ \to 4$ jet events due to signal and background processes, after all cuts, for a 200 fb^{-1} event sample at an e^+e^- linear collider at 1.5 TeV in the center of mass, from [75]. Three different models for the signal are compared to the Standard Model background.

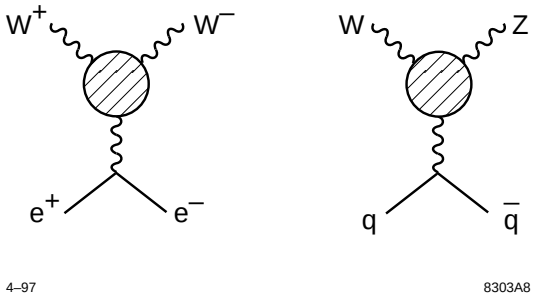

Figure 41: Collider processes which involve vector boson pair-production.

rate. Since the hadronic decay captures the full energy-momentum of the weak boson, the total momentum vector of the boson pair can be measured. This, again, is fortunate, because the dominant backgrounds to WW scattering through new strong interactions come from the photon-induced processes $\gamma\gamma \to W^+W^-$ and $\gamma e \to ZW\nu$. The first of these backgrounds can be dramatically reduced by insisting that the final two-boson system has a transverse momentum between 50 and 300 GeV, corresponding to the phenomenon we noted in (196) that longitudinally polarized weak bosons are typically emitted with a transverse momentum of order m_W. This cut should be accompanied by a forward electron and positron veto to remove processes with an initial photon which has been radiated from one of the fermion lines.

The expected signal and background after cuts, in $e^+e^- \to \nu\overline{\nu}W^+W^-$ and $e^+e^- \to \nu\overline{\nu}Z^0Z^0$, at a center-of-mass energy of 1.5 TeV, are shown in Figure 40 [75]. The signal is shown for a number of different models and is compared to the Standard Model expectation for transversely polarized boson pair production. In the most favorable cases of 1 TeV resonances in the $I = 0$ or $I = 1$ channel, resonance structure is apparent in the signal, but in models with higher resonance masses one must again rely on observing an enhancement over the predicted Standard Model backgrounds. At an e^+e^- collider, one has the small advantage that these backgrounds come from electroweak processes and can therefore be precisely estimated.

Recently, it has been shown that the process $WW \to t\bar{t}$ can be observed at an e^+e^- linear collider at 1.5 TeV [76]. This reaction probes the involvement of the top quark in the new strong interactions. If the W and top quark masses have a common origin, the same resonances which appear in WW scattering should also appear in this reaction. However, some models, for example, Hill's topcolor [77], attribute the top quark mass to interactions specific to the third generation which lead to top pair condensation. The study of $WW \to t\bar{t}$ can directly address this issue experimentally.

5.5 New strong interactions in W pair-production

In addition to providing direct WW scattering processes, new strong interactions can affect collider processes by creating a resonant enhancement of fermion pair annihilation in to weak bosons. The most important reactions for studying this effect are shown in Figure 41. As with the processes studied in Section 5.4, these occur both in the pp and e^+e^- collider environment.

The effect is easy to understand by a comparison to the familiar strong interactions.

In the same way that the boson-boson scattering processes described in the previous section were analogous to pion-pion scattering, the strong interaction enhancement of W pair production is analogous to the behavior of the pion form factor. We might parametrize the enhancement of the amplitude for fermion pair annihilation into longitudinally polarized W bosons by a form factor $F_\pi(q^2)$. In QCD, the pion form factor receives a large enhancement from the ρ resonance. Similarly, if the new strong interactions contain a strong $I = 1$ resonance, the amplitude for longitudinally polarized W pair production should be multiplied by the factor

$$F_\pi(q^2) = \frac{-M_1^2 + iM_1\Gamma_1}{q^2 - M_1^2 + iM_1\Gamma_1} \ , \tag{198}$$

where M_1 and Γ_1 are the mass and width of the resonance. If there is no strong resonance, the new strong interactions still have an effect on this channel, but it may be subtle and difficult to detect. A benchmark is that the phase of the new pion form factor is related to the pion-pion scattering phase shift in the $I = 1$ channel,

$$\arg F_\pi(s) = \delta_1(s) \ ; \tag{199}$$

this result is true for any strong-interaction model as long as $\pi\pi \to 4\pi$ processes are not important at the given value of s [78].

At the LHC, an $I = 1$ resonance in the new strong interactions can be observed as an enhancement in $pp \to WZ + X$, with both W and Z decaying to leptons, as long as the resonance is sufficiently low in mass that its peak occurs before the $q\overline{q}$ luminosity spectrum cuts off. The ATLAS collaboration has demonstrated a sensitivity up to masses of 1.6 TeV [79]. The signal for a 1 TeV resonance is quite dramatic, as demonstrated in Figure 42.

Also shown in this figure is an estimate of a related effect that appears in some but not all models, the production of an $I = 0$, $J = 1$ resonance analogous to the ω in QCD, which then decays to 3 new pions or to $\pi\gamma$. Though the first of these modes is not easily detected at the LHC, the latter corresponds to the final state $Z^0\gamma$, which can be completely reconstructed if the Z^0 decays to $\ell^+\ell^-$.

At an e^+e^- collider, the study of the new pion form factor can be carried a bit farther. The process $e^+e^- \to W^+W^-$ is the most important single process in high-energy e^+e^- annihilation, with a cross section greater than that for all annihilation processes to quark pairs. If one observes this reaction in the topology in which one W decays hadronically and the other leptonically, the complete event can be reconstructed including the signs of the W bosons. The W decay angles contain information on the boson polarizations. So it is possible to measure the pair production cross section to an accuracy of a few percent, and also to extract the contribution from W bosons with longitudinal polarization. The experimental techniques for this analysis have been reviewed in [80].

Because an $I = 1$ resonance appears specifically in the pair-production of longitudinally polarized W bosons, the resonance peak in the cross section has associated with it an effect in the W polarizations which is significant even well below the peak. This effect is seen in Figure 43, which shows the differential cross section for W pair production at a fixed angle as a function of center-of-mass energy, in a minimal technicolor model with the $I = 1$ technirho resonance at 1.8 TeV. By measuring the amplitude for longitudinal

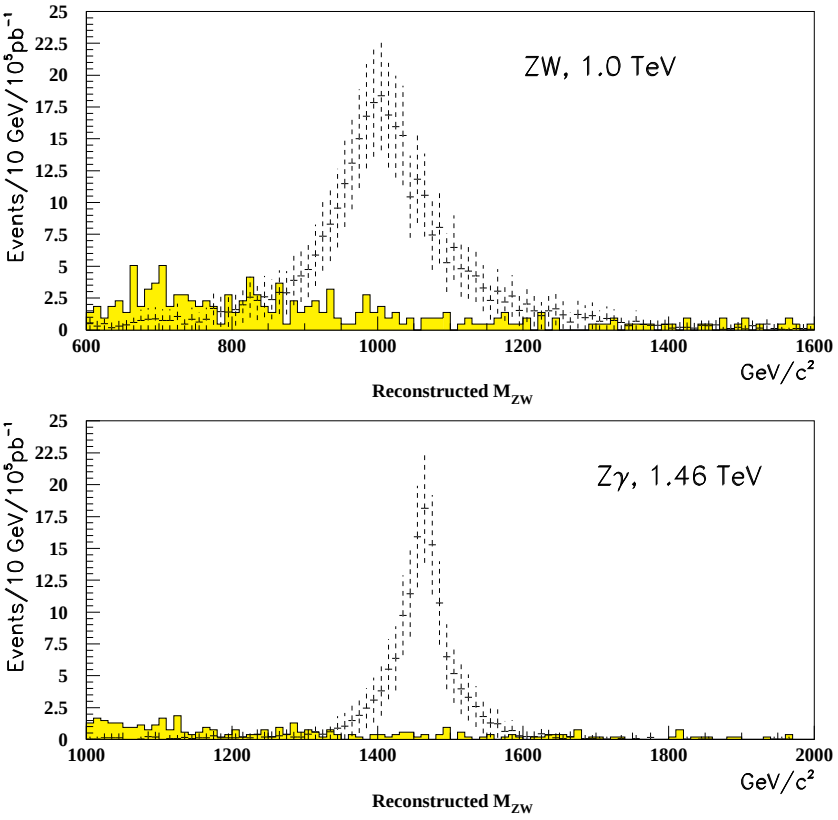

Figure 42: Reconstructed masses at the LHC for new strong interaction resonances decaying into gauge boson pairs, from [28]: (a) a 1 TeV techni-ρ resonance decaying into WZ and observed in the 3-lepton final state; (b) a 1.46 TeV techni-ω decaying into γZ and observed in the $\gamma\ell^+\ell^-$ final state.

W pair production accurately, then, it is possible to look for $I = 1$ resonances which are well above threshold. In addition, measurement of the interference between the transverse and longitudinal W pair production amplitudes allows one to determine the phase of the new pion form factor [80]. This effect is present even in models with no resonant behavior, simply by virtue of the relation (199) and the model-independent leading term in (193). Figure 44 shows the behavior of the new pion form factor as an amplitude in the complex plane as a function of the center-of-mass energy in the nonresonant and resonant cases.

The expectations for the measurement of the new pion form factor at a 1.5 TeV linear collider, from simulation results of Barklow [80], are show in Figure 45. The estimated sensitivity of the measurement is compared to the expectations from a model incorporating the physics I have just described [81]. A nonresonant model with scattering in the $I = 1$ channel given only by the scattering length term in (193) is already distinguished from a model with no new strong interactions at the 4.6 σ level, mainly by the measurement of the imaginary part of F_π. In addition, the measurement of the resonance effect (198) in the real part of F_π can distinguish the positions of $I = 1$ resonances more than a factor two above the collider center-of-mass energy.

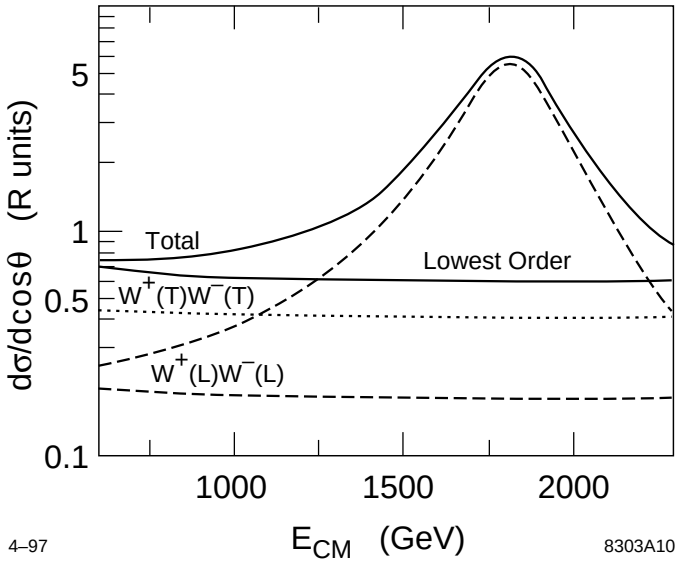

Figure 43: Technirho resonance effect on the differential cross section for $e^+e^- \to W^+W^-$ at $\cos\theta = -0.5$. The figure shows the effect on the various W polarization states.

5.6 Overview of WW scattering experiments

It is interesting to collect together and summarize the various probes for resonances in the new strong interactions that I have described in the previous two sections. I have described both direct studies of WW scattering processes and indirect searches for resonances through their effect on fermion annihilation to boson pairs. With the LHC and the e^+e^- linear collider, these reactions would be studied in a number of channels spanning all of the cases listed in (191). Of course, with fixed energy and luminosity, we can only probe so far into each channel. It is useful to express this reach quantitatively and to ask whether it should give a sufficient picture of the resonance structure that might be found.

There is a well-defined way to estimate how far one must reach to have interesting sensitivity to new resonances. The model-independent lowest order expressions for the $\pi\pi$ scattering amplitudes

$$\mathcal{M}_I = 32\pi e^{i\delta_I} \frac{s}{A_I} \cdot \begin{cases} 1 & J = 0 \\ 3\cos\theta & J = 1 \end{cases} , \tag{200}$$

violate unitarity when s becomes sufficiently large, and this gives a criterion for the value of s by which new resonances must appear [69]. The unitarity violation begins for $s = A_I/2$; with the values of the A_I given in (194), we find the bounds

$$I = 0 \ : \quad \sqrt{s} < 1.3 \text{ TeV} , \qquad I = 1 \ : \quad \sqrt{s} < 3.0 \text{ TeV} . \tag{201}$$

For comparison, if we scale up the QCD resonance masses by the factor (18), we find a techni-ρ mass of 2.0 TeV, well below the the $I = 1$ unitarity bound given in (201). It is interesting to compare these goals to the reach expected for the experiments we have described.

One of the working groups at the recent Snowmass summer study addressed the question of estimating the sensitivity to new strong interaction resonances in each of the boson-boson scattering channels that will be probed by the high-energy colliders [82].

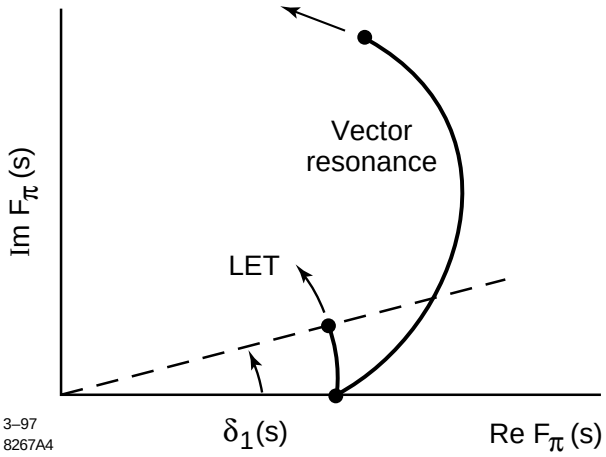

Figure 44: Dependence of $F_\pi(s)$ on energy, in models without and with a new strong interaction resonance in the $I = J = 1$ channel.

Their results are reproduced in Table 1. Results are given for experiments at the LHC and at a 1.5 TeV e^+e^- linear collider, with luminosity samples of 100 fb^{-1} per experiment. The method of the study was to use simulation data from the literature to estimate the sensitivity to the parameters M_I in (193), allowing just this one degree of freedom per channel. Situations with multiple resonances with coherent or cancelling effects were not considered. Nevertheless, the determination of these basic parameters should give a general qualitative picture of the new strong interactions. The estimates of the sensitivity to these parameters go well beyond the goals set in (201).

If new strong interactions are found, further experiments at higher energy will be necessary to characterize them precisely. Eventually, we will need to work out the detailed hadron spectroscopy of these new interactions, as was done a generation ago for QCD. Some techniques for measuring this spectrum seem straightforward if the high energy accelerators will be available. For example, one could measure the spectrum of $J = 1$ resonances from the cross section for e^+e^- or $\mu^+\mu^-$ annihilation to multiple longitudinal W and Z bosons. I presume that there are also elegant spectroscopy experiments that can be done in high-energy pp collisions, though these have not yet been worked out. It may be interesting to think about this question. If the colliders of the next generation do discover these new strong interactions, the new spectroscopy will be a central issue of particle physics twenty years from now.

5.7 Observable effects of extended technicolor

Beyond these general methods for observing new strong interactions, which apply to any model in which electroweak symmetry breaking has a strong-coupling origin, each specific model leads to its own model-dependent predictions. Typically, these predictions can be tested at energies below the TeV scale, so they provide phenomena that can be explored before the colliders of the next generation reach their ultimate energy and luminosity. On the other hand, these predictions are specific to their context. Excluding one such phenomenon rules out a particular model but not necessarily the whole class of strong-coupled theories. We have seen an example of this already in Section 5.2, where the strong constraints on technicolor models from precision electroweak physics force viable

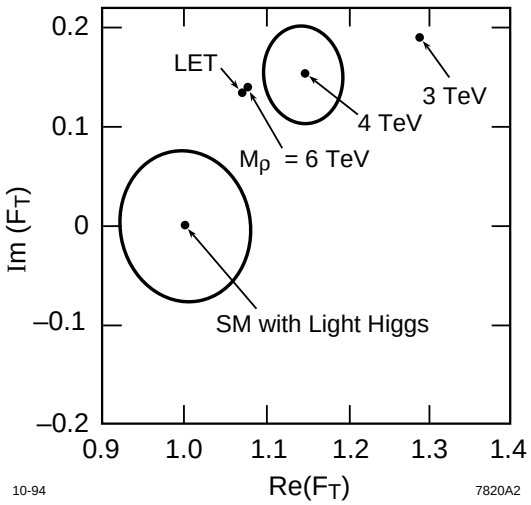

Figure 45: Determination of the new pion form factor an an e^+e^- linear collider at 1.5 TeV with an unpolarized data sample of 200 fb^{-1}, from [80]. The simulation results are compared to model with a high-mass $I = 1$ resonance and the model-independent contribution to pion-pion scattering. The contour about the light Higgs point (with no new strong interactions) is a 95% confidence contour; that about the point $M = 4$ TeV is a 68% confidence contour.

models to have particular dynamical behavior but do not exclude these models completely.

In this section, I would like to highlight three such predictions specifically associated with technicolor theories. These three phenomena illustrate the range of possible effects that might be found. A systematic survey of the model-dependent predictions of models of strongly-coupled electroweak symmetry breaking is given in [82].

All three of these predictions are associated with the extended technicolor mechanism of quark and lepton mass generation described at the end of Section 5.1 and in Figure 32. To see the first prediction, note from the figure that the Standard Model quantum numbers of the external fermion must be carried either by the techniquark or by the ETC gauge boson. The simplest possibility is to assign the techniquarks the quantum numbers of a generation of quarks and leptons [55]. Call these fermions (U, D, N, E). The pions of the technicolor theory, the Goldstone bosons of spontaneously broken chiral $SU(2)$, have the quantum numbers

$$\pi^+ \sim \overline{U}\gamma^5 D + \overline{N}\gamma^5 E \ , \pi^0 \sim \overline{U}\gamma^5 U - \overline{D}\gamma^5 D + \overline{N}\gamma^5 N - \overline{E}\gamma^5 E \ . \tag{202}$$

But the theory contains many more pseudoscalar mesons. In fact, in the absence of the coupling to $SU(3) \times SU(2) \times U(1)$, the model has the global symmetry $SU(8) \times SU(8)$ (counting each techniquark as three species), which would be spontaneously broken to a vector $SU(8)$ symmetry by dynamical techniquark mass generation. This would produce an $SU(8)$ representation of Goldstone bosons, 63 in all. Of these, three are the Goldstone bosons eaten by the $W^\pm$ and Z^0 in the Higgs mechanism. The others comprise four color singlet bosons, for example,

$$P^+ \sim \frac{1}{3}\overline{U}\gamma^5 D - \overline{N}\gamma^5 E \ , \tag{203}$$

Table 1: LHC and linear collider ('NLC') sensitivity to resonances in the new strong interactions, from [82]. 'Reach' gives the value of the resonance mass corresponding to an enhancement of the cross section for boson-boson scattering at the 95% confidence level obtained in Section VIB2. 'Sample' gives a representative set of errors for the determination of a resonance mass from this enhancement. 'Eff. $\mathcal{L}$ Reach' gives the estimate of the resonance mass for a 95% confidence level enhancement. All of these estimates are based on simple parametrizations in which a single resonance dominates the scattering cross section.

Machine	Parton Level Process	I	Reach	Sample	Eff. $\mathcal{L}$ Reach
LHC	$qq' \to qq'ZZ$	0	1600	1500^{+100}_{-70}	1500
LHC	$q\overline{q} \to WZ$	1	1600	1550^{+50}_{-50}	
LHC	$qq' \to qq'W^+W^+$	2	1950	2000^{+250}_{-200}	
NLC	$e^+e^- \to \nu\overline{\nu}ZZ$	0	1800	1600^{+180}_{-120}	2000
NLC	$e^+e^- \to \nu\overline{\nu}t\overline{t}$	0	1600	1500^{+450}_{-160}	
NLC	$e^+e^- \to W^+W^-$	1	4000	3000^{+180}_{-150}	

four color triplets, for example,

$$P_3 \sim \overline{U}\gamma^5 E \ , \tag{204}$$

and four color octets, for example,

$$P_8^+ \sim \overline{U}\gamma^5 t^a D \ , \tag{205}$$

where t^a is a 3×3 $SU(3)$ generator. These additional particles are known as *pseudo-Goldstone bosons* or, more simply, *technipions*.

Phenomenologically, the technipions resemble Higgs bosons with the same Standard Model quantum numbers. They are produced in e^+e^- annihilation at the same rate as for pointlike charged bosons. The idea of Higgs bosons with nontrivial color is usually dismissed in studies of the Higgs sector because this structure is not 'minimal'; however, we see that these objects appear naturally from the idea of technicolor. The colored objects are readily pair-produced at proton colliders, and the neutral isosinglet color-octet state can also be singly produced through gluon-gluon fusion [83].

The masses of the technipions arise from Standard Model radiative corrections and from ETC interactions; these are expected to be of the order of a few hundred GeV. Technipions decay by a process in which the techniquarks exchange an ETC boson and convert to ordinary quarks and leptons. This decay process favors decays to heavy flavors, for example, $P_8^+ \to \overline{t}b$. In this respect, too, the technipions resemble Higgs bosons of a highly nonminimal Higgs sector resulting from an underlying composite structure.

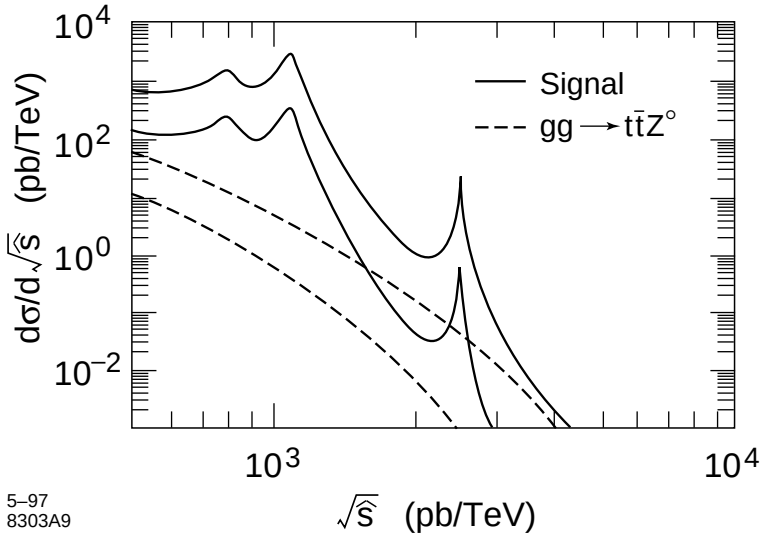

Figure 46: Cross section for the production of ETC boson pair states in pp collisions, from [84]. The $\overline{E}E$ states are observed as $t\bar{t}Z^0$ systems of definite invariant mass. The two sets of curves correspond to signal and Standard Model background (with the requirement $|p_\perp(t)| > 50$ GeV) for pp center-of-mass energies of 10 and 20 TeV.

If ETC bosons are needed to generate mass in technicolor models, it is interesting to ask whether these bosons can be observed directly. In (177), I showed that the ETC boson associated with the top quark should have a mass of about 1 TeV, putting it within the mass range accessible to the LHC. Arnold and Wendt considered a particular signature of ETC boson pair production at hadron colliders [84]. They assumed (in contrast to the assumptions of the previous few paragraphs) that the ETC bosons carry color; this allows these bosons to be pair-produced in gluon-gluon collisions. Because ETC bosons carry technicolor, they will not be produced as free particles; rather, the ETC boson pair will form a technihadron $\overline{E}E$. These hadrons will decay when the ETC boson emits a top quark and turns into a techniquark, $E \to T\bar{t}$. When both ETC bosons have decayed, we are left with a technicolor pion, which is observed as a longitudinally polarized Z^0. The full reaction is

$$gg \to \overline{E}E \to \overline{E}T + \bar{t} \to Z^0 + t + \bar{t} \ , \tag{206}$$

in which the tZ^0 system and the $Z^0 t\bar{t}$ systems both form definite mass combinations corresponding to technihadrons. The cross section for this reaction is shown in Figure 46. Note that the multiple peaks in the signal show contributions from both the $J = 0$ and the $J = 2$ bound states of ETC bosons.

A second manifestation of ETC dynamics is less direct, but it is visible at lower eneriges. To understand this effect, go back to the elementary ETC gauge boson coupling that produces the top quark mass,

$$\Delta\mathcal{L} = g_E E_\mu \overline{Q}_L \gamma^\mu T_L \ , \tag{207}$$

where $Q_L = (t, b)_L$ and $T_L = (U, D)_L$. If we put this interaction together with a corresponding coupling to the right-handed quarks, we obtain the term (174) which leads to

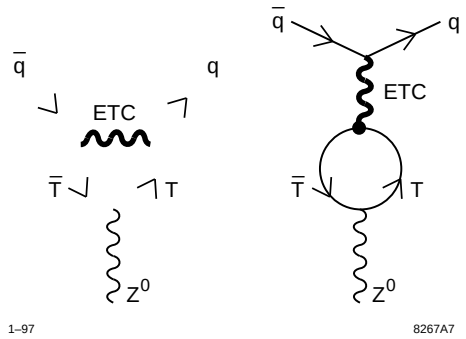

Figure 47: Modification of the $Z^0 b\overline{b}$ and $Z^0 t\overline{t}$ vertices by ETC interactions.

the fermion masses. On the other hand, we could contract the vertex (207) with its own Hermitian conjugate. This gives the vertex

$$i\Delta\mathcal{L} = (ig_E \overline{Q}_L \gamma^\mu T_L)\frac{-i}{-m_E^2}(ig_E \overline{T}_L \gamma_\mu Q_L) \ . \tag{208}$$

By a Fierz transformation [5], this expression can be rearranged into

$$i\Delta\mathcal{L} = \frac{-ig_E^2}{m_E^2}(\overline{Q}_L \gamma^\mu \tau^a Q_L)(\overline{T}_L \gamma_\mu \tau^a T_L) \ , \tag{209}$$

where τ^a are the weak isospin matrices. The last factor gives just the technicolor currents which couple to the weak interaction vector bosons. Thus, we can replace this factor by

$$\overline{T}_L \gamma_\mu \tau^3 T_L \to \frac{1}{4}\frac{e}{cs} f_\pi^2 Z_\mu \tag{210}$$

Then this term has the interpretation of a technicolor modification of the $Z \to b\overline{b}$ and $Z \to t\overline{t}$ vertices [85].

It is not difficult to estimate the size of this effect. Writing the new contribution to the Z^0 vertex together with the Standard Model contributions, we have

$$\Delta\mathcal{L} = \frac{e}{cs} Z_\mu \overline{Q}_L \gamma^\mu \left\{ \tau^3 - s^2 Q - \frac{g_E^2}{2m_E^2} f_\pi^2 \tau^3 \right\} Q_L \ . \tag{211}$$

For the left-handed b, $\tau^3 = -\frac{1}{2}$, and so the quantity in brackets is

$$\begin{aligned} g_L^b &= -\frac{1}{2} + \frac{1}{3}s^2 + \frac{1}{4}\frac{g_E^2}{m_E^2} f_\pi^2 \\ &= (g_L^b)_{\rm SM} \left(1 - \frac{1}{2}\frac{m_t}{4\pi f_\pi} \right) \ , \end{aligned} \tag{212}$$

where in the last line I have used (177) to estimate g_E/m_E. The value of the correction, when squared, is about 6% and would tend to decrease the branching ratio for $Z^0 \to b\overline{b}$.

The effect that we have estimated is that of the first diagram in Figure 47. In more complicated models of ETC [56, 86, 87], effects corresponding to both of the diagrams shown in the figure contribute, and can also have either sign. Typically, the two types of diagrams cancel in the $Z^0 b\overline{b}$ coupling and add in the $Z^0 t\overline{t}$ coupling [88]. Thus, it is interesting to study this effect experimentally in e^+e^- experiments both at the Z^0 resonance and at the $t\overline{t}$ threshold.

5.8 Recapitulation

In this section, I have discussed the future experimental program of particle physics for the case in which electroweak symmetry breaking has its origin in new strong interactions. We have discussed model-independent probes of the new strong interaction sector and experiments which probe specific aspects of technicolor models. In this case, as opposed to the case of supersymmetry, some of the most important experiments can only be done at very high energies and luminosities, corresponding to the highest values being considered for the next generation of colliders. Nevertheless, I have argued that, if plans now proposed can be realized, these experiments form a rich program which provides a broad experimental view of the new interactions.

Two sets of contrasting viewpoints appeared in our analysis. The first was the contrast between experiments that test model-dependent as opposed to model-independent conclusions. The search for technipions, for corrections to the $Zt\bar{t}$ vertex, and for other specific manifestations of technicolor theories can be carried out at energies well below the 1 TeV scale. In fact, the precision electroweak experiments and the current precision determination of the $Z^0 \to b\bar{b}$ branching ratio already strongly constrain technicolor theories. However, such constraints can be evaded by clever model-building. If an anomaly predicted by technicolor is found, it will be important and remarkable. But in either case, we will need to carry out the TeV-energy experiments to see the new interactions directly and to clearly establish their properties.

The second set of contrasts, which we saw also in our study of supersymmetry, comes from the different viewpoints offered by pp and e^+e^- colliders. In the search for anomalies, the use of both types of experiments clearly offers a broader field for discovery. But these two types of facilities also bring different information to the more systematic program of study of the new strong interactions summarized in Table 1. The table makes quantitative the powerful capabilities of the LHC to explore the new strong interaction sector. But it also shows that an e^+e^- linear collider adds to the LHC an exceptional sensitivity in the $I = 1$ channel, reaching well past the unitarity bound, and sensitivity to the process $W^+W^- \to t\bar{t}$, which tests the connection between the new strong interactions and the top quark mass generation. Again in this example, we see how the LHC and the linear collider, taken together, provide the information for a broad and coherent picture of physics beyond the standard model.

6. Conclusions

This concludes our grand tour of theoretical ideas about what physics waits for us at this and the next generation of high-energy colliders. I have structured my presentation around two specific concrete models of new physics—supersymmetry and technicolor. These models contrast greatly in their details and call for completely different experimental programs. Nevertheless, they have some common features that I would like to emphasize.

First of all, these models give examples of solutions to the problem I have argued is the highest-priority problem in elementary particle physics, the mechanism of electroweak symmetry breaking. Much work has been devoted to 'minimal' solutions to this problem, in which the future experimental program should be devoted to finding a few, or even just one, Higgs scalar bosons. It is possible that Nature works in this way. But, for myself, I do not believe it. Through these examples, I have tried to explain a very different view

of electroweak symmetry breaking, that this phenomenon arises from a new principle of physics, and that its essential simplicity is found not by counting the number of particles in the model but by understanding that the model is built around a coherent physical mechanism. New principles have deep implications, and we have seen in our two examples that these can lead to a broad and fascinating experimental program.

If my viewpoint is right, these new phenomena are waiting for us, perhaps already at the LEP 2 and Tevatron experiments of the next few years, and at the latest at the LHC and the e^+e^- linear collider. If the new physical principle that we are seeking explains the origin of Z and W masses, it cannot be too far away. In each of the models that I have discussed, I have given a quantitative estimate of the energy reach required. At the next generation of colliders, we will be there.

For those of you who are now students of elementary particle physics, this conclusion comes with both discouraging and encouraging messages. The discouragement comes from the long time scale required to construct new accelerator facilities and to carry out the large-scale experiments that are now required on the frontier. Some of your teachers can remember a time when a high-energy physics experiment could be done in one year. Today, the time scale is of order ten years, or longer if the whole process of designing and constructing the accelerator is considered.

The experiments that I have described put a premium not only on high energy but also high luminosity. This means that not only the experiments but also the accelerator designs required for these studies will require careful thinking and brilliant new ideas. During the school, Alain Blondel was fond of repeating, 'Inverse picobarns must be earned!' The price of inverse femtobarns is even higher. Thus, I strongly encourage you to become involved in the problems of accelerator design and the interaction of accelerators with experiments, to search for solutions to the challenging problems that must be solve to carry out experiments at 1 TeV and above.

The other side of the message is filled with promise. If we can have the patience to wait over the long time intervals that our experiments require, and to solve the technical problems that they pose, we will eventually arrive at the physics responsible for electroweak symmetry breaking. If the conception that I have argued for in these lectures is correct, this will be genuinely a new fundamental scale in physics, with new interactions and a rich phenomenological structure. Though the experimental discovery and clarification of this structure will be complex, the accelerators planned for the next generation—the LHC and the e^+e^- linear collider—will provide the powerful tools and analysis methods that we will require. This is the next frontier in elementary particle physics, and it is waiting for you. Enjoy it when it arrives!

Acknowledgments

I am grateful to Belen Gavela, Matthias Neubert, and Nick Ellis for inviting me to speak at the European School, to Alain Blondel, Susannah Tracy, and Egil Lillestol for providing the very pleasant arrangements for the school, to the students at the school for their enthusiasm and for their criticisms, and to Erez Etzion, Morris Swartz, and Ian Hinchliffe for comments on the manuscript. This work was supported by the Department of Energy under contract DE–AC03–76SF00515.

REFERENCES

[1] S. Weinberg, *Phys. Rev.* D **19**, 1277 (1979).
[2] L. Susskind, *Phys. Rev.* D **20**, 2619 (1979).
[3] M. Weinstein, *Phys. Rev.* D **8**, 2511 (1973).
[4] P. Sikivie, L. Susskind, M. Voloshin, and V. Zakharov, *Nucl. Phys.* B **173**, 189 (1980).
[5] M. E. Peskin and D. V. Schroeder, *An Introduction to Quantum Field Theory*. (Addison-Wesley, Reading, Mass., 1995).
[6] M. Lindner, *Z. Phys.* C **31**, 295 (1986).
[7] H. Georgi, H. R. Quinn, and S. Weinberg, *Phys. Rev. Lett.* **33**, 451 (1974).
[8] I. Hinchliffe, in *Review of Particle Properties*, *Phys. Rev.* D **54**, 1 (1996).
[9] R. Raja, to appear in the Proceedings of the 1997 Moriond Workshop on Electroweak Interactions.
[10] M. Sher, in *Perspectives in Higgs Physics*, G. Kane, ed. (World Scientific, Singapore, 1992).
[11] P. Langacker and J. Erler, hep-ph/9703428, and in *Review of Particle Properties*, *Phys. Rev.* D **54**, 1 (1996).
[12] C. T. Hill, *Phys. Rev.* D **24**, 691 (1981).
[13] R. Haag, J. T. Lopuszanski, and M. Sohnius, *Nucl. Phys.* B **88**, 257 (1975).
[14] S. Coleman and J. Mandula, *Phys. Rev.* **159**, 1251 (1967).
[15] B. Zumino, *Nucl. Phys.* B **89**, 535 (1975).
[16] J. Iliopoulos and B. Zumino, *Nucl. Phys.* B **76**, 310 (1974).
[17] M Grisaru, W. Siegel, and M. Rocek, *Nucl. Phys.* B **159**, 429 (1979).
[18] L. Girardello and M. T. Grisaru, *Nucl. Phys.* B **194**, 65 (1982).
[19] L. E. Ibáñez and G. G. Ross, in *Perspectives in Higgs Physics*, G. Kane, ed. (World Scientific, Singapore, 1992).
[20] G. L. Kane, C. Kolda, L. Roszkowski, and J. D. Wells, *Phys. Rev.* D **49**, 6173 (1994).
[21] F. Gabbiani and A. Masiero, *Nucl. Phys.* B **322**, 235 (1989); F. Gabbiani, E. Gabrielli, A. Masiero, and L. Silvestrini, *Nucl. Phys.* B **477**, 321 (1996).
[22] S. Dimopoulos and H. Georgi, *Nucl. Phys.* B **193**, 150 (1981).
[23] N. Sakai, *Z. Phys.* C **11**, 153 (1981).
[24] Y. Nir and N. Seiberg, *Phys. Lett.* B **309**, 337 (1993); M. Leurer, Y. Nir, and N. Seiberg, *Nucl. Phys.* B **309**, 337 (1993).
[25] D. M. Pierce and A. Papadopoulos, *Nucl. Phys.* B **430**, 278 (1994); D. M. Pierce, J. A. Bagger, K. Matchev, and R.-J. Zhang, *Nucl. Phys.* B **491**, 3 (1997).
[26] M. Dine, A. E. Nelson, Y. Nir, and Y. Shirman, *Phys. Rev.* D **53**, 2658 (1996).
[27] J. Bagger, U. Nauenberg, X. Tata, and A. White, hep-ph/9612359, to appear in the Proceedings of the 1996 DPF/DPB Snowmass Summer Study, D. Cassel and R. Siemann, eds.
[28] ATLAS Collaboration, Technical Proposal, CERN/LHCC/94-43.
[29] J. L. Feng and T. Moroi, hep-ph/9612333.
[30] J. A. Bagger, K. Matchev, D. M. Pierce, and R.-J. Zhang, *Phys. Rev.* D **55**, 3188 (1997).
[31] M. E. Peskin, *Prog. Theor. Phys. Suppl.* **123**, 507 (1996).
[32] D. Decamp, *et al.*(ALEPH Collaboration), *Phys. Repts.* **216**, 253 (1992).

[33] H. Baer, V. Barger, D. Karatas, and X. Tata, *Phys. Rev.* D **36**, 96 (1987); H. Baer, X. Tata, and J. Woodside, *Phys. Rev.* D **42**, 1568 (1990).
[34] R. M. Barnett, J. F. Gunion, and H. E. Haber, *Phys. Rev.* D **37**, 1892 (1988).
[35] H. Baer, X. Tata, and J. Woodside, *Phys. Rev.* D **45**, 142 (1992).
[36] S. Dimopoulos, M. Dine, S. Raby, and S. Thomas, *Phys. Rev. Lett.* **76**, 3494 (1996).
[37] J. Ellis, K. Enqvist, D. Nanopoulos, and F. Zwirner, *Mod. Phys. Lett* A **1**, 57 (1986).
[38] R. Barbieri and G. Giudice, *Nucl. Phys.* B **306**, 63 (1988).
[39] G. Anderson and D. Castaño, *Phys. Rev.* D **52**, 1693 (1995).
[40] G. F. Giudice, *et al.*, hep-ph/9602207.
[41] D. Amidei and R. Brock, eds., *Future Electroweak Physics at the Fermilab Tevatron.* FERMILAB-Pub-96/082.
[42] I. Hinchliffe, F. E. Paige, M. D. Shapiro, J. Soderqvist, and W. Yao, *Phys. Rev.* D **55**, 5520 (1997).
[43] G. Loew, *et al.*, *International Linear Collider Technical Review Committee Report 1995.* SLAC-Report-471 (1995).
[44] S. Kuhlman, *et al.*, *Physics and Technology of the Next Linear Collider.* BNL 52-502, Fermilab-PUB-96/112, LBNL-PUB-5425, SLAC report 485, UCRL-ID-124160 (1996).
[45] T. Tsukamoto, K. Fujii, H. Murayama, M. Yamaguchi, and Y. Okada, *Phys. Rev.* D **51**, 3153 (1995).
[46] M. M. Nojiri, K. Fujii, and T. Tsukamoto, *Phys. Rev.* D **54**, 6756 (1996).
[47] M. N. Danielson, *et al.*, to appear in the Proceedings of the 1996 DPF/DPB Snowmass Summer Study, D. Cassel and R. Siemann, eds.
[48] J. L. Feng, M. E. Peskin, H. Murayama, and X. Tata, *Phys. Rev.* D **52**, 1418 (1995).
[49] J. L. Feng and D. E. Finnell, *Phys. Rev.* D **49**, 2369 (1994).
[50] LHC Study Group, *The Large Hadron Collider: Conceptual Design.* CERN/AC/95-05 (LHC) (1995).
[51] S. Basa, Marseille Ph. D. thesis, 1994.
[52] H. Baer, C.-H. Chen, F. Paige, and X. Tata, *Phys. Rev.* D **50**, 4508 (1994).
[53] S. Dimopoulos and L. Susskind, *Nucl. Phys.* B **155**, 237 (1979).
[54] E. Eichten and K. Lane, *Phys. Lett.* B **90**, 125 (1980).
[55] E. Farhi and L. Susskind, *Phys. Rev.* D **20**, 3404 (1979).
[56] R. S. Chivukula, E. Gates, E. H. Simmons and J. Terning, *Phys. Lett.* B **311**, 157 (1993); R. S. Chivukula, E. H. Simmons and J. Terning, *Phys. Lett.* B **331**, 383 (1994).
[57] S. Glashow, J. Iliopoulos, and L. Maiani, *Phys. Rev.* D **2**, 1285 (1970).
[58] E. Eichten, K. Lane, and J. Preskill, *Phys. Rev. Lett.* **45**, 225 (1980).
[59] S. Dimopoulos and J. Ellis, *Nucl. Phys.* B **182**, 505 (1982).
[60] S. Dimopoulos, H. Georgi, and S. Raby, *Phys. Lett.* B **127**, 101 (1983).
[61] L. Randall, *Nucl. Phys.* B **403**, 122 (1993).
[62] H. Georgi, *Nucl. Phys.* B **416**, 699 (1994).
[63] S. Raby, *Nucl. Phys.* B **187**, 446 (1981).
[64] M. E. Peskin and T. Takeuchi, *Phys. Rev. Lett.* **65**, 964 (1990), *Phys. Rev.* D **46**, 381 (1992).
[65] B. Holdom, *Phys. Rev.* D **24**, 1441 (1981).

[66] T. Appelquist and J. Terning, *Phys. Lett.* B **315**, 139 (1993).
[67] J. M. Cornwall, D. N. Levin, and G. Tiktopoulos, *Phys. Rev.* D **10**, 1145 (1974).
[68] C. E. Vayonakis, *Lett. Nuov. Cim.* **17**, 383 (1976).
[69] B. W. Lee, C. Quigg, and H. B. Thacker, *Phys. Rev. Lett.* **38**, 883 (1977), *Phys. Rev.* D **16**, 1519 (1977).
[70] M. S. Chanowitz and M. K. Gaillard, *Nucl. Phys.* B **261**, 379 (1985).
[71] G. Källén, *Elementary Particle Physics*. (Addison-Wesley, Reading, Mass., 1964).
[72] M. Chanowitz, M. Golden, and H. Georgi, *Phys. Rev. Lett.* **57**, 2344 (1986), *Phys. Rev.* D **36**, 1490 (1987).
[73] S. Dawson, *Nucl. Phys.* B **249**, 42 (1985).
[74] J. Bagger, V. Barger, K. Cheung, J. Gunion, T. Han, G. A. Ladinsky, R. Rosenfeld, and C. P. Yuan, *Phys. Rev.* D **49**, 1246 (1994), **52**, 3878 (1995).
[75] V. Barger, K. Cheung, T. Han and R. Phillips, Phys. Rev. *Phys. Rev.* D **52**, 3815 (1995).
[76] T. L. Barklow, to appear in the Proceedings of the 1996 DPF/DPB Snowmass Summer Study, D. Cassel and R. Siemann, eds.
[77] C. T. Hill, *Phys. Lett.* B **266**, 419 (1991), **345**, 483 (1995).
[78] J. D. Bjorken and S. D. Drell, *Relativistic Quantum Fields*, Ch. 18.13. (McGraw-Hill, New York, 1965).
[79] C. E. Wulz, in Proceedings of the International Europhysics Conference on High-Energy Physics, EPS HEP 95, J. Lemonne, C. Vander Velde, and F. Verbeure, eds. (World Scientific, Singapore, 1996).
[80] T. L. Barklow, in *Physics and Experiments with Linear Colliders*, A. Miyamoto, Y. Fujii, T. Matsui, and S. Iwata, eds. (World Scientific, Singapore, 1996).
[81] M. E. Peskin, in *Physics in Collision 4*, A. Seiden, ed. (Éditions Frontières, Gif, 1984).
[82] T. L. Barklow, G. Burdman, R. S. Chivukula, B. A. Dobrescu, P. S. Drell, N. Hadley, W. B. Kilgore, M. E. Peskin, J. Terning, and D. R. Wood, hep-ph/9704217, to appear in the Proceedings of the 1996 DPF/DPB Snowmass Summer Study, D. Cassel and R. Siemann, eds.
[83] E. Eichten and K. Lane, hep-ph/9609297, 9609298, to appear in the Proceedings of the 1996 DPF/DPB Snowmass Summer Study, D. Cassel and R. Siemann, eds.
[84] P. Arnold and C. Wendt, *Phys. Rev.* D **33**, 1873 (1986).
[85] R. S. Chivukula, S. B. Selipsky, and E. H. Simmons, *Phys. Rev. Lett.* **69**, 575 (1992).
[86] N. Kitazawa, *Phys. Lett.* B **313**, 395 (1993); K. Hagiwara and N. Kitazawa, *Phys. Rev.* D **52**, 5374 (1995).
[87] G.-H. Wu, *Phys. Rev. Lett.* **74**, 4137 (1995).
[88] H. Murayama, in *Physics and Experiments with Linear Colliders*, A. Miyamoto, Y. Fujii, T. Matsui, and S. Iwata, eds. (World Scientific, Singapore, 1996).